GRAN SASSO SCIENCE INSTITUTE
SCHOOL OF ADVANCED STUDIES
Scuola Universitaria Superiore

CHALMERS
UNIVERSITY OF TECHNOLOGY

Unveiling the nature of dark matter with direct detection experiments

Vanessa Zema

PhD Thesis Defence
Gran Sasso Science Institute - Zoom meeting
10 September 2020

DARK MATTER SEARCH

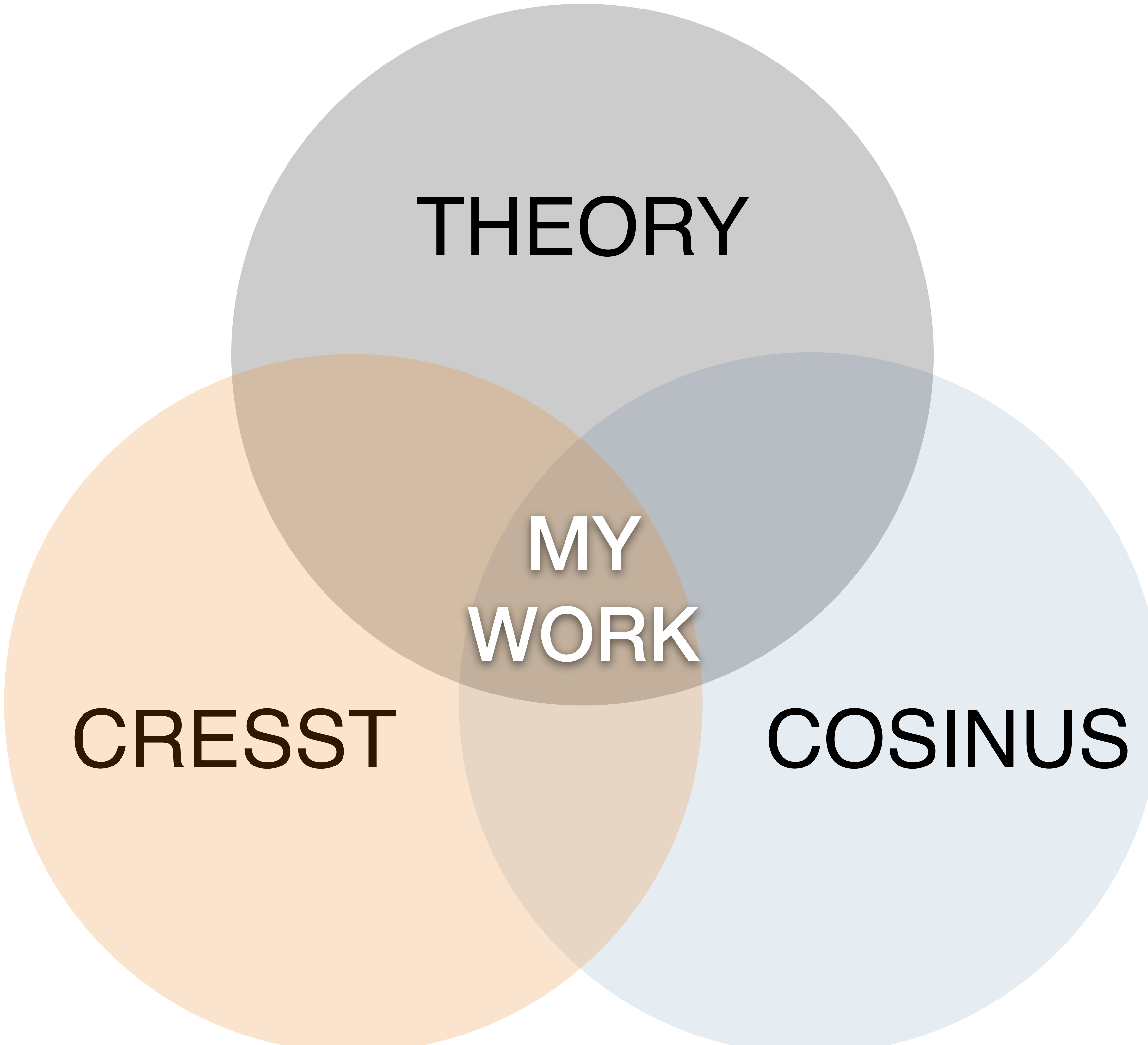

Outline

- Evidence for dark matter (DM)
- Generalities of DM direct detection (DD)
- DM DD effective field theory: two applications
- DM search with the CRESST experiment
- COSINUS phenomenology

Outline

- Evidence for dark matter (DM)
- Generalities of DM direct detection (DD)
- DM DD effective field theory: two applications
- DM search with the CRESST experiment
- COSINUS phenomenology

Introduction

Outline

- Evidence for dark matter (DM)
- Generalities of DM direct detection (DD)

→ Introduction

- DM DD effective field theory: two applications
- DM search with the CRESST experiment
- COSINUS phenomenology

→ Studies and Results

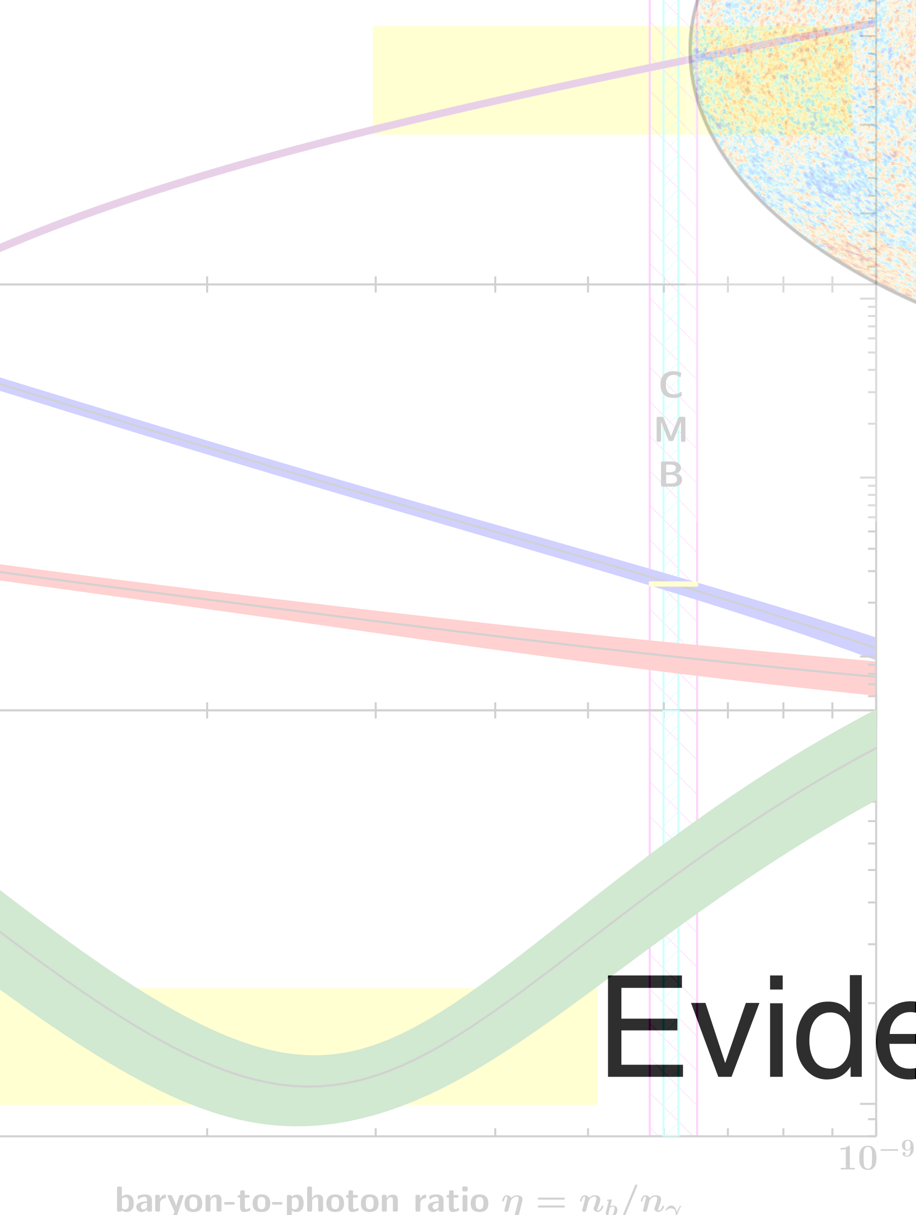

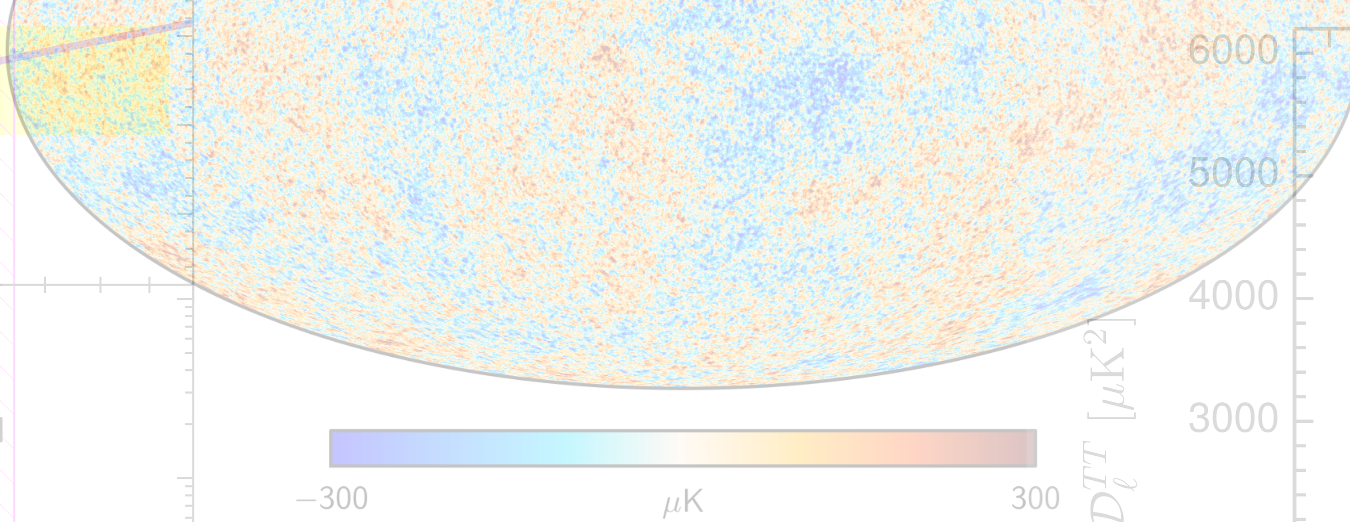

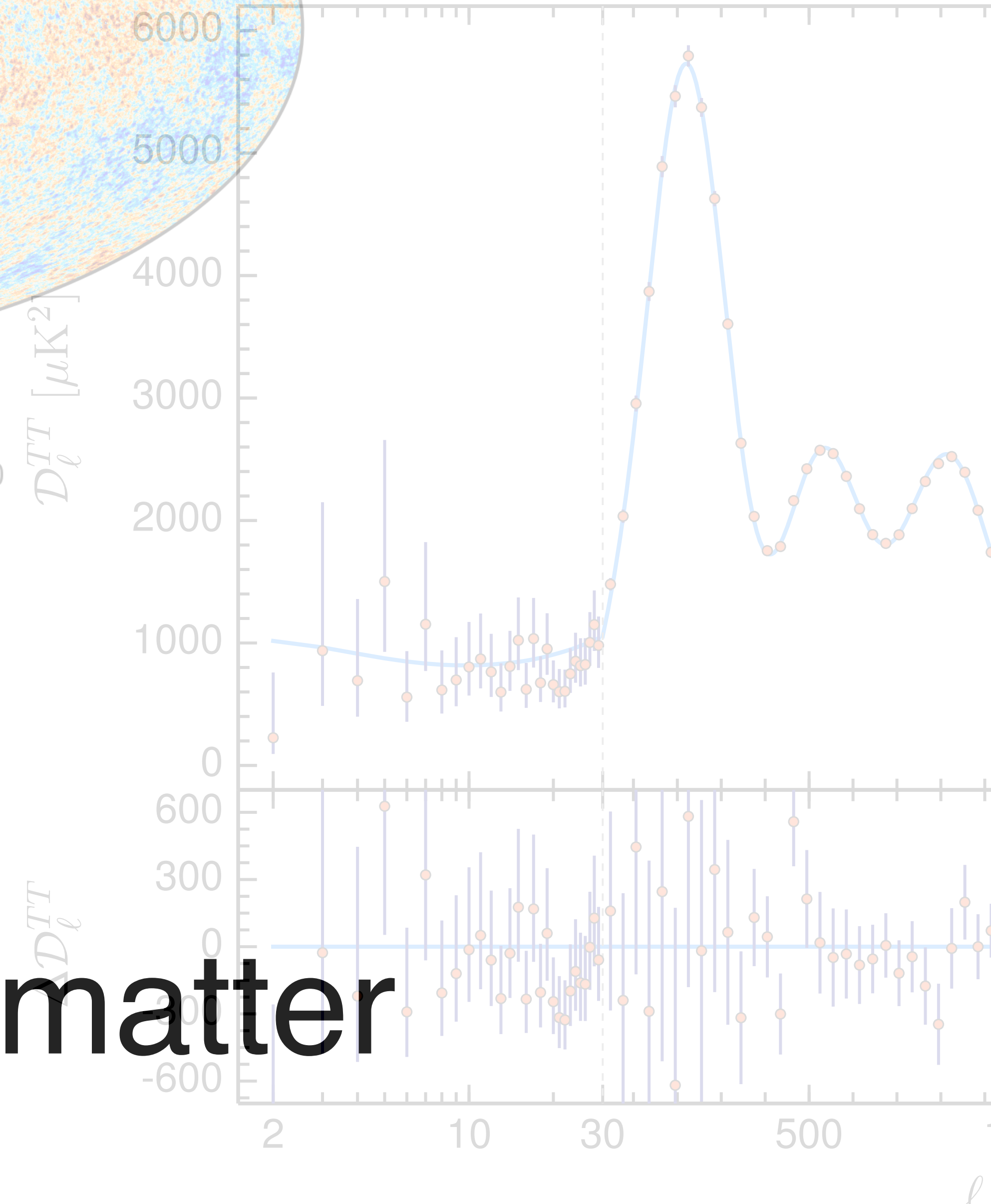

Evidence for dark matter

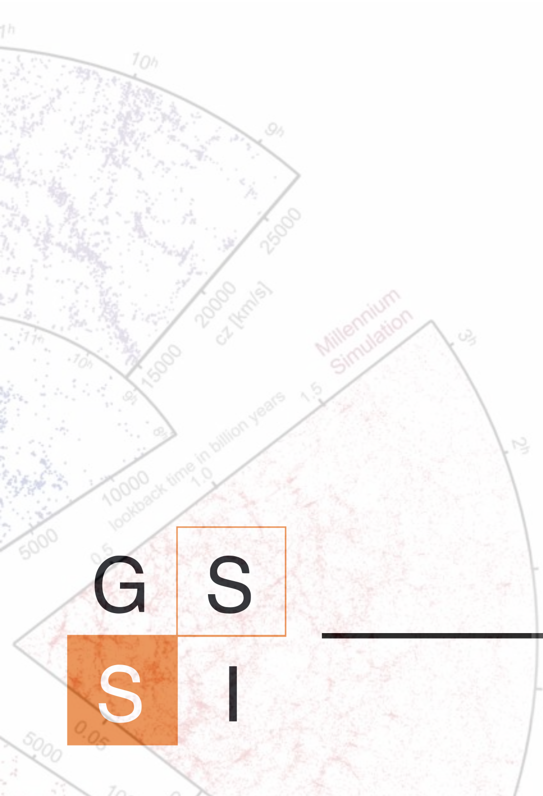

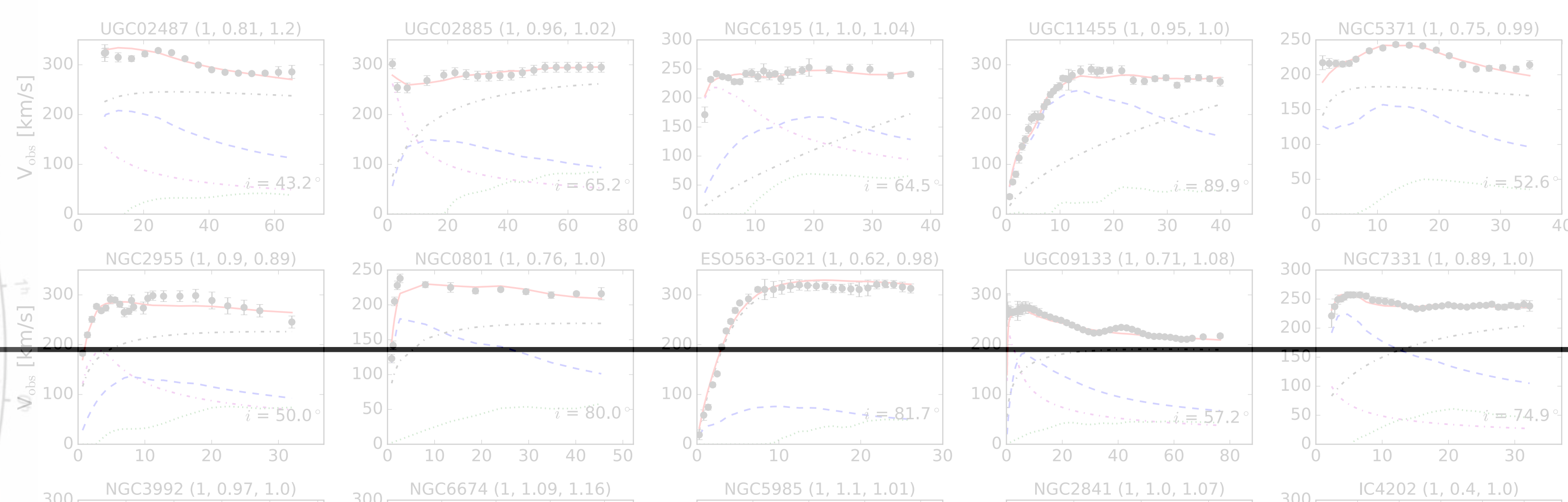

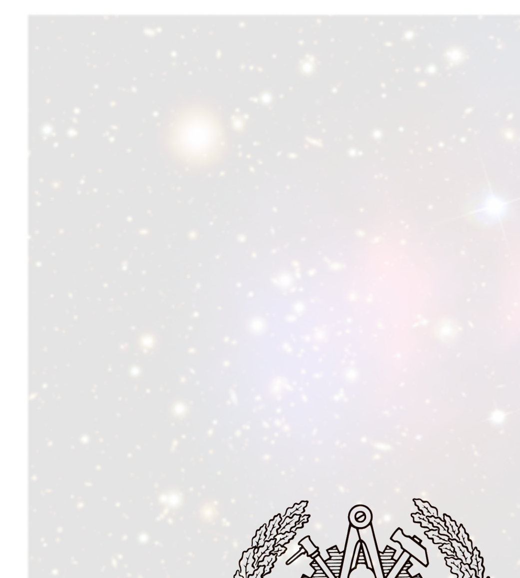

Evidence for dark matter (DM)

Does the Universe contain non-baryonic DM?

$$\Omega_m > \Omega_b$$

Total matter density parameter

Baryonic matter density parameter

Evidence for dark matter (DM)

Does the Universe contain non-baryonic DM?

$$\Omega_m > \Omega_b$$

Total matter density parameter

Baryonic matter density parameter

1. How many baryons are in the Universe?

- Big Bang Nucleosynthesis (BBN)
- Recombination era - Cosmic microwave background (CMB)
- Astronomical measurements

Evidence for dark matter (DM)

1. How many baryons are in the Universe?
   - Big Bang Nucleosynthesis (BBN)
   - Recombination era - Cosmic microwave background (CMB)
   - Astronomical measurement
2. Does the Universe contain non-baryonic DM?
   - Cosmic Microwave Background (CMB)
   - Large scale structure formation

Does the Universe contain non-baryonic DM?

Evidence from CMB

CMB $\longrightarrow$ Black body $\longrightarrow$ $T(\theta, \phi)$

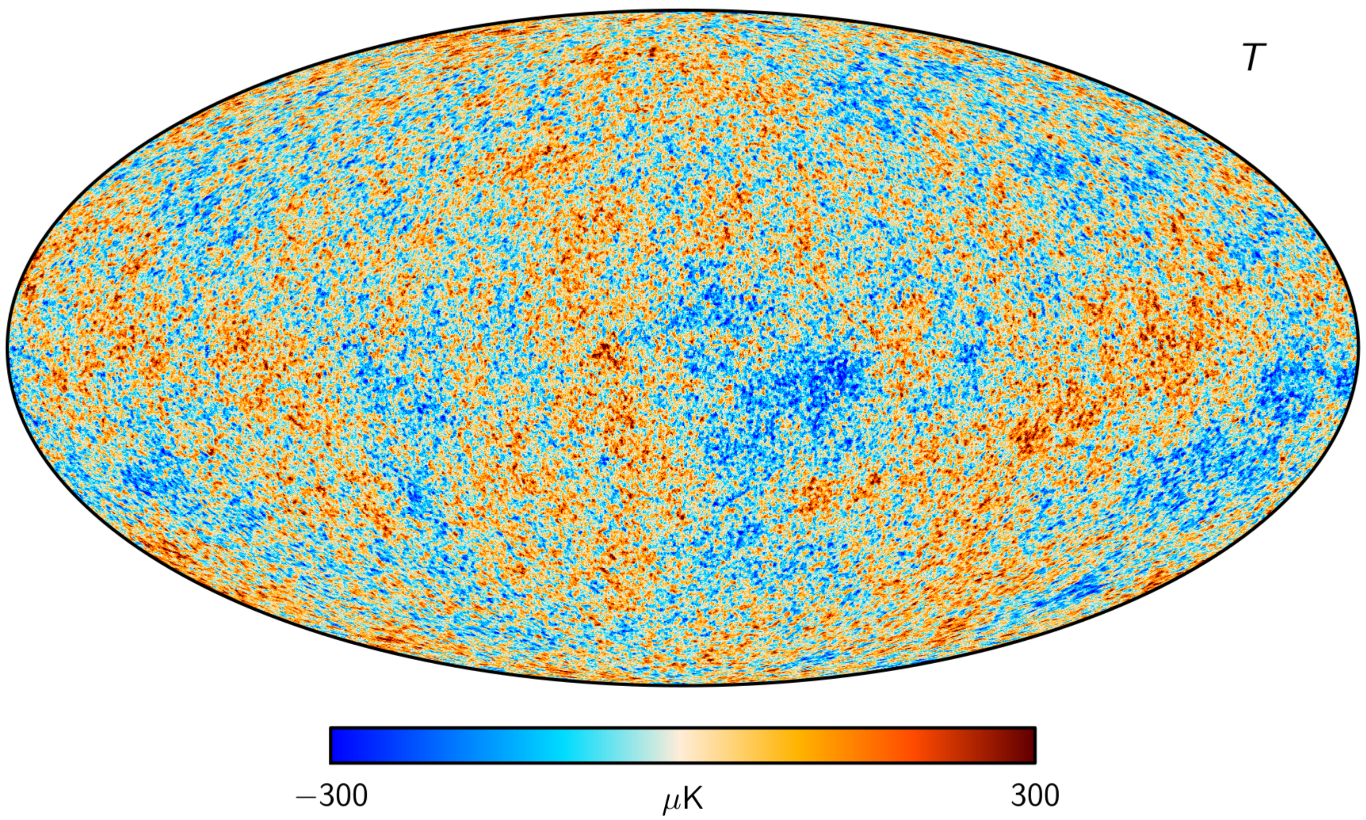

https://wiki.cosmos.esa.int/planck-legacy-archive/index.php/Main_Page

Observable: angular power spectrum

$$D^{TT}(\theta) = \left\langle \frac{\delta T}{T}(n_1)\frac{\delta T}{T}(n_2) \right\rangle$$

Does the Universe contain non-baryonic DM?

Evidence from CMB

N. Aghanim et al. Planck 2018 results. VI. Cosmological parameters. 2018.

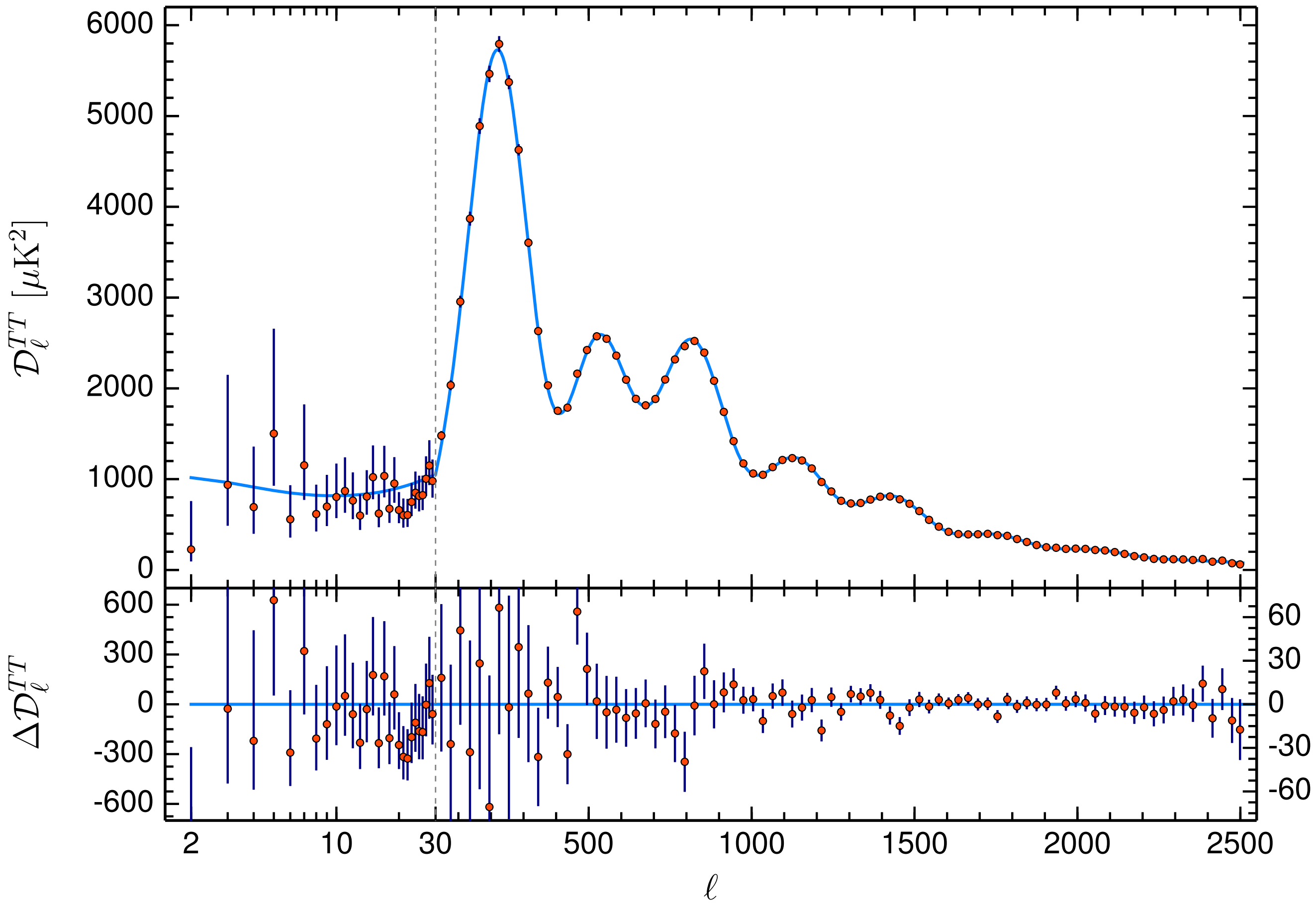

$$\Omega_m h^2 = 0.1430 \pm 0.0011$$

$$\Omega_b h^2 = 0.02230 \pm 0.00020$$

$$\Omega_c h^2 = 0.1200 \pm 0.0012$$

$$\boxed{\Omega_m > \Omega_b}$$

GS
SI

Does the Universe contain non-baryonic DM?

Evidence from large scale structure formation

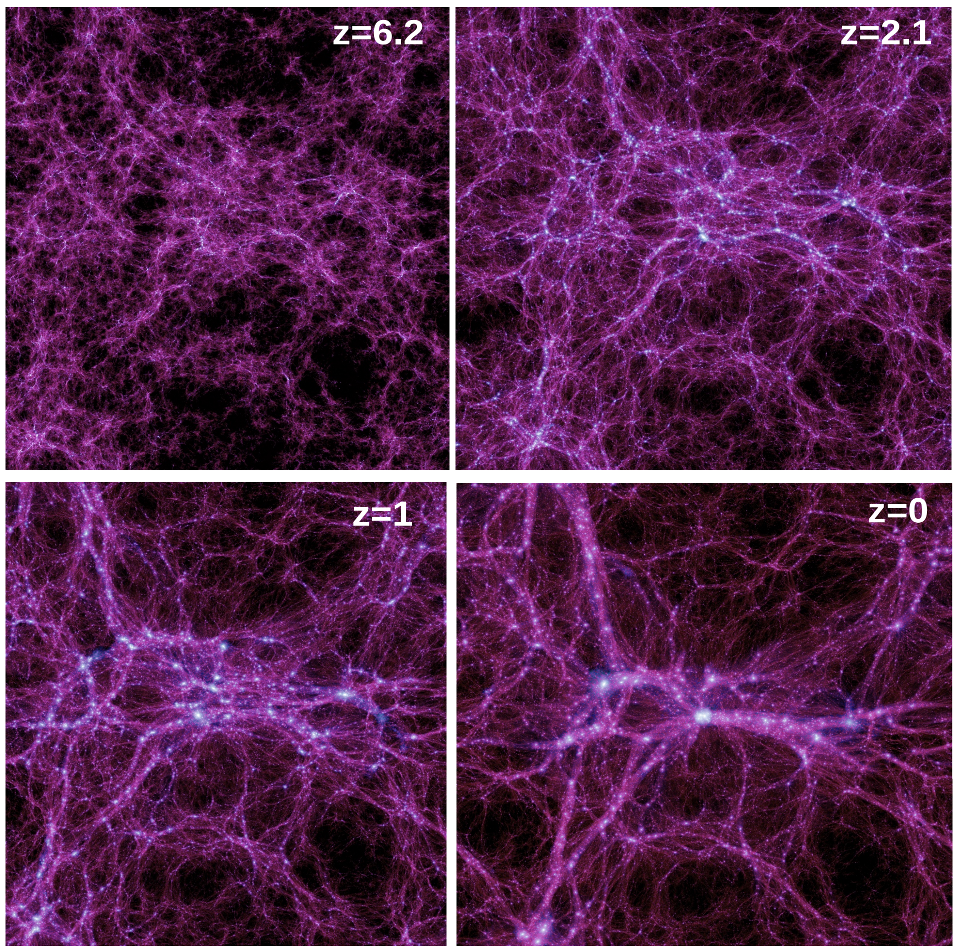

Mon. Not. Roy. Astron. Soc., 398:1150, 2009.

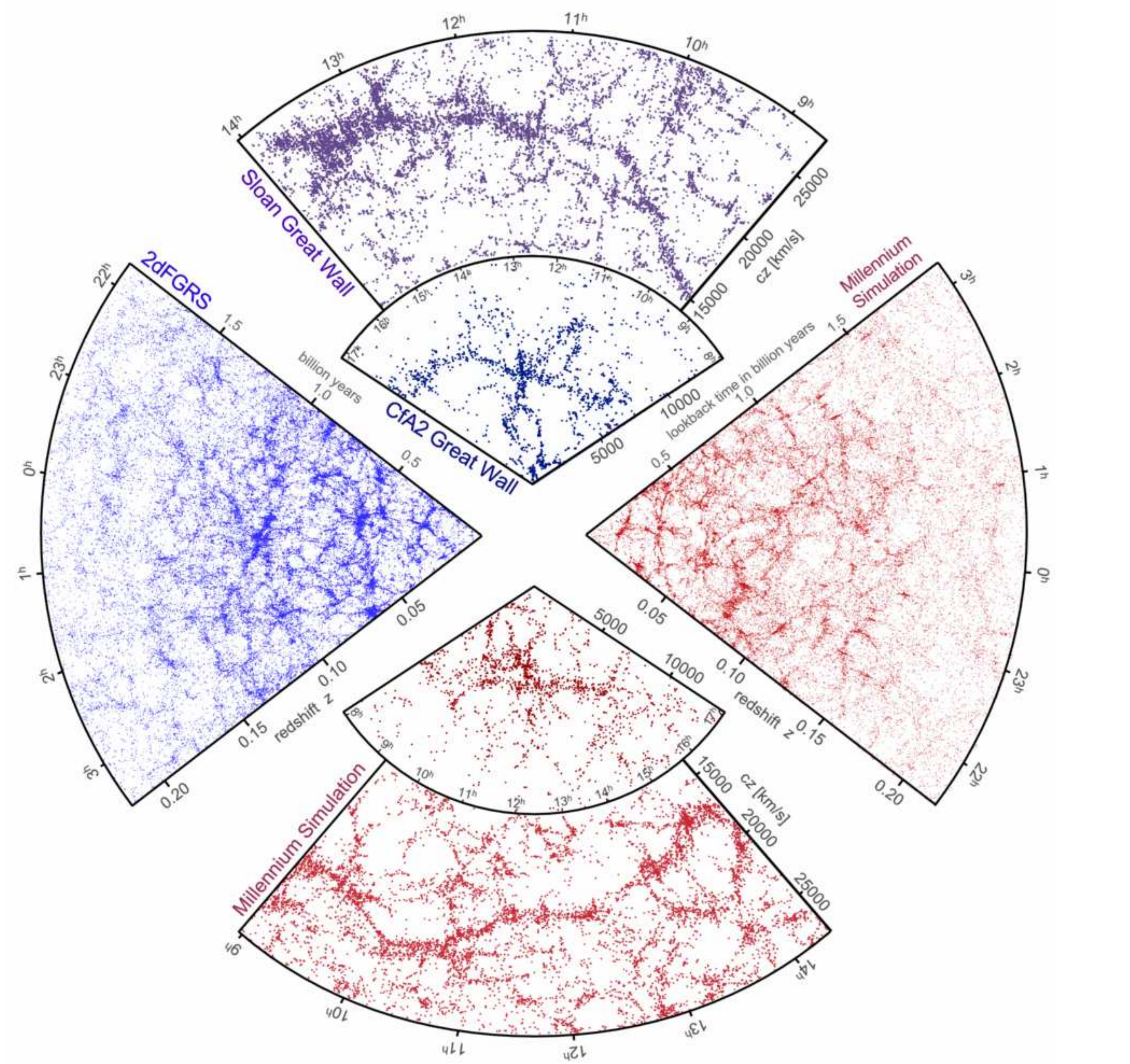

The large-scale structure of the Universe. Nature, 440:1137, 2006

Evidence for dark matter (DM)

1. How many baryons are in the Universe?
   - Big Bang Nucleosynthesis (BBN)
   - Recombination era - Cosmic microwave background (CMB)
2. Does the Universe contain non-baryonic DM?
   - Cosmic Microwave Background (CMB)
   - Large scale structure formation

Evidence for DM at astrophysical scale

- Gravitational lensing
- Galactic rotation curves

G S
S I

Does the Universe contain non-baryonic DM?

Evidence from gravitational lensing, e.g. *Bullet cluster*

Annual Review of Astronomy and Astrophysics, 48:87{125, 2010}

Does the Universe contain non-baryonic DM?

Evidence from spiral galaxy velocity rotation curves

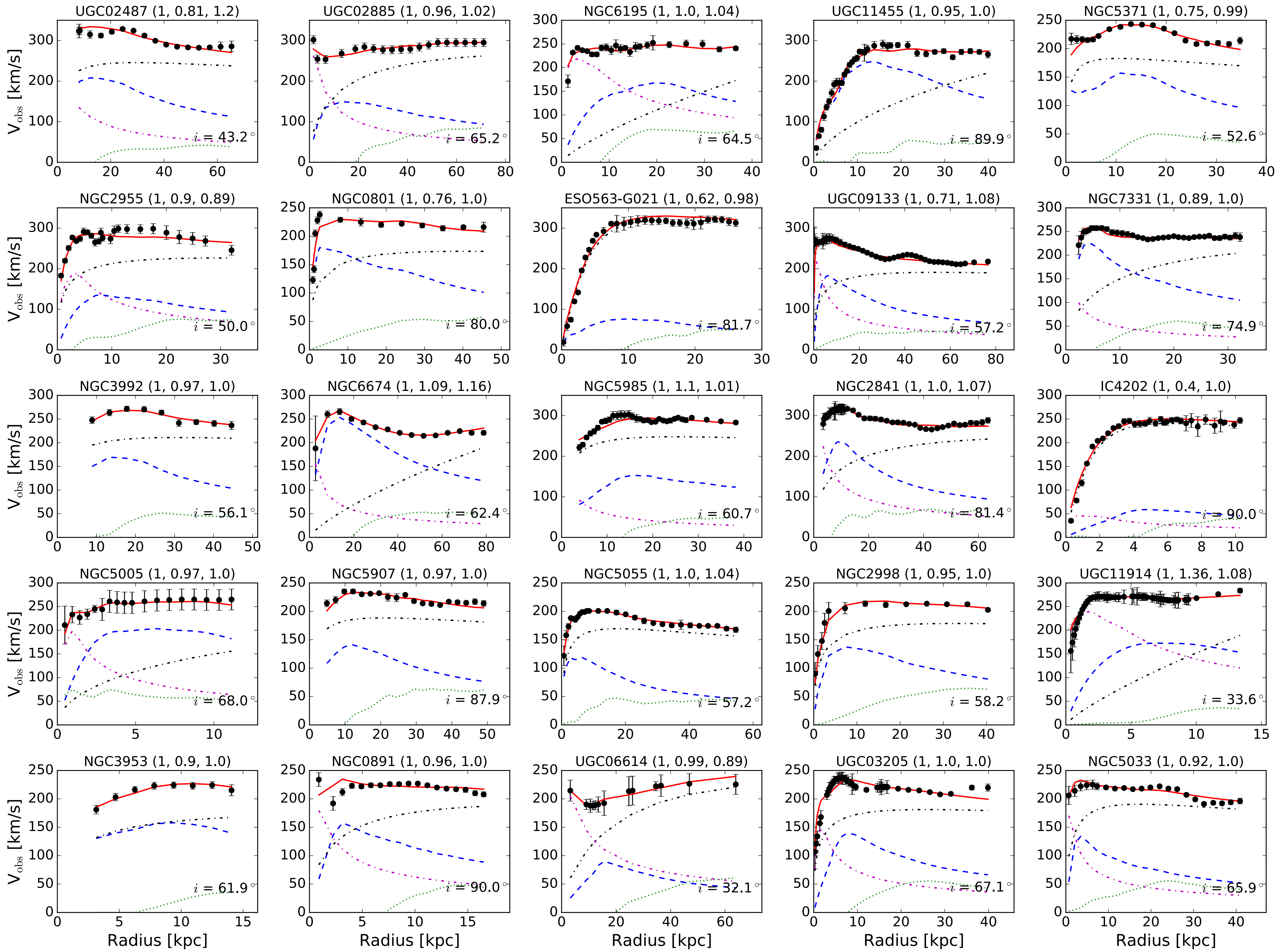

The Astronomical Journal, 152(6):157, 2016

Alternative to DM

Example: MoND

M. Milgrom. *A Modification of the Newtonian dynamics as a possible alternative to the hidden mass hypothesis*. Astrophys. J., 270:365-370, 1983.

Phenomenological modification of Newtonian dynamics which reproduces experimental rotation curves

$$\begin{cases} g = g_N & if \quad g \gg a_0 \\ g = g_N \frac{a_0}{g} & if \quad g \ll a_0 \end{cases}$$

$$g\ m\ r = m\ V_C^2 \quad \rightarrow V_C^2 = g\ r = \sqrt{g_N\ a_0}\ r = \sqrt{G_N\ M\ a_0} = const$$

No fundamental theory of modified gravity have been found <u>yet</u> which can explain all the gravitational observations at the same time

G S S I

Missing mass problem

Dark matter

Modify gravity

Missing mass problem

Dark matter

Modify gravity

Particle

- MAcroscopic Compact Halo Objects (MACHOs)
  - Primordial Black Holes (PBH)

Missing mass problem

Dark matter

Modify gravity

Particle

- MAcroscopic Compact Halo Objects (MACHOs)
  - Primordial Black Holes (PBH)

Ruled out as the main component of DM

Phys. Rev. Lett., 121(14):141101, 2018.

G S
S I

Missing mass problem

Dark matter

Modify gravity

Particle

- MAcroscopic Compact Halo Objects (MACHOs)
  - Primordial Black Holes (PBH)

G S
S I

Selected dark matter particle models

Selected dark matter particle models

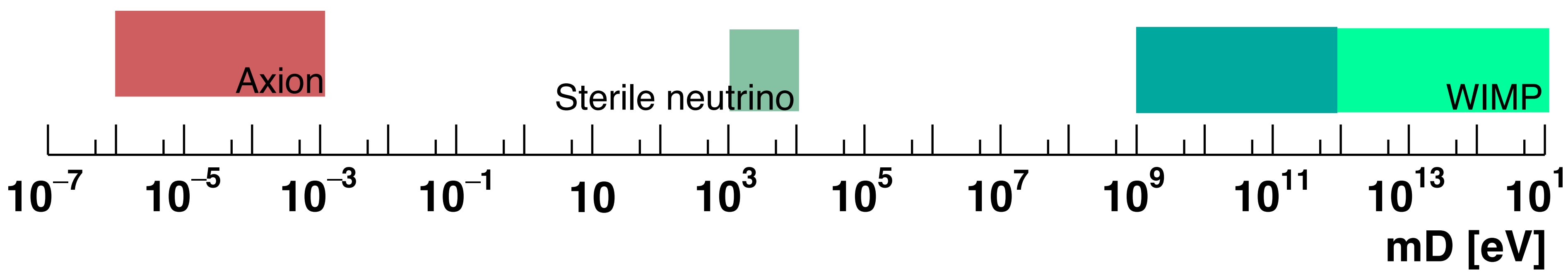

V. Zema, Master thesis, University of Rome La Sapienza, 2016

Selected dark matter particle models

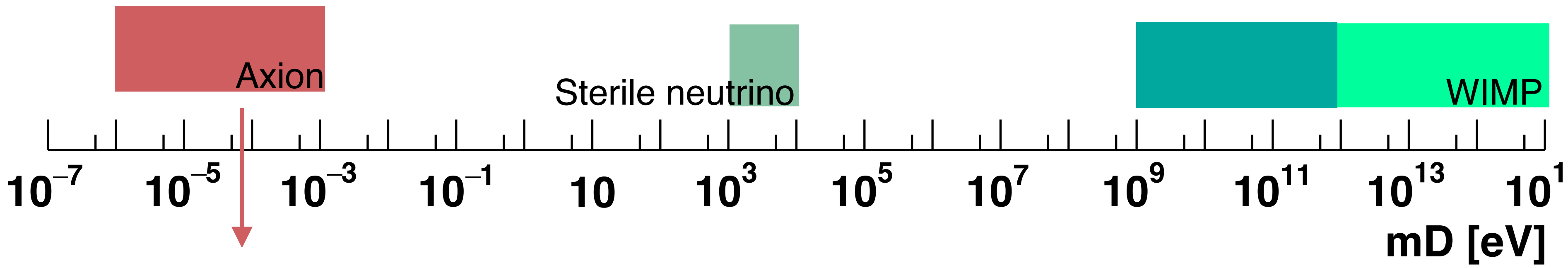

- Pseudoscalar particle
- Roberto Peccei and Helen Quinn's model
- Solution of the strong CP violation problem
- $m_a \rightarrow 10^{-6} - 10^{-3} eV$

V. Zema, Master thesis, University of Rome La Sapienza, 2016

Selected dark matter particle models

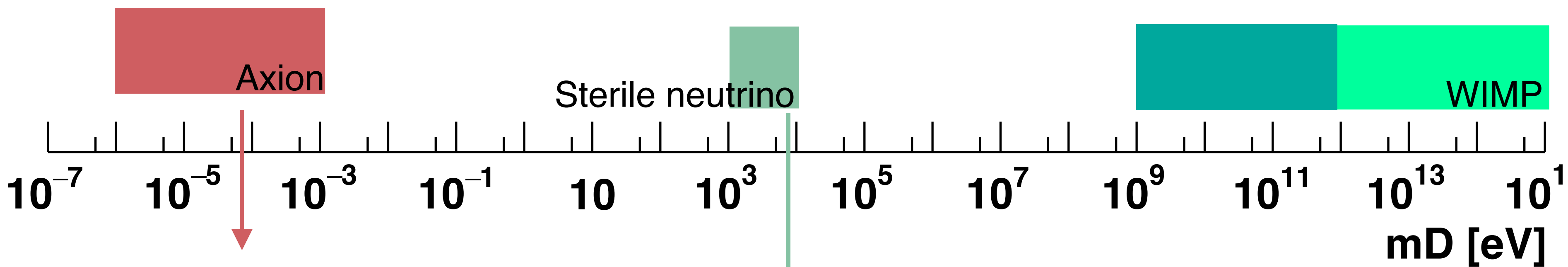

V. Zema, Master thesis, University of Rome La Sapienza, 2016

- Pseudoscalar particle
- Roberto Peccei and Helen Quinn's model
- Solution of the strong CP violation problem
- $m_a \to 10^{-6} - 10^{-3} eV$

- Fermionic particle
- Right handed massive neutrino
- Promising candidate as extension of the standard model if involved in the neutrino mass term
- $m_N \sim \mathcal{O}(\mathrm{keV})$

Selected dark matter particle models

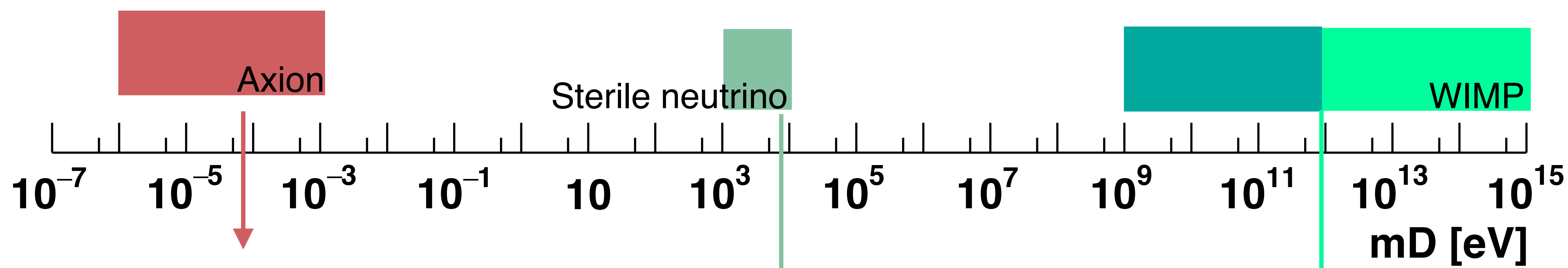

V. Zema, Master thesis, University of Rome La Sapienza, 2016

- Pseudoscalar particle
- Roberto Peccei and Helen Quinn's model
- Solution of the strong CP violation problem
- $m_a \rightarrow 10^{-6} - 10^{-3} eV$

- Fermionic particle
- Right handed massive neutrino
- Promising candidate as extension of the standard model if involved in the neutrino mass term
- $m_N \sim \mathcal{O}(\mathrm{keV})$

- Weakly Interactive Massive Particle
- Thermal relic
- Supersymmetric provides the neutralino as WIMP candidate
- $m_\chi \rightarrow \mathrm{GeV} - \mathrm{TeV}$ the most investigated
- Most of the experiments search for WIMP

GSSI

Selected dark matter particle models

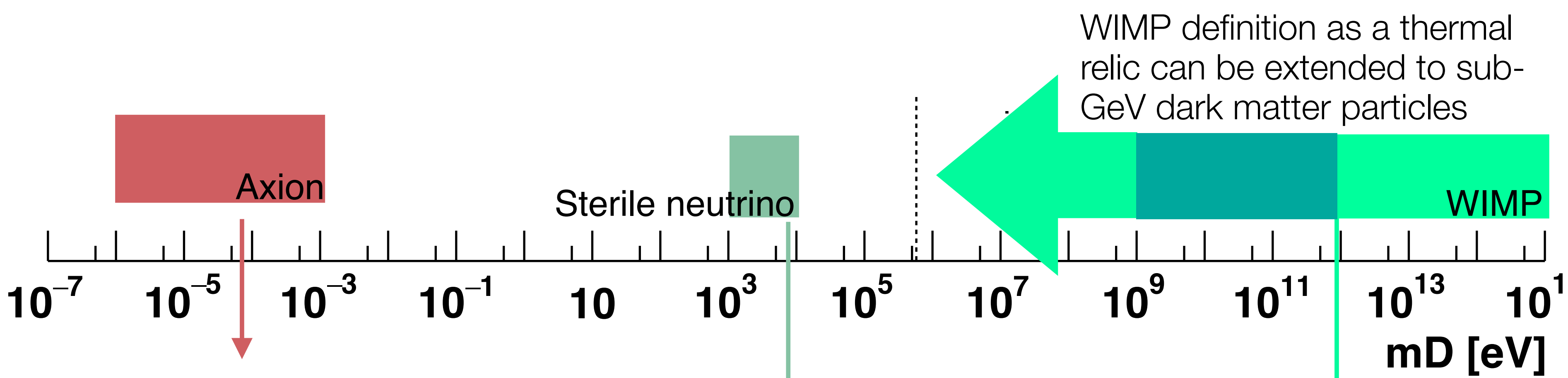

V. Zema, Master thesis, University of Rome La Sapienza, 2016

- Pseudoscalar particle
- Roberto Peccei and Helen Quinn's model
- Solution of the strong CP violation problem
- $m_a \to 10^{-6} - 10^{-3} eV$

- Fermionic particle
- Right handed massive neutrino
- Promising candidate as extension of the standard model if involved in the neutrino mass term
- $m_N \sim \mathcal{O}(\mathrm{keV})$

- Weakly Interactive Massive Particle
- Thermal relic
- Supersymmetric provides the neutralino as WIMP candidate
- $m_\chi \to \mathrm{GeV} - \mathrm{TeV}$ the most investigated
- Most of the experiments search for WIMP

GSSI

Detection techniques

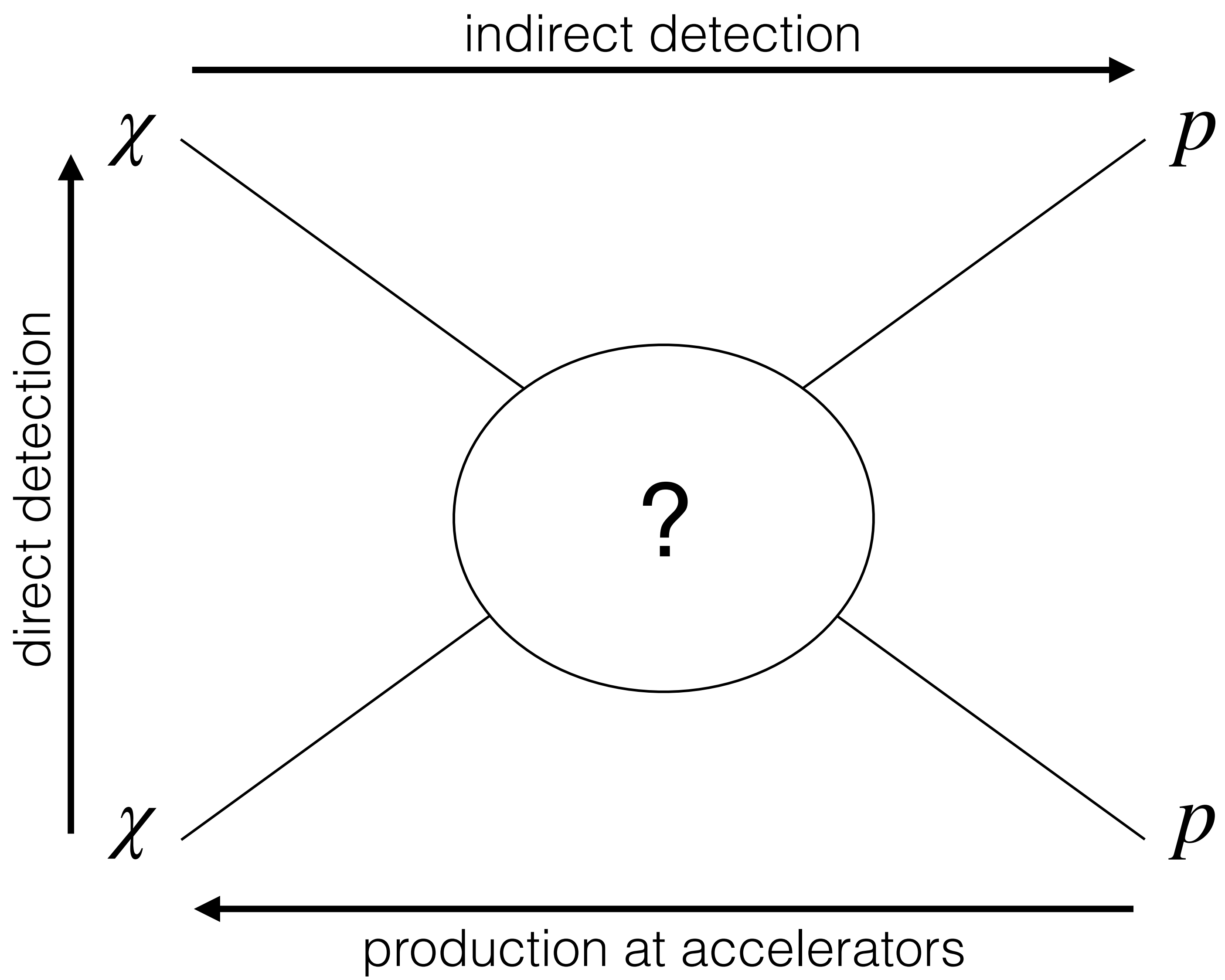

Detection techniques

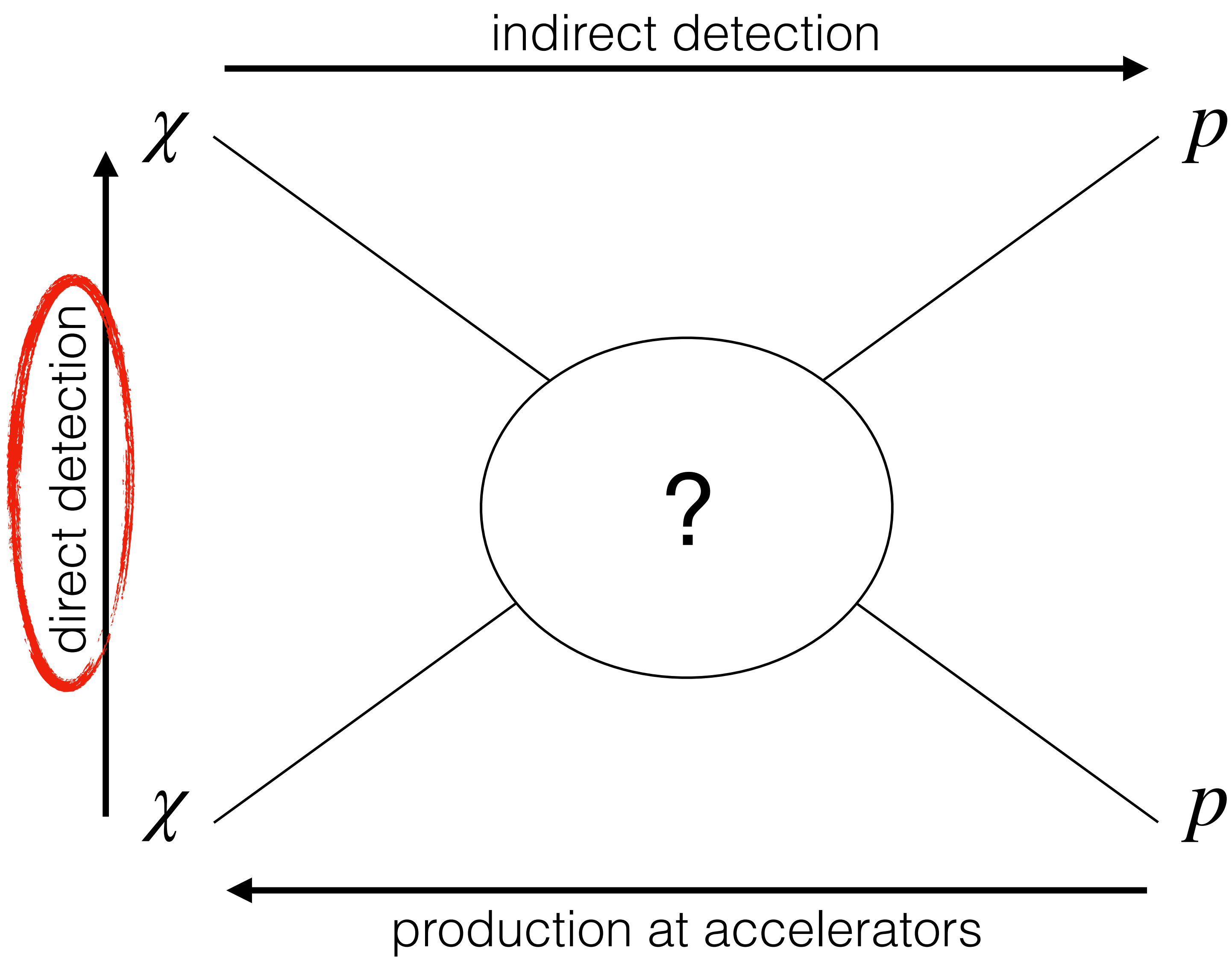

Generalities of
dark matter direct detection

Generalities of dark matter direct detection

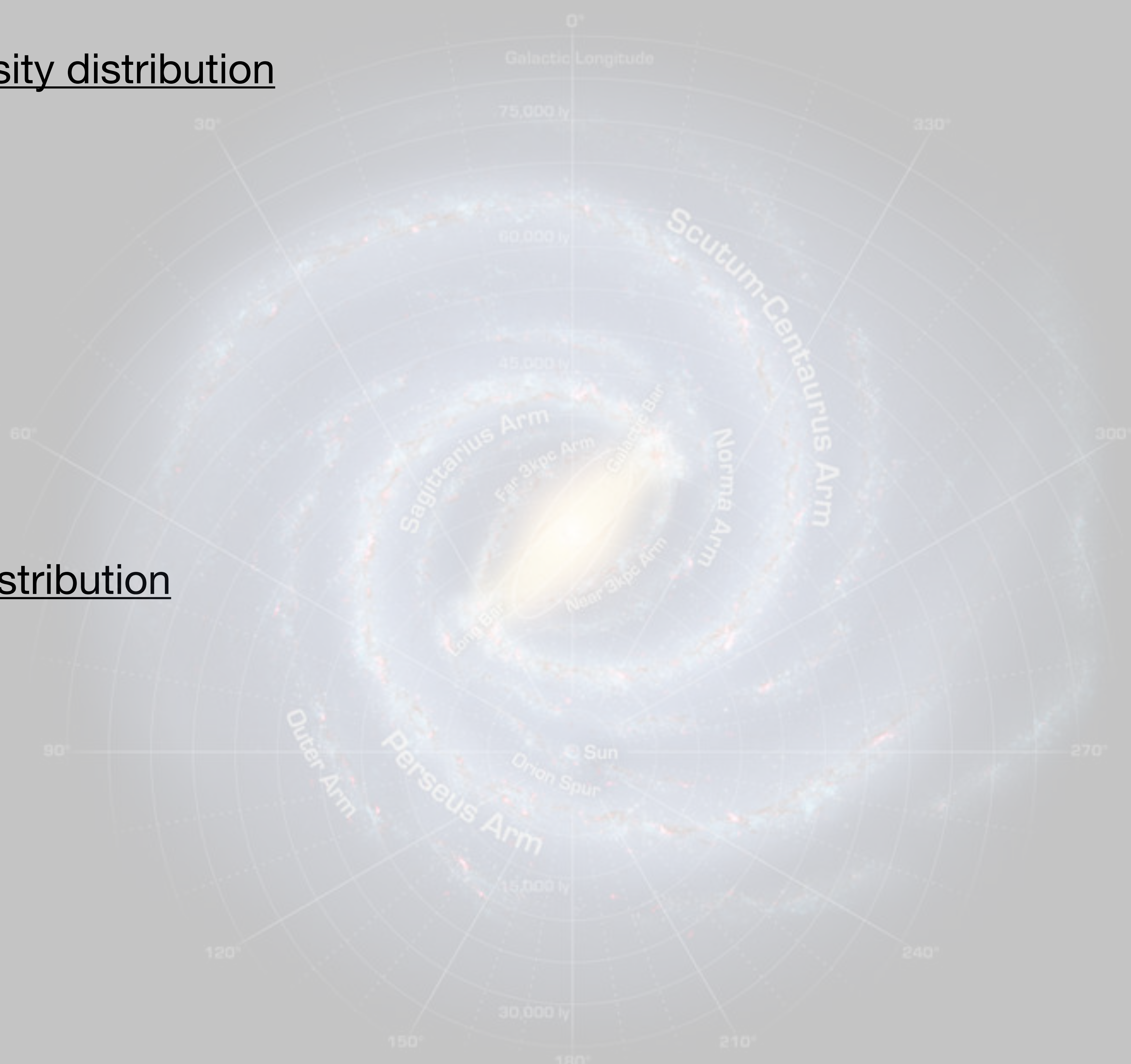

DM mass density distribution

DM velocity distribution

DM mass density distribution

The most accurate DM-halo mass density profile is the spherically symmetric Einasto profile

$$\rho(r) = \rho_{-2}\; exp\; \left\{ -\frac{2}{\alpha}\left[\left(\frac{r}{r_{-2}}\right)^{\alpha} - 1\right]\right\}$$

Jaan Einasto. *On the construction of a composite model for the galaxy and on the determination of the system of galactic parameters.* Trudy Astrozicheskogo Instituta Alma-Ata, 5:87-100, 1965.

Houjun Mo, Frank Van den Bosch, and Simon White. *Galaxy formation and evolution.* Galaxy formation and evolution. Cambridge University Press, 2010.

DM velocity distribution

Generalities of dark matter direct detection

DM mass density distribution

The most accurate DM-halo mass density profile is the spherically symmetric Einasto profile

$$\rho(r) = \rho_{-2}\ exp\ \left\{ -\frac{2}{\alpha}\left[\left(\frac{r}{r_{-2}}\right)^{\alpha} - 1\right]\right\}$$

Jaan Einasto. *On the construction of a composite model for the galaxy and on the determination of the system of galactic parameters.* Trudy Astrozicheskogo Instituta Alma-Ata, 5:87-100, 1965.

Houjun Mo, Frank Van den Bosch, and Simon White. *Galaxy formation and evolution.* Galaxy formation and evolution. Cambridge University Press, 2010.

DM velocity distribution

Simulations show that the **Maxwell-Boltzmann distribution function** is the most accurate velocity distribution in the Solar neighbourhood when also the role of baryons is included in the simulations

Nassim Bozorgnia and Gianfranco Bertone. *Implications of hydrodynamical simulations for the interpretation of direct dark matter searches*. Int. J. Mod. Phys., A32(21):1730016, 2017.

DM mass density distribution

The most accurate DM-halo mass density profile is the spherically symmetric Einasto profile

$$\rho(r) = \rho_{-2}\, exp\, \left\{ -\frac{2}{\alpha}\left[\left(\frac{r}{r_{-2}}\right)^{\alpha} - 1\right]\right\}$$

Jaan Einasto. *On the construction of a composite model for the galaxy and on the determination of the system of galactic parameters.* Trudy Astrozicheskogo Instituta Alma-Ata, 5:87-100, 1965.

Houjun Mo, Frank Van den Bosch, and Simon White. *Galaxy formation and evolution.* Galaxy formation and evolution. Cambridge University Press, 2010.

DM velocity distribution

Simulations show that the **Maxwell-Boltzmann distribution function** is the most accurate velocity distribution in the Solar neighbourhood when also the role of baryons is included in the simulations

Nassim Bozorgnia and Gianfranco Bertone. *Implications of hydrodynamical simulations for the interpretation of direct dark matter searches.* Int. J. Mod. Phys., A32(21):1730016, 2017.

DM is on average at rest in the galactic reference frame

$$|\mathbf{v}_{\chi}^{gal}| \approx 0$$

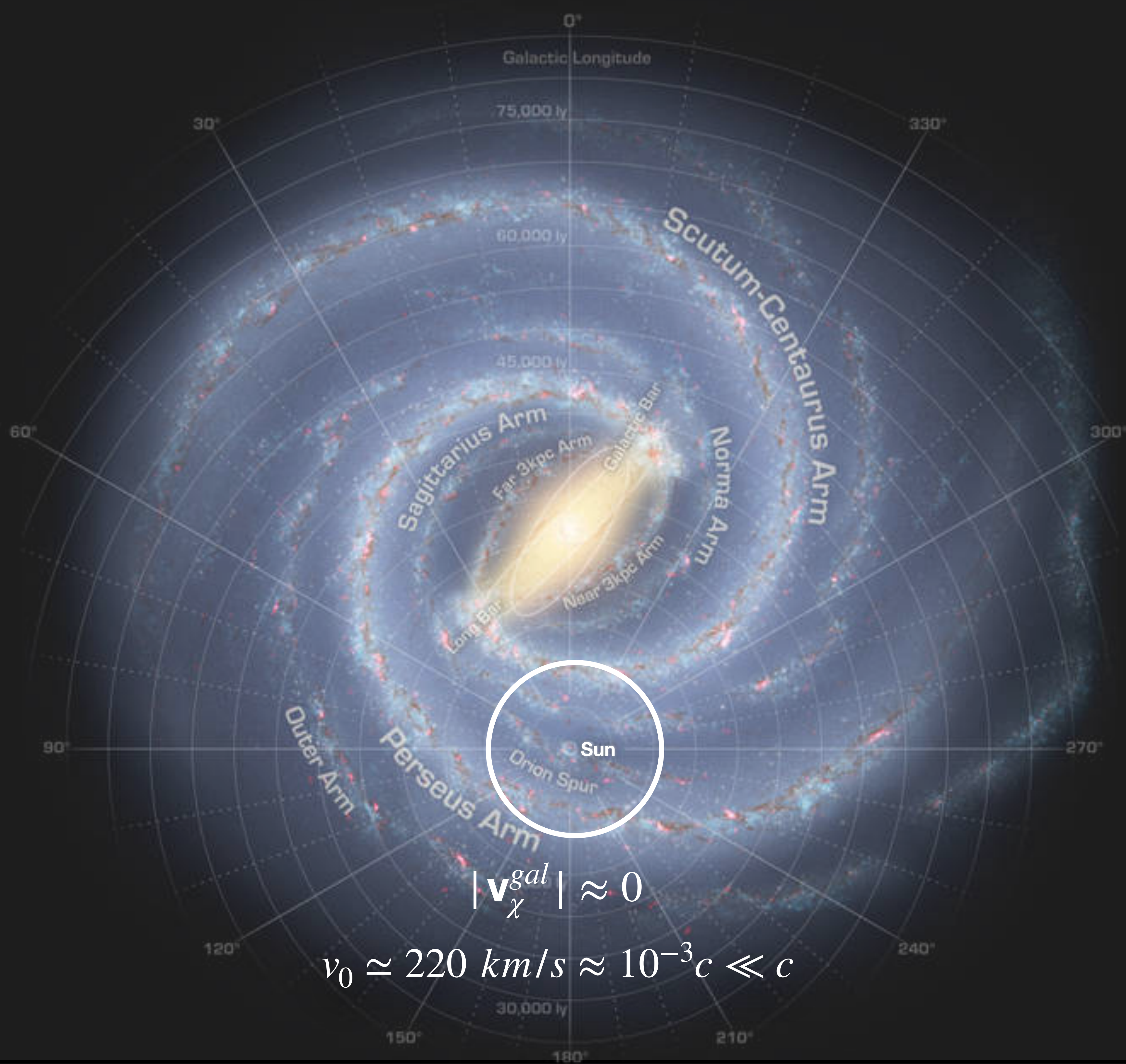

$$|\mathbf{v}_\chi^{gal}| \approx 0$$

$$v_0 \simeq 220\ km/s \approx 10^{-3}c \ll c$$

Generalities of dark matter direct detection

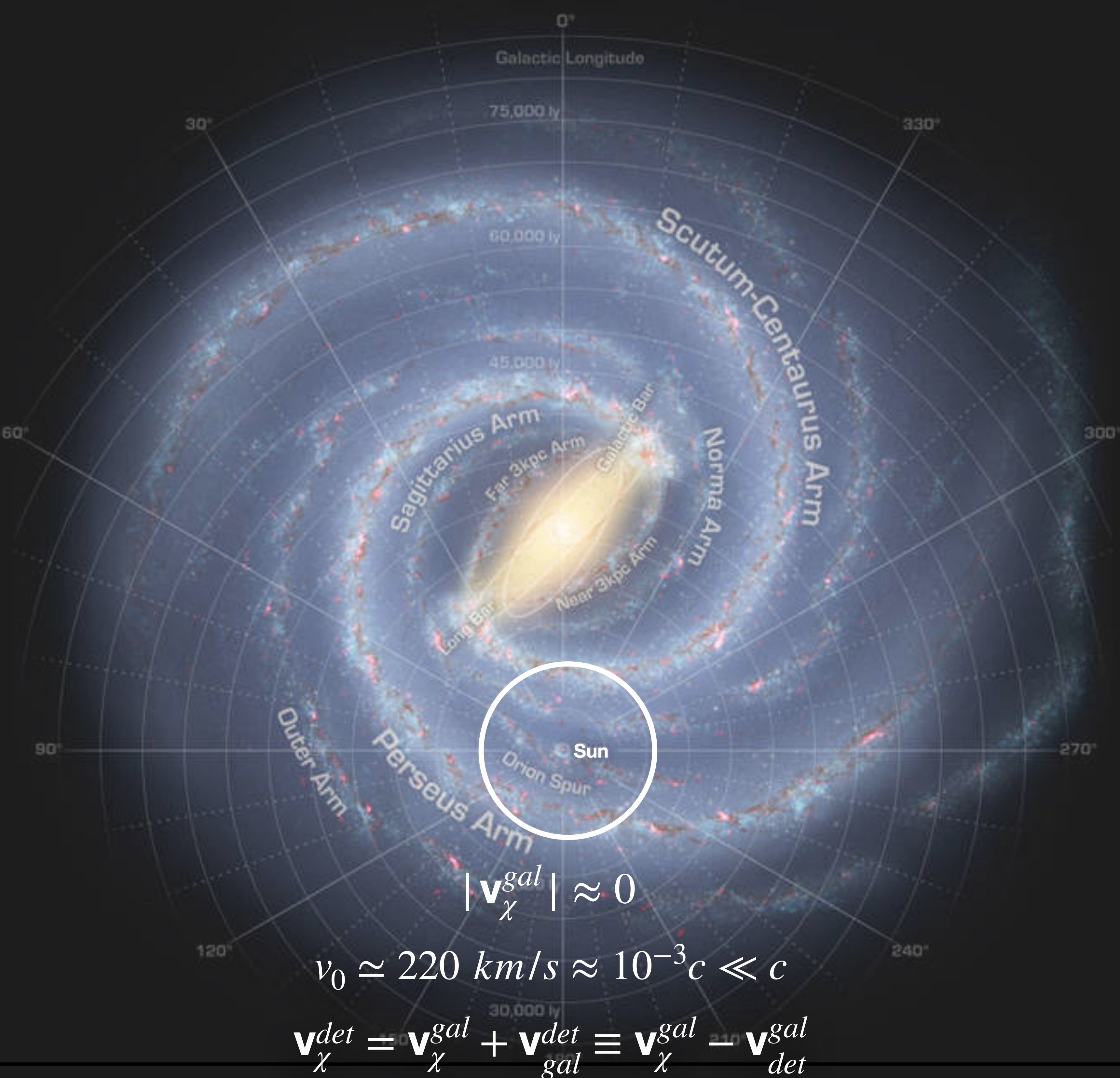

$$|\mathbf{v}_{\chi}^{gal}| \approx 0$$

$$v_0 \simeq 220\ km/s \approx 10^{-3}c \ll c$$

$$\mathbf{v}_{\chi}^{det} = \mathbf{v}_{\chi}^{gal} + \mathbf{v}_{gal}^{det} \equiv \mathbf{v}_{\chi}^{gal} - \mathbf{v}_{det}^{gal}$$

Generalities of dark matter direct detection

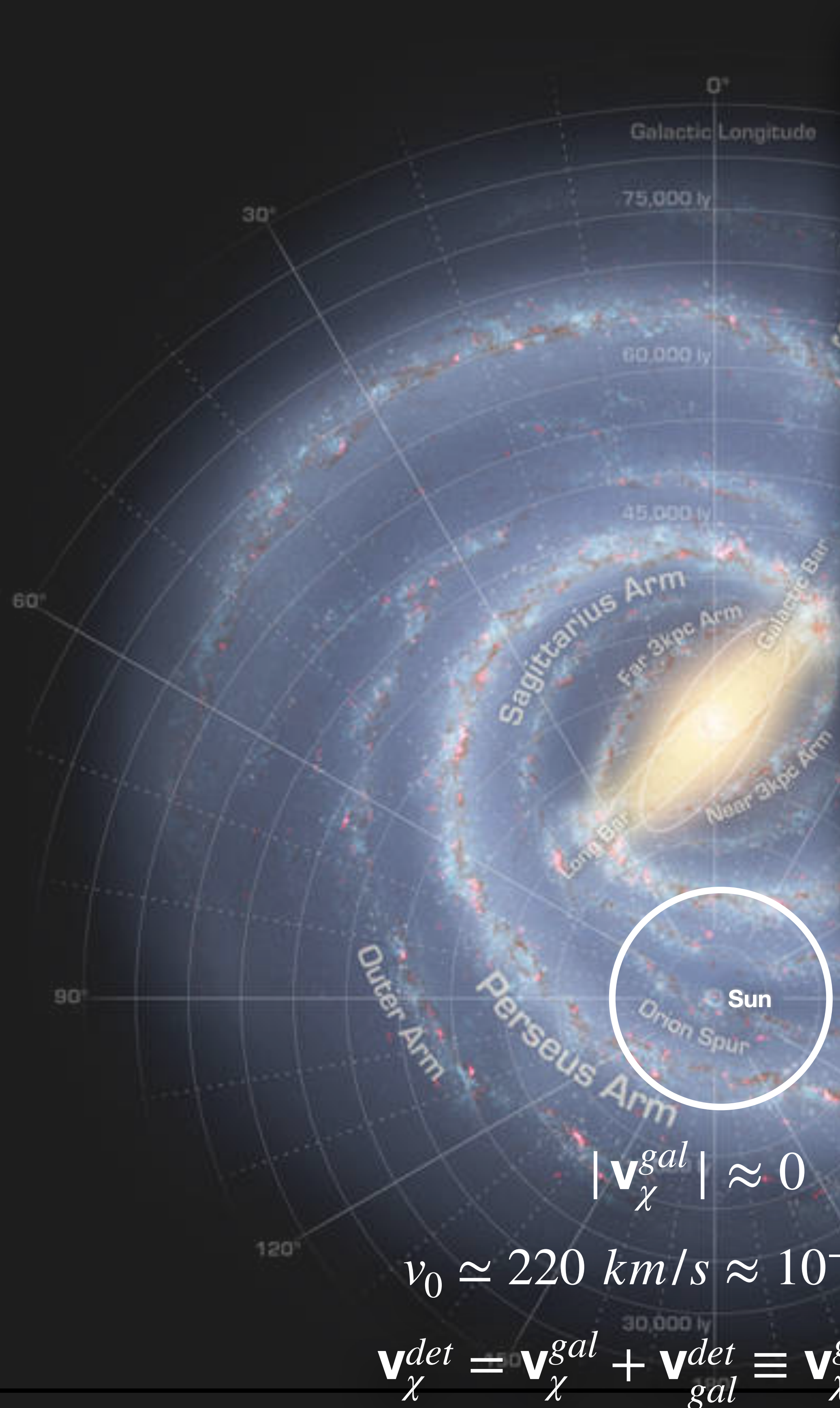

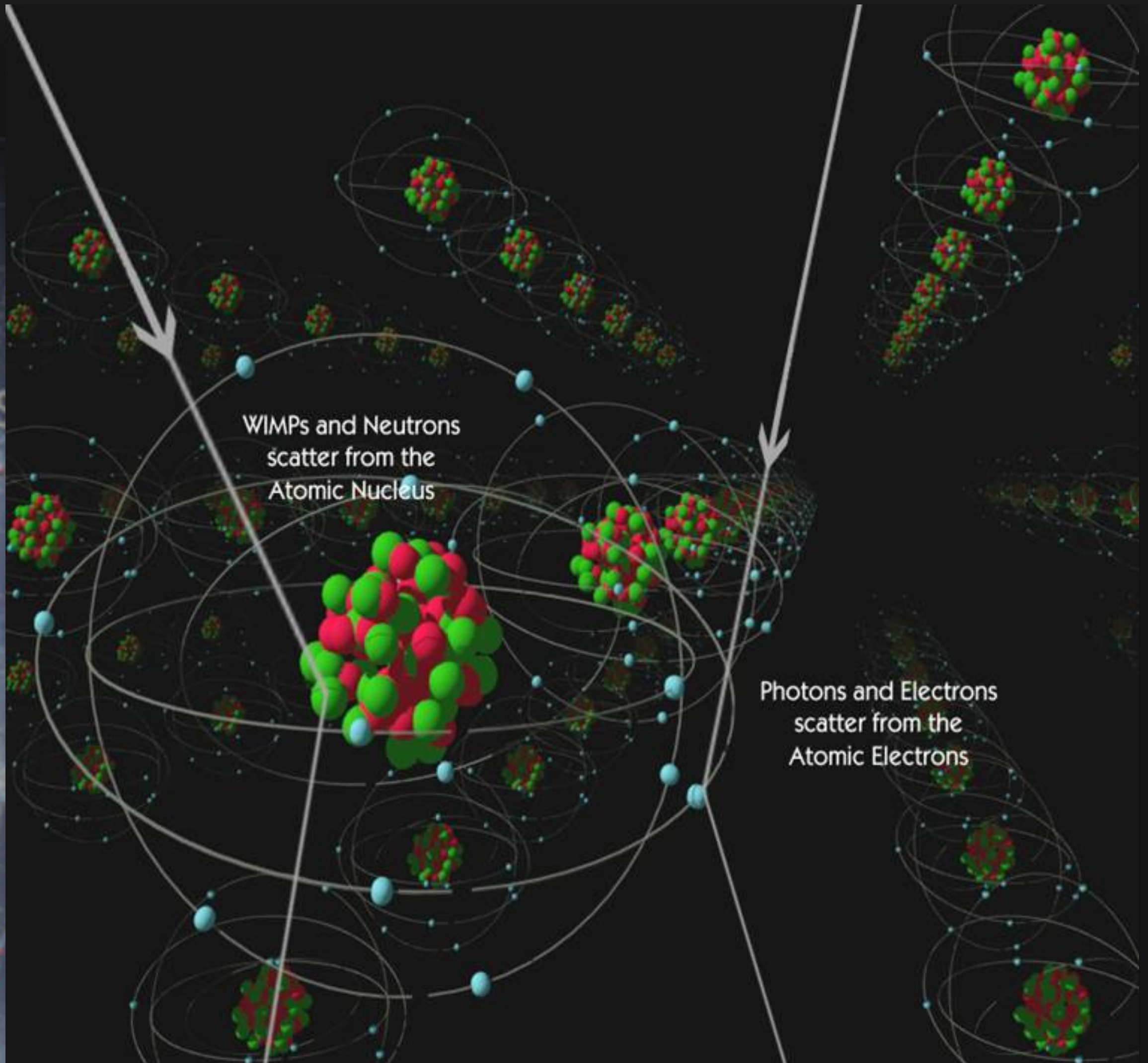

http://cdms.berkeley.edu/Education/DMpages/science/directDetection.shtml

$$|\mathbf{v}_\chi^{gal}| \approx 0$$

$$v_0 \simeq 220\ km/s \approx 10^{-3}c \ll c$$

$$\mathbf{v}_\chi^{det} = \mathbf{v}_\chi^{gal} + \mathbf{v}_{gal}^{det} \equiv \mathbf{v}_\chi^{gal} - \mathbf{v}_{det}^{gal}$$

G S
S I

Generalities of dark matter direct detection

Two observables:

1. Energy spectrum
2. Annually modulating energy spectrum

$$R = N_T \, \phi \, \sigma$$

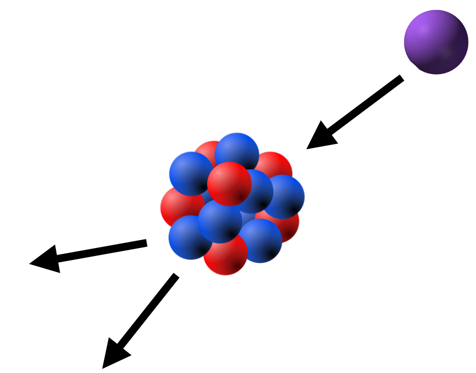

G S
S I

Generalities of dark matter direct detection

Two observables:

1. Energy spectrum
2. Annually modulating energy spectrum

$$R = N_T \, \phi \, \sigma$$

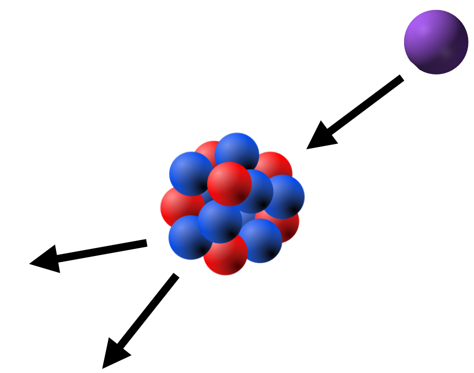

$$\frac{\mathrm{dR}}{\mathrm{dE_R}} = \frac{\rho_\chi}{m_\chi m_T} \int_{|\mathbf{v}_\chi^{det}|>v_{min}}^{|\mathbf{v}_\chi^{det}+\mathbf{v}_{det}^{gal}|<v_{esc}} d\mathbf{v}_\chi^{det} \, |\mathbf{v}_\chi^{det}| \, f(\mathbf{v}_\chi^{det} + \mathbf{v}_{det}^{gal}) \, \frac{\mathrm{d}\sigma}{\mathrm{dE_R}}(E_R, \mathbf{v}_\chi^{det})$$

G S
S I

Generalities of dark matter direct detection

Two observables:

1. Energy spectrum
2. Annually modulating energy spectrum

$$R = N_T \, \phi \, \sigma$$

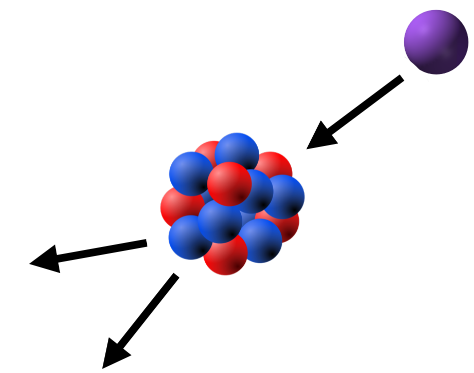

$$\frac{\mathrm{dR}}{\mathrm{dE_R}} = \frac{\rho_\chi}{m_\chi m_T} \int_{|\mathbf{v}_\chi^{det}|>v_{min}}^{|\mathbf{v}_\chi^{det}+\mathbf{v}_{det}^{gal}|<v_{esc}} d\mathbf{v}_\chi^{det} \, |\mathbf{v}_\chi^{det}| \, f(\mathbf{v}_\chi^{det} + \mathbf{v}_{det}^{gal}) \, \frac{\mathrm{d}\sigma}{\mathrm{dE_R}}(E_R, \mathbf{v}_\chi^{det})$$

Generalities of dark matter direct detection

Two observables:

1. Energy spectrum
2. Annually modulating energy spectrum

$$R = N_T \phi \sigma$$

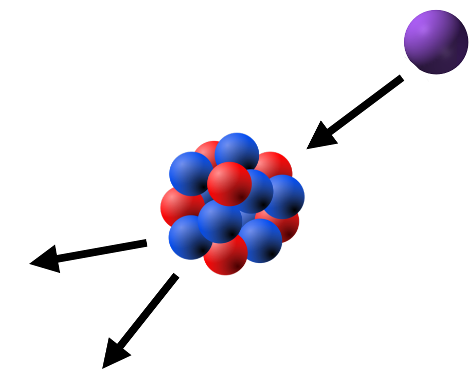

$$\frac{\mathrm{dR}}{\mathrm{dE_R}} = \frac{\rho_\chi}{m_\chi m_T}\int_{|\mathbf{v}_\chi^{det}|>v_{min}}^{|\mathbf{v}_\chi^{det}+\mathbf{v}_{det}^{gal}|<v_{esc}} d\mathbf{v}_\chi^{det}\,|\mathbf{v}_\chi^{det}|\,f(\mathbf{v}_\chi^{det}+\mathbf{v}_{det}^{gal})\,\frac{\mathrm{d}\sigma}{\mathrm{dE_R}}(E_R, \mathbf{v}_\chi^{det})$$

Generalities of dark matter direct detection

Two observables:

1. Energy spectrum
2. Annually modulating energy spectrum

$$R = N_T \phi \sigma$$

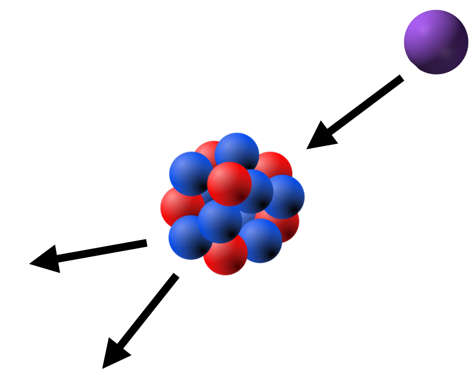

$$\frac{\mathrm{dR}}{\mathrm{dE_R}} = \frac{\rho_\chi}{m_\chi m_T} \int_{|\mathbf{v}_\chi^{det}|>v_{min}}^{|\mathbf{v}_\chi^{det}+\mathbf{v}_{det}^{gal}|<v_{esc}} d\mathbf{v}_\chi^{det}\, |\mathbf{v}_\chi^{det}|\, f(\mathbf{v}_\chi^{det} + \mathbf{v}_{det}^{gal}) \frac{\mathrm{d}\sigma}{\mathrm{dE_R}}(E_R, \mathbf{v}_\chi^{det})$$

Generalities of dark matter direct detection

Two observables:

1. Energy spectrum
2. Annually modulating energy spectrum

$$R = N_T \phi \sigma$$

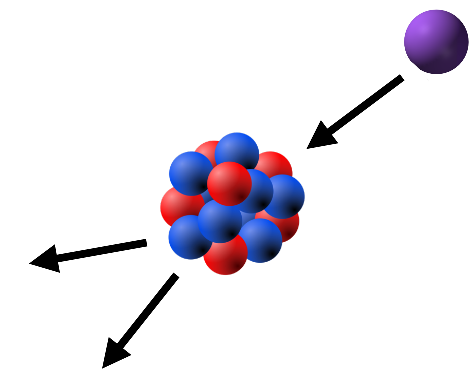

$$\frac{\mathrm{dR}}{\mathrm{dE_R}} = \frac{\rho_\chi}{m_\chi m_T} \int_{|\mathbf{v}_\chi^{det}|>v_{min}}^{|\mathbf{v}_\chi^{det}+\mathbf{v}_{det}^{gal}|<v_{esc}} d\mathbf{v}_\chi^{det} \, |\mathbf{v}_\chi^{det}| \, f(\mathbf{v}_\chi^{det} + \mathbf{v}_{det}^{gal}) \frac{\mathrm{d}\sigma}{\mathrm{dE_R}}(E_R, \mathbf{v}_\chi^{det})$$

$$f(\mathbf{v}_\chi^{gal}) \equiv f(\mathbf{v}_\chi^{det} - \mathbf{v}_{gal}^{det}) = \begin{cases} \frac{1}{N_{esc}} \left(\frac{1}{\pi v_0^2} \right)^{3/2} e^{-(\mathbf{v}_\chi^{det} - \mathbf{v}_{gal}^{det})^2 / v_0^2}, & for \ |\mathbf{v}_\chi^{det} - \mathbf{v}_{gal}^{det}| < v_{esc}^{gal} \\ 0, & otherwise \end{cases}$$

Samuel K. Lee, Mariangela Lisanti, and Benjamin R. Safdi. Dark-Matter Harmonics Beyond Annual Modulation. JCAP, 1311:033, 2013.

Truncated Standard Halo Model (SHM)

Generalities of dark matter direct detection

Two observables:

1. Energy spectrum
2. Annually modulating energy spectrum

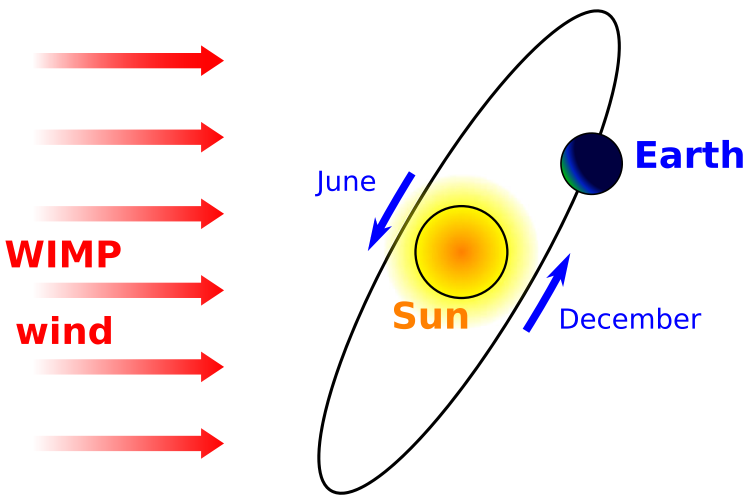

Two observables:

1. Energy spectrum
2. Annually modulating energy spectrum

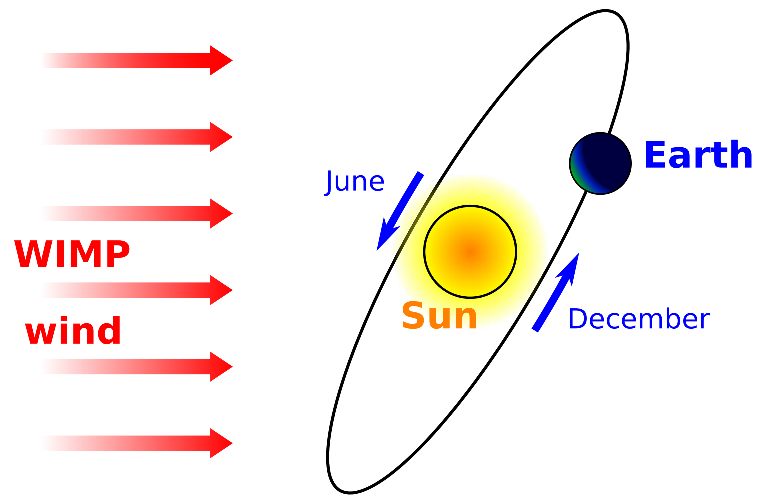

$$\mathbf{v}^{det}_{gal}(t) = \mathbf{v}^{\odot}_{gal} + \mathbf{v}^{det}_{\odot}(t) \longrightarrow f(\mathbf{v}^{gal}_{\chi}(t))$$ with period 1 year

Generalities of dark matter direct detection

Two observables:

1. Energy spectrum
2. Annually modulating energy spectrum

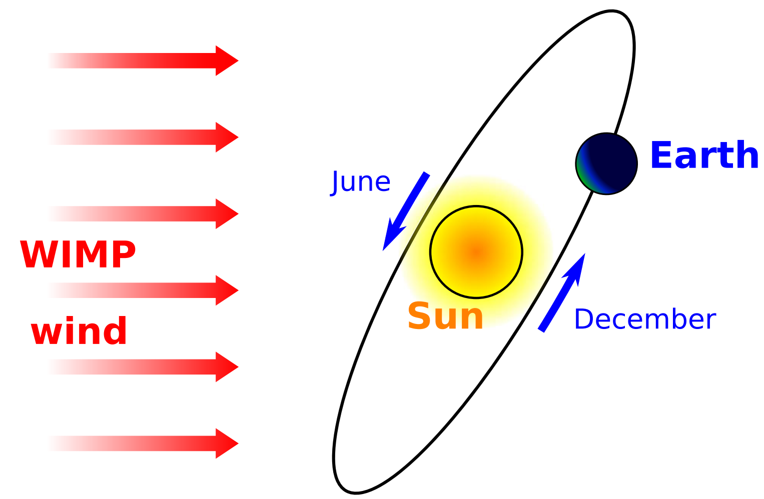

$$\mathbf{v}_{gal}^{det}(t) = \mathbf{v}_{gal}^{\odot} + \mathbf{v}_{\odot}^{det}(t) \longrightarrow f(\mathbf{v}_{\chi}^{gal}(t))$$ with period 1 year

$$\boxed{\frac{\mathrm{d}R(t)}{\mathrm{d}E_R} = A_0 + \sum_{n=1}^{\infty} A_n \cos n\omega(t-t_0) + \sum_{n=1}^{\infty} B_n \sin n\omega(t-t_0)}$$

Samuel K. Lee, Mariangela Lisanti, and Benjamin R. Safdi. Dark-Matter Harmonics Beyond Annual Modulation. JCAP, 1311:033, 2013.

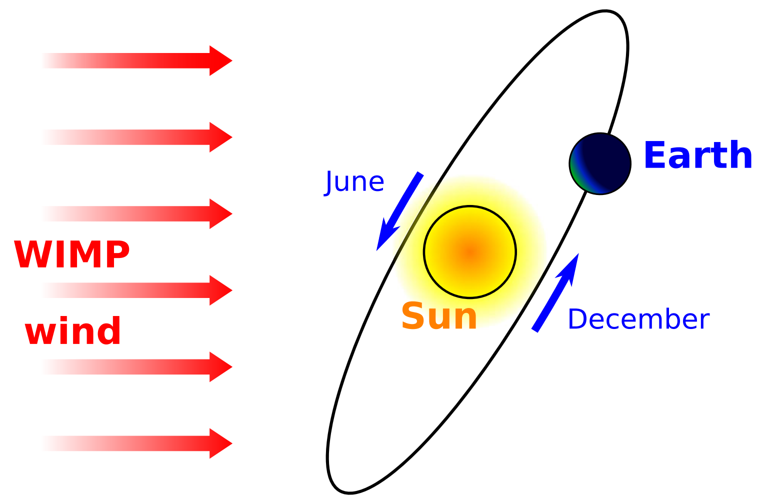

Two observables:

1. Energy spectrum
2. Annually modulating energy spectrum

$$\mathbf{v}_{gal}^{det}(t) = \mathbf{v}_{gal}^{\odot} + \mathbf{v}_{\odot}^{det}(t) \longrightarrow f(\mathbf{v}_{\chi}^{gal}(t))$$ with period 1 year

$$\boxed{\frac{\mathrm{d}R(t)}{\mathrm{d}E_R} = A_0 + \sum_{n=1}^{\infty} A_n \cos n\omega(t-t_0) + \sum_{n=1}^{\infty} B_n \sin n\omega(t-t_0)}$$

Samuel K. Lee, Mariangela Lisanti, and Benjamin R. Safdi. Dark-Matter Harmonics Beyond Annual Modulation. JCAP, 1311:033, 2013.

$$\boxed{\frac{\mathrm{d}R(t)}{\mathrm{d}E_R} \approx A_0 + A_1 \cos \omega(t-t_0)}$$

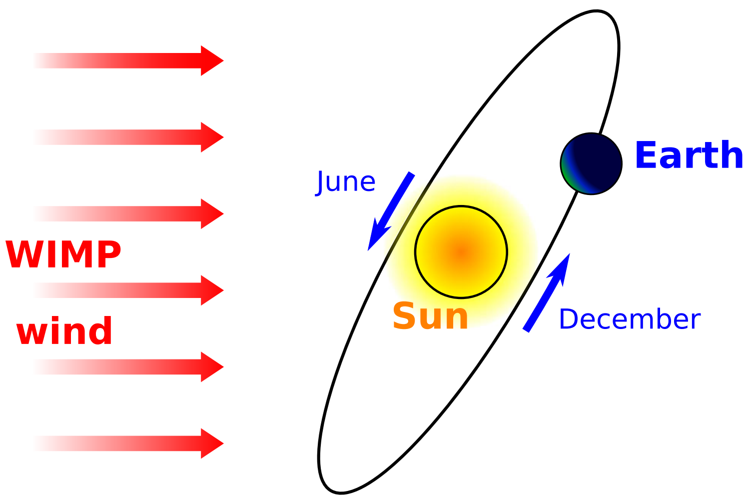

Two observables:

1. Energy spectrum
2. Annually modulating energy spectrum

$$\mathbf{v}_{gal}^{det}(t) = \mathbf{v}_{gal}^{\odot} + \mathbf{v}_{\odot}^{det}(t) \longrightarrow f(\mathbf{v}_{\chi}^{gal}(t))$$ with period 1 year

$$\boxed{\frac{\mathrm{d}R(t)}{\mathrm{d}E_R} = A_0 + \sum_{n=1}^{\infty} A_n \cos n\omega(t-t_0) + \sum_{n=1}^{\infty} B_n \sin n\omega(t-t_0)}$$

Samuel K. Lee, Mariangela Lisanti, and Benjamin R. Safdi. Dark-Matter Harmonics Beyond Annual Modulation. JCAP, 1311:033, 2013.

Halo anisotropy: gravitational focusing

G S
S I

Generalities of dark matter direct detection

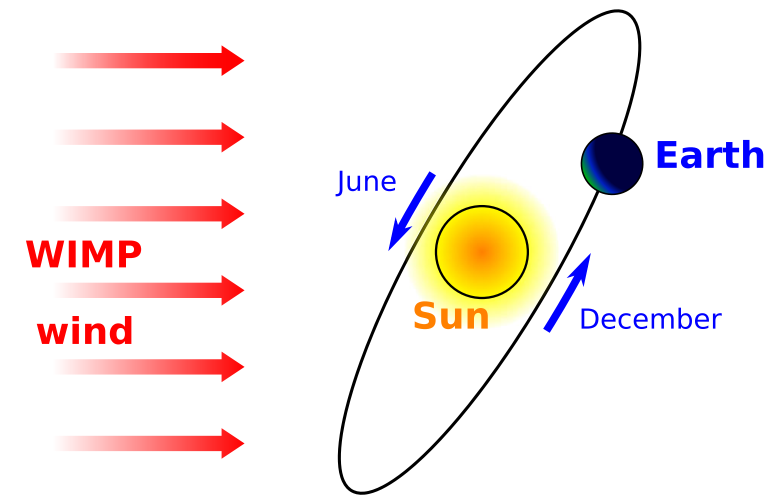

Two observables:

1. Energy spectrum
2. Annually modulating energy spectrum

$$\mathbf{v}^{det}_{gal}(t) = \mathbf{v}^{\odot}_{gal} + \mathbf{v}^{det}_{\odot}(t) \longrightarrow f(\mathbf{v}^{gal}_{\chi}(t)) \quad \text{with period 1 year}$$

$$\boxed{\frac{\mathrm{d}R(t)}{\mathrm{d}E_R} = A_0 + \sum_{n=1}^{\infty} A_n \cos n\omega(t-t_0) + \sum_{n=1}^{\infty} B_n \sin n\omega(t-t_0)}$$

Samuel K. Lee, Mariangela Lisanti, and Benjamin R. Safdi. Dark-Matter Harmonics Beyond Annual Modulation. JCAP, 1311:033, 2013.

Halo anisotropy: gravitational focusing

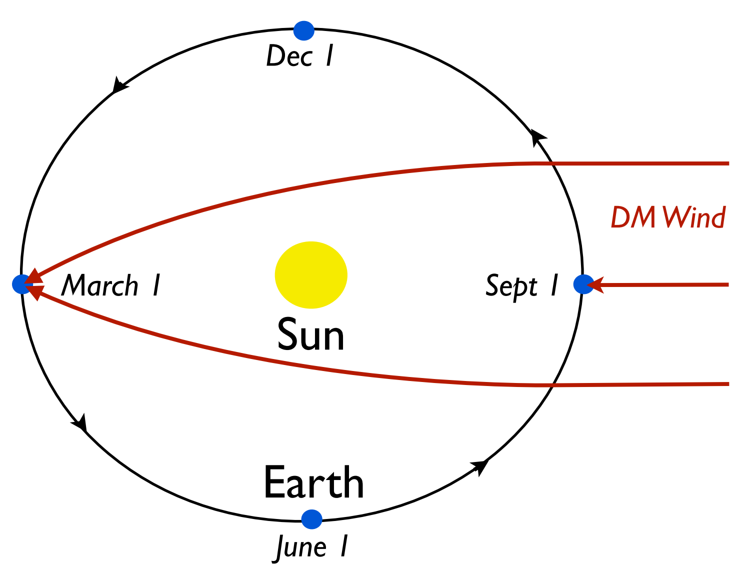

Two observables:

1. Energy spectrum
2. Annually modulating energy spectrum

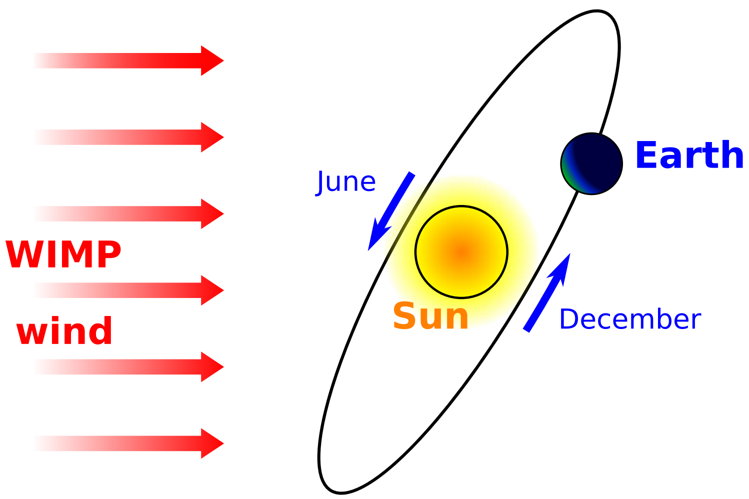

$$\mathbf{v}_{gal}^{det}(t) = \mathbf{v}_{gal}^{\odot} + \mathbf{v}_{\odot}^{det}(t) \longrightarrow f(\mathbf{v}_{\chi}^{gal}(t))$$ with period 1 year

$$\boxed{\frac{\mathrm{d}R(t)}{\mathrm{d}E_R} = A_0 + \sum_{n=1}^{\infty} A_n \cos n\omega(t-t_0) + \sum_{n=1}^{\infty} B_n \sin n\omega(t-t_0)}$$

Samuel K. Lee, Mariangela Lisanti, and Benjamin R. Safdi. Dark-Matter Harmonics Beyond Annual Modulation. JCAP, 1311:033, 2013.

Halo anisotropy: gravitational focusing

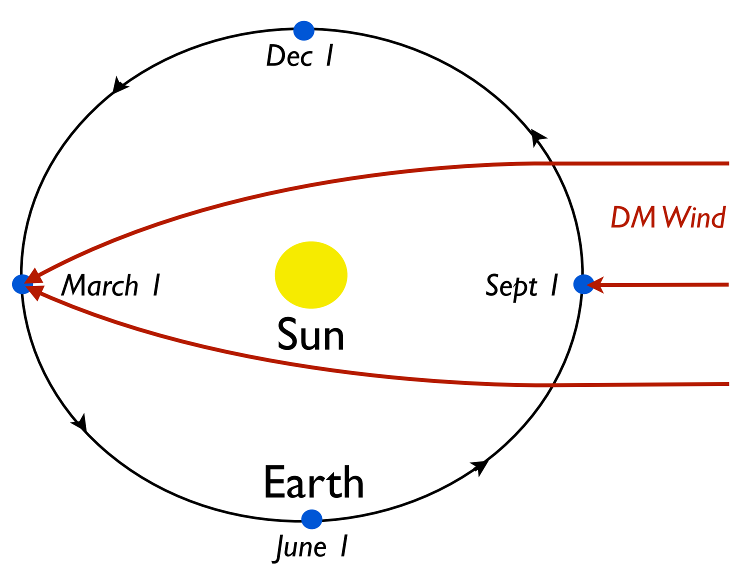

Time of the year of maximum differential rate

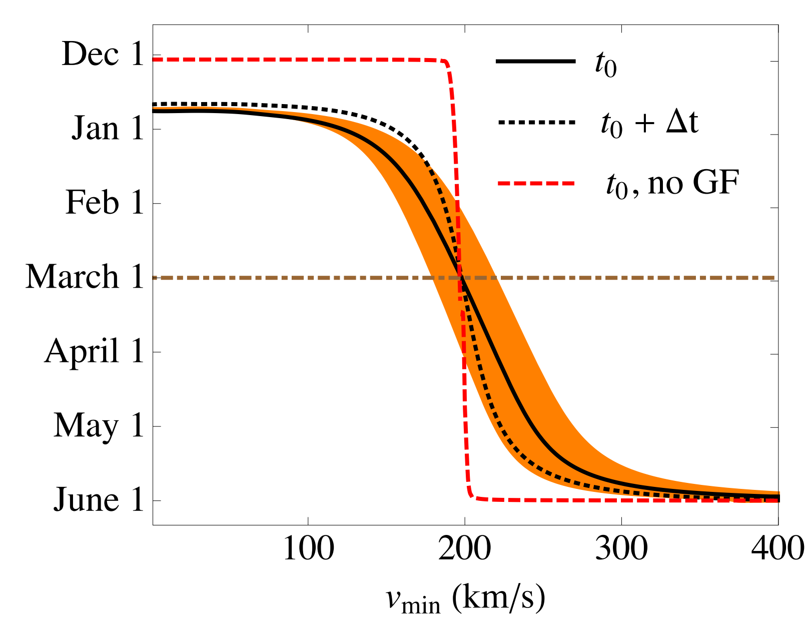

Samuel K. Lee, Mariangela Lisanti, Annika H. G. Peter, and Benjamin R. Safdi. Effect of Gravitational Focusing on Annual Modulation in Dark-Matter Direct-Detection Experiments. Phys. Rev. Lett., 112(1):011301, 2014.

$$\frac{\mathrm{d}\sigma}{\mathrm{d}E_R} \propto |\mathscr{M}_{NR}|^2$$

Generalities of dark matter direct detection

$$\frac{\mathrm{d}\sigma}{\mathrm{d}E_R} \propto |\mathscr{M}_{NR}|^2$$

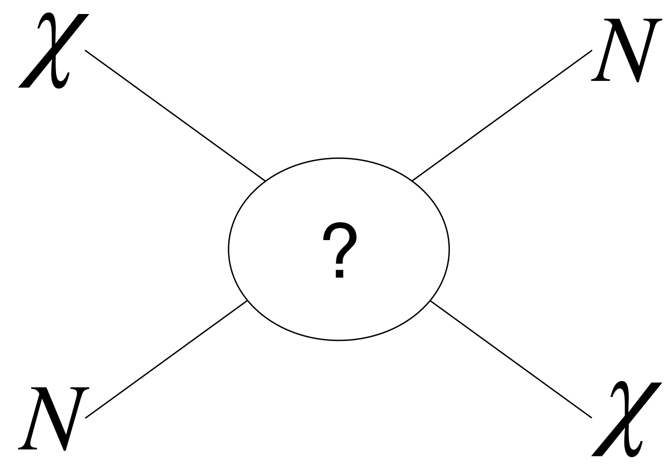

$$\frac{\mathrm{d}\sigma}{\mathrm{d}E_R} \propto |\mathscr{M}_{NR}|^2$$

Convention: spin independent (SI) and spin dependent (SD) interactions:

$$\mathcal{O}_{SI} = \bar{\chi}\chi\bar{N}\,N$$
$$\mathcal{O}_{SD} = \bar{\chi}\gamma^{\mu}\gamma^{5}\chi\bar{N}\gamma_{\mu}\gamma^{5}N$$

Generalities of dark matter direct detection

$$\frac{\mathrm{d}\sigma}{\mathrm{d}E_R} \propto |\mathscr{M}_{NR}|^2$$

Convention: spin independent (SI) and spin dependent (SD) interactions:

$$\mathcal{O}_{SI} = \bar{\chi}\chi\bar{N}\,N$$
$$\mathcal{O}_{SD} = \bar{\chi}\gamma^{\mu}\gamma^{5}\chi\bar{N}\gamma_{\mu}\gamma^{5}N$$

$\xrightarrow{\text{point like and NR approximation}}$

$$\left.\frac{\mathrm{d}\sigma_{SI}}{\mathrm{d}E_R}\right|_{q=0} = \frac{2\ m_T}{\pi v^2}\,[Z\,f_p + (A-Z)f_n]^2$$
$$\left.\frac{\mathrm{d}\sigma_{SD}}{\mathrm{d}E_R}\right|_{q=0} = 2\ m_T\frac{8G_F^2}{(2J_T+1)v^2}\,S_A(0)$$

G S S I

Generalities of dark matter direct detection

$$\frac{\mathrm{d}\sigma}{\mathrm{d}E_R} \propto |\mathscr{M}_{NR}|^2$$

Convention: spin independent (SI) and spin dependent (SD) interactions:

$$\mathcal{O}_{SI} = \bar{\chi}\chi\bar{N}\,N$$
$$\mathcal{O}_{SD} = \bar{\chi}\gamma^{\mu}\gamma^{5}\chi\bar{N}\gamma_{\mu}\gamma^{5}N$$

$\xrightarrow{\text{point like and NR approximation}}$

$$\left.\frac{\mathrm{d}\sigma_{SI}}{\mathrm{d}E_R}\right|_{q=0} = \frac{2\ m_T}{\pi v^2}\,[Z\,f_p + (A-Z)f_n]^2$$
$$\left.\frac{\mathrm{d}\sigma_{SD}}{\mathrm{d}E_R}\right|_{q=0} = 2\ m_T\frac{8G_F^2}{(2J_T+1)v^2}\,S_A(0)$$

If the nucleus cannot be considered as point like, nuclear *form factors* must be included

$$\frac{\mathrm{d}\sigma}{\mathrm{d}E_R} = \left.\frac{\mathrm{d}\sigma}{\mathrm{d}E_R}\right|_{q=0} \cdot F(q)$$

Conventionally, Helm form factor for SI interactions (see Lewin & Smith, 1996)
Axial structure function for SD interactions (see Engel, Pittel & Vogel, 1992)

Generalities of dark matter direct detection

https://supercdms.slac.stanford.edu/dark-matter-limit-plotter

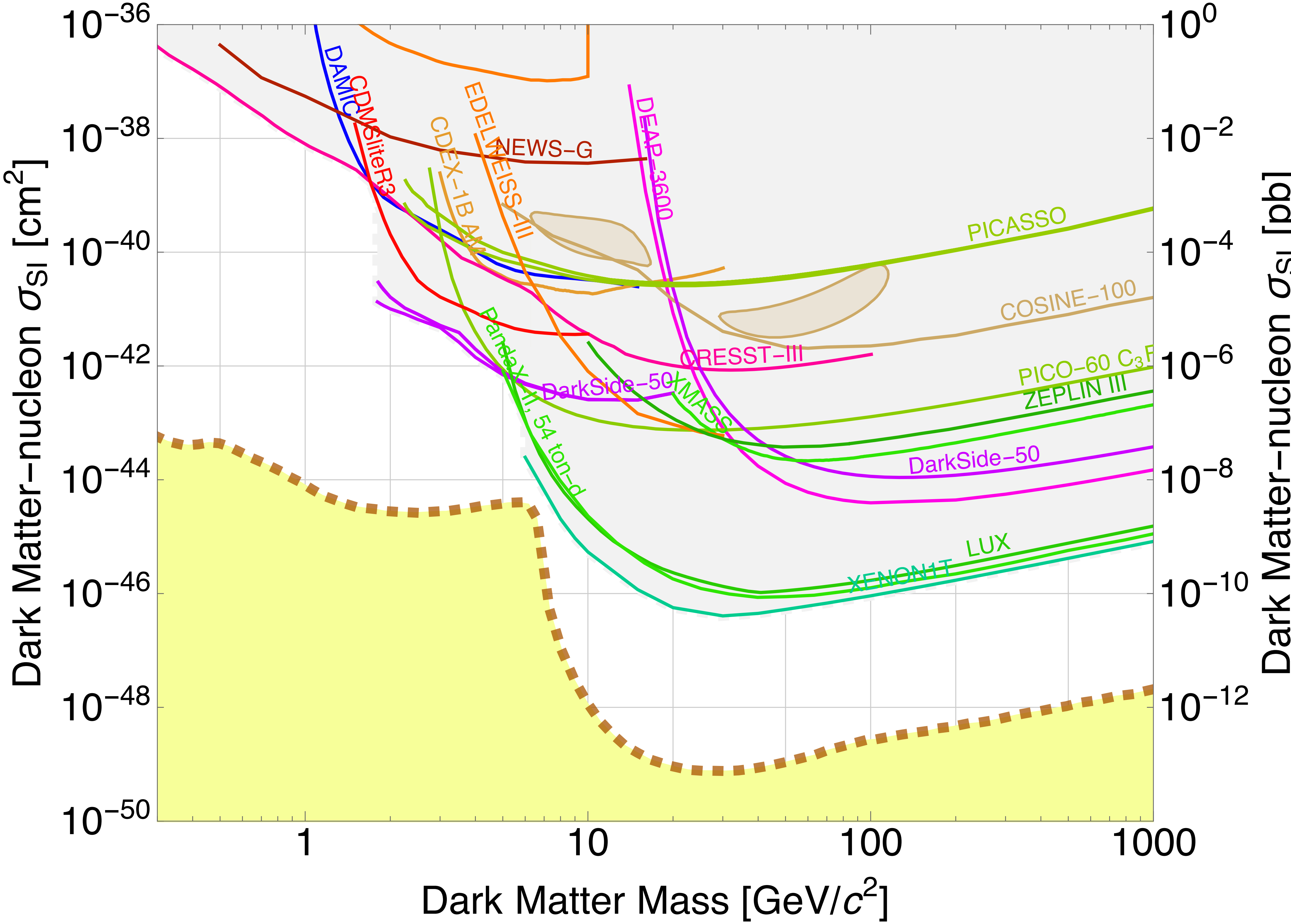

https://supercdms.slac.stanford.edu/dark-matter-limit-plotter

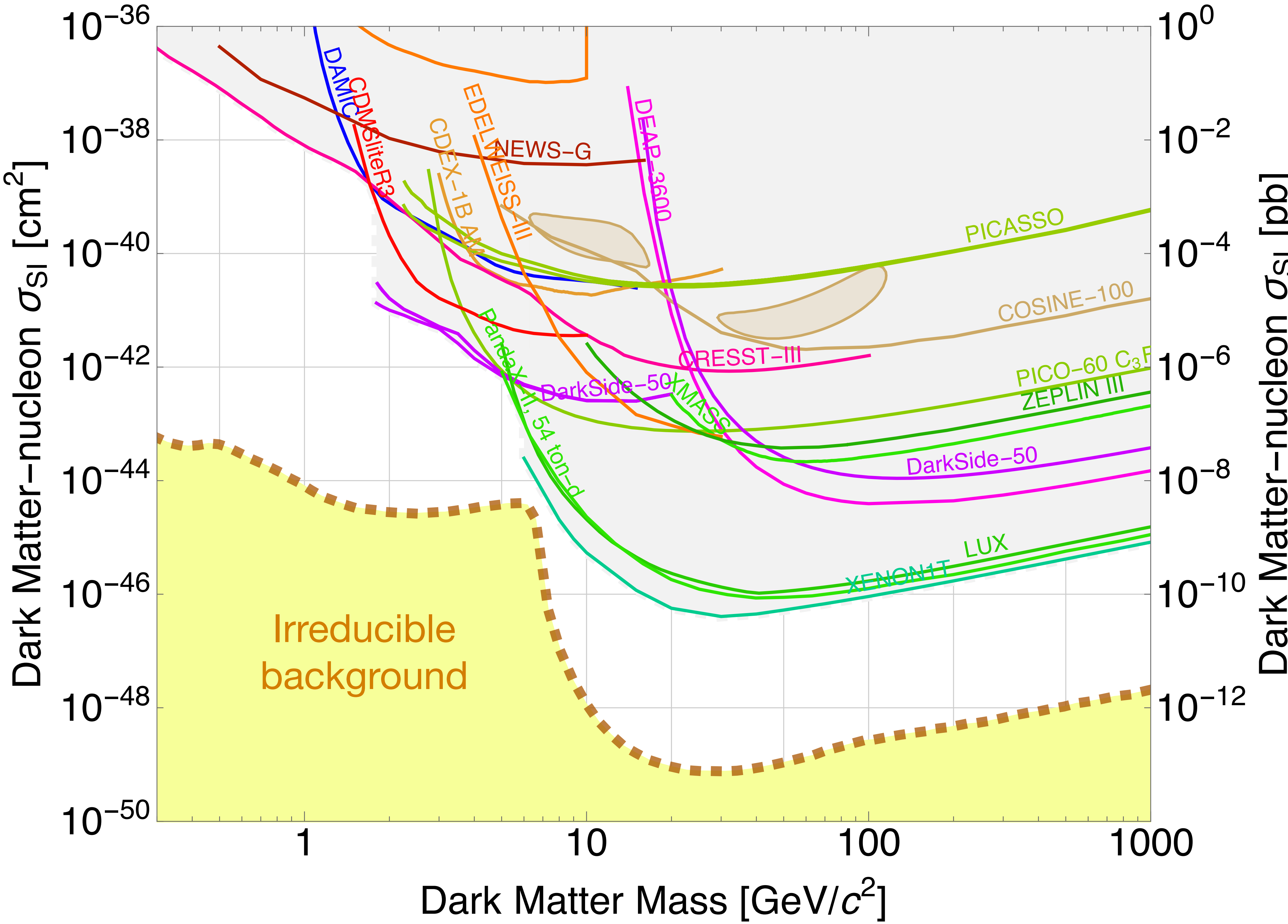

https://supercdms.slac.stanford.edu/dark-matter-limit-plotter

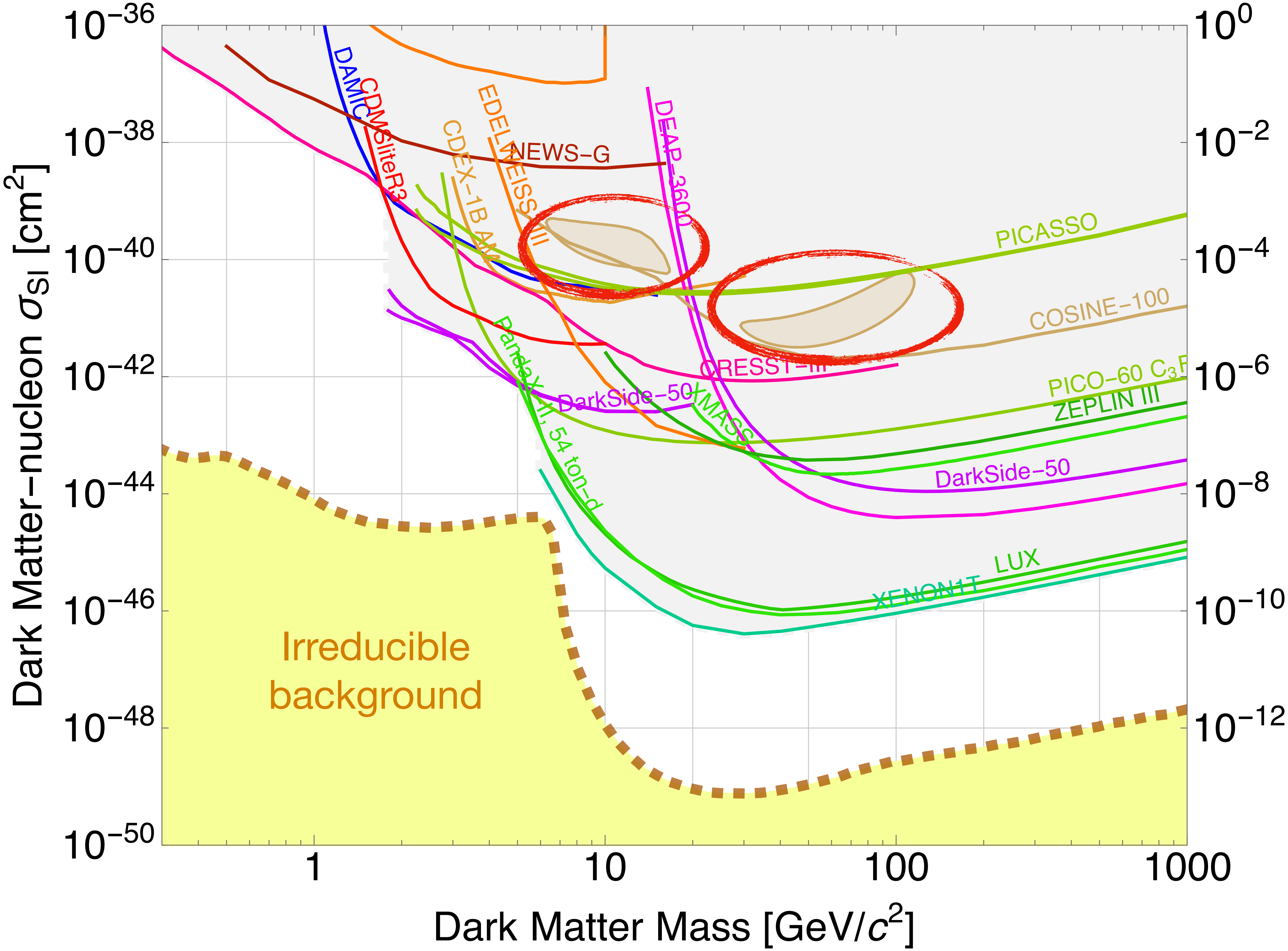

Generalities of dark matter direct detection

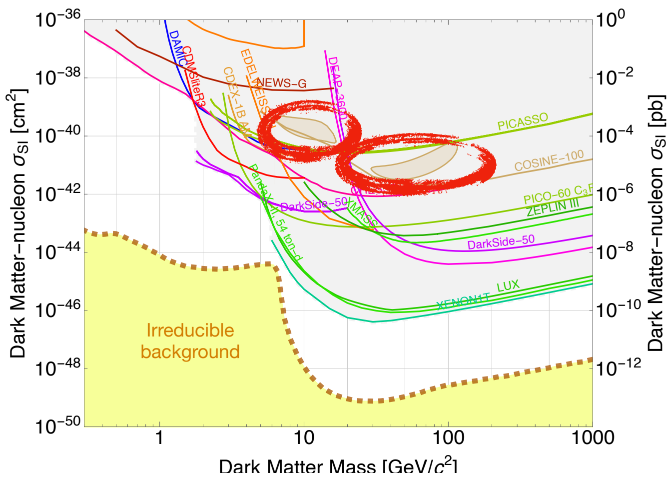

The case of DAMA/LIBRA

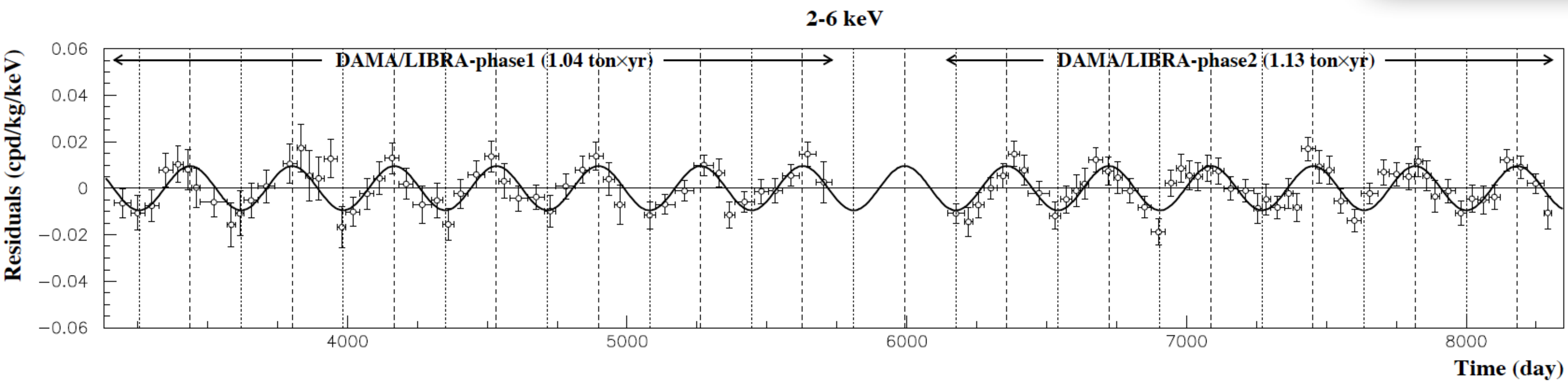

	Phase-I+Phase-II
Total exposure (ton $\times$ yr):	2.17
Statistical significance:	12.0σ
Period (yr):	0.9987 ± 0.0008
Phase (days):	145 ± 5
Amplitude ($[\text{day kg keV}]^{-1}$):	0.0096 ± 0.0008

R. Bernabei et al. *First Model Independent Results from DAMA/LIBRA-Phase2*. Universe, 4(11):116, 2018

G S S I

Generalities of dark matter direct detection

https://supercdms.slac.stanford.edu/dark-matter-limit-plotter

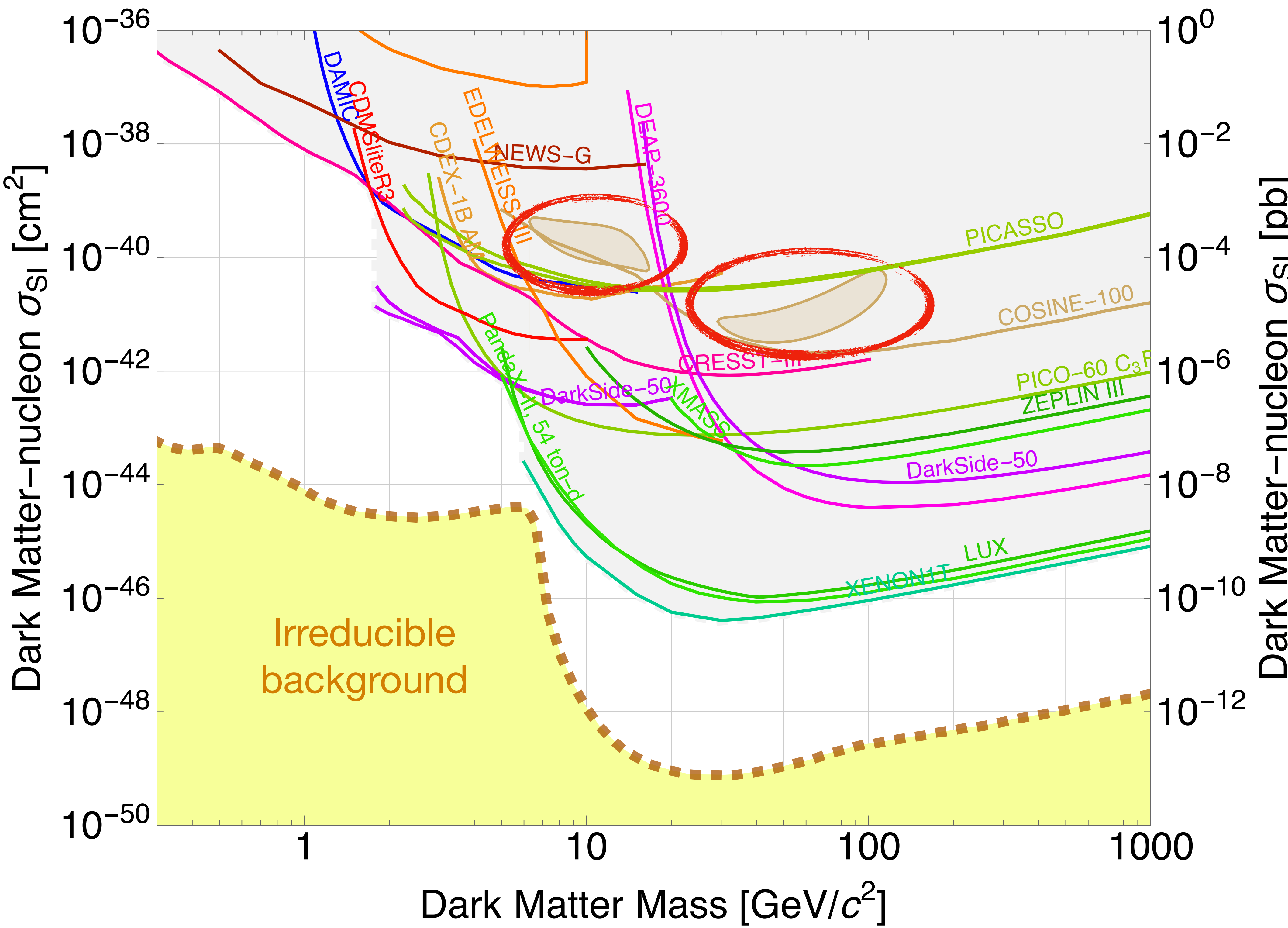

Dark matter direct detection effective field theory: two applications

G S
S I

Non-relativistic effective field theory (NREFT)

A. Liam Fitzpatrick, Wick Haxton, Emanuel Katz, Nicholas Lubbers, and Yiming Xu. *The Effective Field Theory of Dark Matter Direct Detection*. JCAP, 1302:004, 2013.

JiJi Fan, Matthew Reece, and Lian-Tao Wang. Non-relativistic effective theory of dark matter direct detection. JCAP, 11:042, 2010.

$$\frac{\mathrm{d}\sigma}{\mathrm{d}E_R} \propto |\mathscr{M}_{NR}|^2$$

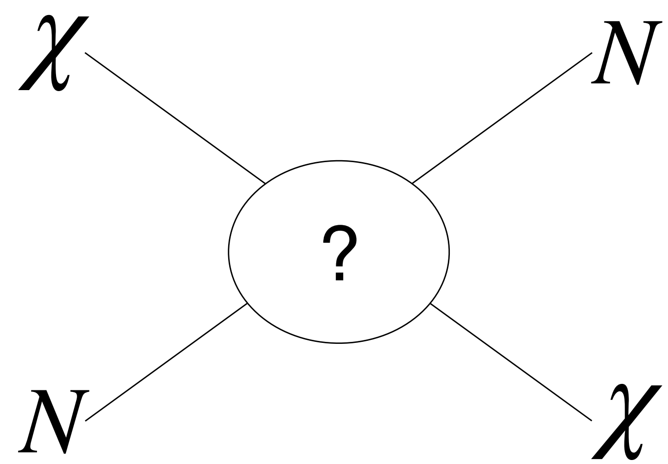

DM direct detection EFT: two applications

Non-relativistic effective field theory (NREFT)

A. Liam Fitzpatrick, Wick Haxton, Emanuel Katz, Nicholas Lubbers, and Yiming Xu. *The Effective Field Theory of Dark Matter Direct Detection*. JCAP, 1302:004, 2013.

JiJi Fan, Matthew Reece, and Lian-Tao Wang. Non-relativistic effective theory of dark matter direct detection. JCAP, 11:042, 2010.

$$\frac{\mathrm{d}\sigma}{\mathrm{d}E_R} \propto |\mathscr{M}_{NR}|^2$$

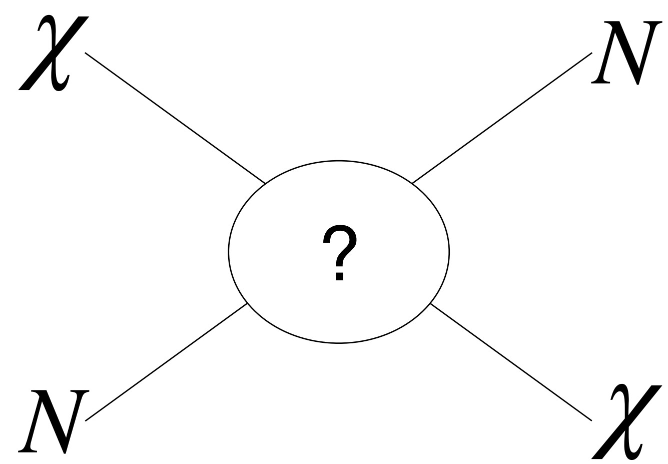

Non-relativistic effective field theory (NREFT)

A. Liam Fitzpatrick, Wick Haxton, Emanuel Katz, Nicholas Lubbers, and Yiming Xu. *The Effective Field Theory of Dark Matter Direct Detection*. JCAP, 1302:004, 2013.

JiJi Fan, Matthew Reece, and Lian-Tao Wang. Non-relativistic effective theory of dark matter direct detection. JCAP, 11:042, 2010.

$$\frac{\mathrm{d}\sigma}{\mathrm{d}E_R} \propto |\mathscr{M}_{NR}|^2$$

$$i\mathscr{M}_{NR} \propto \langle f | \int d^3\mathbf{r}\ \hat{\mathscr{H}}_T | i \rangle$$

G S
S I

Non-relativistic effective field theory (NREFT)

A. Liam Fitzpatrick, Wick Haxton, Emanuel Katz, Nicholas Lubbers, and Yiming Xu. *The Effective Field Theory of Dark Matter Direct Detection*. JCAP, 1302:004, 2013.

JiJi Fan, Matthew Reece, and Lian-Tao Wang. Non-relativistic effective theory of dark matter direct detection. JCAP, 11:042, 2010.

$$\frac{\mathrm{d}\sigma}{\mathrm{d}E_R} \propto |\mathscr{M}_{NR}|^2$$

$$i\mathscr{M}_{NR} \propto \langle f | \int d^3 \hat{\mathscr{H}}_T | \rangle$$

Non-relativistic effective field theory (NREFT)

A. Liam Fitzpatrick, Wick Haxton, Emanuel Katz, Nicholas Lubbers, and Yiming Xu. *The Effective Field Theory of Dark Matter Direct Detection*. JCAP, 1302:004, 2013.

JiJi Fan, Matthew Reece, and Lian-Tao Wang. Non-relativistic effective theory of dark matter direct detection. JCAP, 11:042, 2010.

$$\frac{\mathrm{d}\sigma}{\mathrm{d}E_R} \propto |\mathscr{M}_{NR}|^2$$

$$i\mathscr{M}_{NR} \propto \langle f | \int d^3 \hat{\mathscr{H}}_T | i \rangle$$

$$\hat{\mathscr{H}}_T = \sum_{k=1}^{A} \hat{\mathscr{H}}_k$$

GSSI

Non-relativistic effective field theory (NREFT)

A. Liam Fitzpatrick, Wick Haxton, Emanuel Katz, Nicholas Lubbers, and Yiming Xu. *The Effective Field Theory of Dark Matter Direct Detection*. JCAP, 1302:004, 2013.

JiJi Fan, Matthew Reece, and Lian-Tao Wang. Non-relativistic effective theory of dark matter direct detection. JCAP, 11:042, 2010.

$$\frac{\mathrm{d}\sigma}{\mathrm{d}E_R} \propto |\mathcal{M}_{NR}|^2$$

$$i\mathcal{M}_{NR} \propto \langle f | \int d^3\mathbf{r}\, \hat{\mathcal{H}}_T | i \rangle$$

$$\hat{\mathcal{H}}_T = \sum_{k=1}^{A} \hat{\mathcal{H}}_k$$

GSSI

Non-relativistic effective field theory (NREFT)

A. Liam Fitzpatrick, Wick Haxton, Emanuel Katz, Nicholas Lubbers, and Yiming Xu. *The Effective Field Theory of Dark Matter Direct Detection*. JCAP, 1302:004, 2013.

JiJi Fan, Matthew Reece, and Lian-Tao Wang. Non-relativistic effective theory of dark matter direct detection. JCAP, 11:042, 2010.

$$\frac{\mathrm{d}\sigma}{\mathrm{d}E_R} \propto |\mathscr{M}_{NR}|^2$$

$$i\mathscr{M}_{NR} \propto \langle f| \int d^3\mathbf{r}\, \hat{\mathscr{H}}_T |i\rangle$$

$$\hat{\mathscr{H}}_T = \sum_{k=1}^{A} \hat{\mathscr{H}}_k$$

$$\hat{\mathscr{H}}_k = 2\sum_i \left[c_i^p \left(\frac{1+\tau_3}{2}\right) + c_i^n \left(\frac{1-\tau_3}{2}\right)\right] f_{\hat{\mathscr{O}}_i}(q^2, v^{\perp 2})\hat{\mathscr{O}}_i$$

GS
SI

Non-relativistic effective field theory (NREFT)

A. Liam Fitzpatrick, Wick Haxton, Emanuel Katz, Nicholas Lubbers, and Yiming Xu. *The Effective Field Theory of Dark Matter Direct Detection*. JCAP, 1302:004, 2013.

JiJi Fan, Matthew Reece, and Lian-Tao Wang. Non-relativistic effective theory of dark matter direct detection. JCAP, 11:042, 2010.

$$\frac{\mathrm{d}\sigma}{\mathrm{d}E_R} \propto |\mathscr{M}_{NR}|^2$$

$$i\mathscr{M}_{NR} \propto \langle f | \int d^3\mathbf{r}\, \hat{\mathscr{H}}_T | i \rangle$$

$$\hat{\mathscr{H}}_T = \sum_{k=1}^{A} \hat{\mathscr{H}}_k$$

$$\hat{\mathscr{H}}_k = 2\sum_i \left[c_i^p \left(\frac{1+\tau_3}{2} \right) + c_i^n \left(\frac{1-\tau_3}{2} \right) \right] f_{\hat{\mathcal{O}}_i}(q^2, v^{\perp 2}) \hat{\mathcal{O}}_i$$

GSSI

Non-relativistic effective field theory (NREFT)

A. Liam Fitzpatrick, Wick Haxton, Emanuel Katz, Nicholas Lubbers, and Yiming Xu. *The Effective Field Theory of Dark Matter Direct Detection*. JCAP, 1302:004, 2013.

JiJi Fan, Matthew Reece, and Lian-Tao Wang. Non-relativistic effective theory of dark matter direct detection. JCAP, 11:042, 2010.

$$\frac{\mathrm{d}\sigma}{\mathrm{d}E_R} \propto |\mathcal{M}_{NR}|^2$$

$$i\mathcal{M}_{NR} \propto \langle f| \int d^3\mathbf{r}\, \hat{\mathcal{H}}_T |i\rangle$$

$$\hat{\mathcal{H}}_T = \sum_{k=1}^{A} \hat{\mathcal{H}}_k$$

$$\hat{\mathcal{H}}_k = 2\sum_i \left[c_i^p\left(\frac{1+\tau_3}{2}\right) + c_i^n\left(\frac{1-\tau_3}{2}\right)\right] f_{\hat{\mathcal{O}}_i}(q^2, v^{\perp 2})\hat{\mathcal{O}}_i$$

$$1 \quad iq \quad v^{\perp} \quad S_\chi \quad S_N$$

Non-relativistic effective field theory (NREFT)

A. Liam Fitzpatrick, Wick Haxton, Emanuel Katz, Nicholas Lubbers, and Yiming Xu. *The Effective Field Theory of Dark Matter Direct Detection*. JCAP, 1302:004, 2013.

JiJi Fan, Matthew Reece, and Lian-Tao Wang. Non-relativistic effective theory of dark matter direct detection. JCAP, 11:042, 2010.

$$\frac{\mathrm{d}\sigma}{\mathrm{d}E_R} \propto |\mathscr{M}_{NR}|^2$$

$$i\mathscr{M}_{NR} \propto \langle f | \int d^3\mathbf{r}\, \hat{\mathscr{H}}_T | i \rangle$$

$$\hat{\mathscr{H}}_T = \sum_{k=1}^{A} \hat{\mathscr{H}}_k$$

$$\hat{\mathscr{H}}_k = 2\sum_i \left[c_i^p \left(\frac{1+\tau_3}{2}\right) + c_i^n \left(\frac{1-\tau_3}{2}\right)\right] f_{\hat{\mathcal{O}}_i}(q^2, v^{\perp 2}) \hat{\mathcal{O}}_i$$

$$1 \quad iq \quad v^{\perp} \quad S_\chi \quad S_N$$

$$\mathcal{O}_{SI} = \bar{\chi}\chi\bar{N}N$$

$$\mathcal{O}_{SD} = \bar{\chi}\gamma^\mu\gamma^5\chi\bar{N}\gamma_\mu\gamma^5 N$$

G S
S I

Non-relativistic effective field theory (NREFT)

A. Liam Fitzpatrick, Wick Haxton, Emanuel Katz, Nicholas Lubbers, and Yiming Xu. *The Effective Field Theory of Dark Matter Direct Detection*. JCAP, 1302:004, 2013.

JiJi Fan, Matthew Reece, and Lian-Tao Wang. Non-relativistic effective theory of dark matter direct detection. JCAP, 11:042, 2010.

$$\frac{\mathrm{d}\sigma}{\mathrm{d}E_R} \propto |\mathscr{M}_{NR}|^2$$

$$i\mathscr{M}_{NR} \propto \langle f | \int d^3\mathbf{r}\, \hat{\mathscr{H}}_T | i \rangle$$

$$\hat{\mathscr{H}}_T = \sum_{k=1}^{A} \hat{\mathscr{H}}_k$$

$$\hat{\mathscr{H}}_k = 2\sum_i \left[c_i^p \left(\frac{1+\tau_3}{2}\right) + c_i^n \left(\frac{1-\tau_3}{2}\right)\right] f_{\hat{\mathscr{O}}_i}(q^2, v^{\perp 2}) \hat{\mathscr{O}}_i$$

$$1 \quad iq \quad v^{\perp} \quad S_\chi \quad S_N$$

$$\mathscr{O}_{SI} = \bar{\chi}\chi\bar{N}N \qquad \mathscr{O}_1 = 1_\chi\, 1_N$$

NR reduction $\longrightarrow$

$$\mathscr{O}_{SD} = \bar{\chi}\gamma^\mu\gamma^5\chi\bar{N}\gamma_\mu\gamma^5 N \qquad \mathscr{O}_4 = S_\chi \cdot S_N$$

G S
S I

DM direct detection EFT: two applications

Non-relativistic effective field theory (NREFT)

A. Liam Fitzpatrick, Wick Haxton, Emanuel Katz, Nicholas Lubbers, and Yiming Xu. *The Effective Field Theory of Dark Matter Direct Detection*. JCAP, 1302:004, 2013.

JiJi Fan, Matthew Reece, and Lian-Tao Wang. Non-relativistic effective theory of dark matter direct detection. JCAP, 11:042, 2010.

NREFT application, limitations and subsequent developments

Non-relativistic effective field theory (NREFT)

A. Liam Fitzpatrick, Wick Haxton, Emanuel Katz, Nicholas Lubbers, and Yiming Xu. *The Effective Field Theory of Dark Matter Direct Detection*. JCAP, 1302:004, 2013.

JiJi Fan, Matthew Reece, and Lian-Tao Wang. Non-relativistic effective theory of dark matter direct detection. JCAP, 11:042, 2010.

NREFT application, limitations and subsequent developments

1. The exclusion of light mesons from the theory, motivated by $q \lesssim 200\ MeV$

Non-relativistic effective field theory (NREFT)

A. Liam Fitzpatrick, Wick Haxton, Emanuel Katz, Nicholas Lubbers, and Yiming Xu. *The Effective Field Theory of Dark Matter Direct Detection*. JCAP, 1302:004, 2013.

JiJi Fan, Matthew Reece, and Lian-Tao Wang. Non-relativistic effective theory of dark matter direct detection. JCAP, 11:042, 2010.

NREFT application, limitations and subsequent developments

1. The exclusion of light mesons from the theory, motivated by $q \lesssim 200\ MeV$

2. The use of the shell model for the calculation of the nuclear structure functions

Non-relativistic effective field theory (NREFT)

A. Liam Fitzpatrick, Wick Haxton, Emanuel Katz, Nicholas Lubbers, and Yiming Xu. *The Effective Field Theory of Dark Matter Direct Detection*. JCAP, 1302:004, 2013.

JiJi Fan, Matthew Reece, and Lian-Tao Wang. Non-relativistic effective theory of dark matter direct detection. JCAP, 11:042, 2010.

NREFT application, limitations and subsequent developments

1. The exclusion of light mesons from the theory, motivated by $q \lesssim 200\ MeV$

2. The use of the shell model for the calculation of the nuclear structure functions

3. From the application point of view, the tendency to use single building blocks to derive experimental constraints or phenomenological conclusions, neglecting the matching with the UV-energy-scale.

First application

Annual modulation in NREFT

DM direct detection EFT: two applications

1. Annual modulation in NREFT

Motivations

1. Annual modulation depends on DM interactions

2. Non-standard EFT interactions fit better the latest DAMA results

- Sebastian Baum, Katherine Freese, and Chris Kelso. Dark Matter implications of DAMA/LIBRA-phase2 results. Phys. Lett. B, 789:262{269, 2019

- Sunghyun Kang, Stefano Scopel, Gaurav Tomar, and Jong-Hyun Yoon. DAMA/LIBRA-phase2 in WIMP effective models. JCAP, 1807(07):016, 2018

DM direct detection EFT: two applications

1. Annual modulation in NREFT

Motivations

1. Annual modulation depends on DM interactions

2. Non-standard EFT interactions fit better the latest DAMA results

- Sebastian Baum, Katherine Freese, and Chris Kelso. Dark Matter implications of DAMA/LIBRA-phase2 results. Phys. Lett. B, 789:262{269, 2019

- Sunghyun Kang, Stefano Scopel, Gaurav Tomar, and Jong-Hyun Yoon. DAMA/LIBRA-phase2 in WIMP effective models. JCAP, 1807(07):016, 2018

3. Non-standard EFT interactions might in principle give rise to new, observable phenomena (target dependence)

- Eugenio Del Nobile, Graciela B. Gelmini, and Samuel J. Witte. Target dependence of the annual modulation in direct dark matter searches. Phys. Rev. D, 91(12):121302, 2015

- Eugenio Del Nobile, Graciela B. Gelmini, and Samuel J. Witte. Prospects for detection of target-dependent annual modulation in direct dark matter searches. JCAP, 1602(02):009, 2016.

DM direct detection EFT: two applications

1. Annual modulation in NREFT

Motivations

1. Annual modulation depends on DM interactions

2. Non-standard EFT interactions fit better the latest DAMA results

- Sebastian Baum, Katherine Freese, and Chris Kelso. Dark Matter implications of DAMA/LIBRA-phase2 results. Phys. Lett. B, 789:262{269, 2019

- Sunghyun Kang, Stefano Scopel, Gaurav Tomar, and Jong-Hyun Yoon. DAMA/LIBRA-phase2 in WIMP effective models. JCAP, 1807(07):016, 2018

3. Non-standard EFT interactions might in principle give rise to new, observable phenomena (target dependence)

- Eugenio Del Nobile, Graciela B. Gelmini, and Samuel J. Witte. Target dependence of the annual modulation in direct dark matter searches. Phys. Rev. D, 91(12):121302, 2015

- Eugenio Del Nobile, Graciela B. Gelmini, and Samuel J. Witte. Prospects for detection of target-dependent annual modulation in direct dark matter searches. JCAP, 1602(02):009, 2016.

Goal

Systematic study of the annual modulation properties in NREFT which can help characterising and discriminating the DM signal

Theoretical framework

key point: all the timing information is contained in the relative velocity, **v**(t)

Theoretical framework

key point: all the timing information is contained in the relative velocity, **v**(t)

↓

The relative velocity appears in the differential rate
in the velocity distribution and in the cross-section

$$\frac{\mathrm{dR}}{\mathrm{dE_R}} = \frac{\rho_\chi}{m_\chi m_T} \int d\mathbf{v}\ v\ f(\mathbf{v})\ \frac{\mathrm{d}\sigma(\mathbf{v})}{\mathrm{dE_R}}$$

Theoretical framework

key point: all the timing information is contained in the relative velocity, **v**(t)

↓

The relative velocity appears in the differential rate
in the velocity distribution and in the cross-section

$$\frac{\mathrm{dR}}{\mathrm{dE_R}} = \frac{\rho_\chi}{m_\chi m_T} \int d\mathbf{v}\ v\ f(\mathbf{v})\ \frac{\mathrm{d}\sigma(\mathbf{v})}{\mathrm{dE_R}}$$

Four categories of building-blocks

Theoretical framework

key point: all the timing information is contained in the relative velocity, **v**(t)

$\downarrow$

The relative velocity appears in the differential rate in the velocity distribution and in the cross-section

$$\frac{\mathrm{dR}}{\mathrm{dE_R}} = \frac{\rho_\chi}{m_\chi m_T} \int d\mathbf{v}\; v\, f(\mathbf{v})\, \frac{\mathrm{d}\sigma(\mathbf{v})}{\mathrm{dE_R}}$$

Four categories of building-blocks

$$\begin{array}{ccccc} & \mathcal{O}_1 & \mathcal{O}_5 & \mathcal{O}_7 & \mathcal{O}_{11} \\ & \swarrow & \swarrow & \searrow & \searrow \\ \frac{1}{v^2}\cdot & 1 & (Av^2 + Bv_{min}^2) & (v^2 - v_{min}^2) & v_{min}^2 \end{array}$$

Theoretical framework

key point: all the timing information is contained in the relative velocity, **v**(t)

↓

The relative velocity appears in the differential rate
in the velocity distribution and in the cross-section

$$\frac{\mathrm{dR}}{\mathrm{dE_R}} = \frac{\rho_\chi}{m_\chi m_T} \int d\mathbf{v}\; v\; f(\mathbf{v})\, \frac{\mathrm{d}\sigma(\mathbf{v})}{\mathrm{dE_R}}$$

Four categories of building-blocks

$$\mathcal{O}_1 \quad \mathcal{O}_5 \quad \mathcal{O}_7 \quad \mathcal{O}_{11}$$

↓

$$\frac{\mathrm{dR}}{\mathrm{dE_R}} \propto \left[A(v_{min})\;\eta(v_{min},t) + B(v_{min})\;\tilde{\eta}(v_{min},t)\right]$$

DM direct detection EFT: two applications

1. Annual modulation in NREFT

Theoretical framework

$$\begin{cases} \eta(v_{min}, t) = \int d\mathbf{v}\, \frac{f(\mathbf{v})}{v} \\ \tilde{\eta}(v_{min}, t) = \int d\mathbf{v}\, v\, f(\mathbf{v}) \end{cases}$$

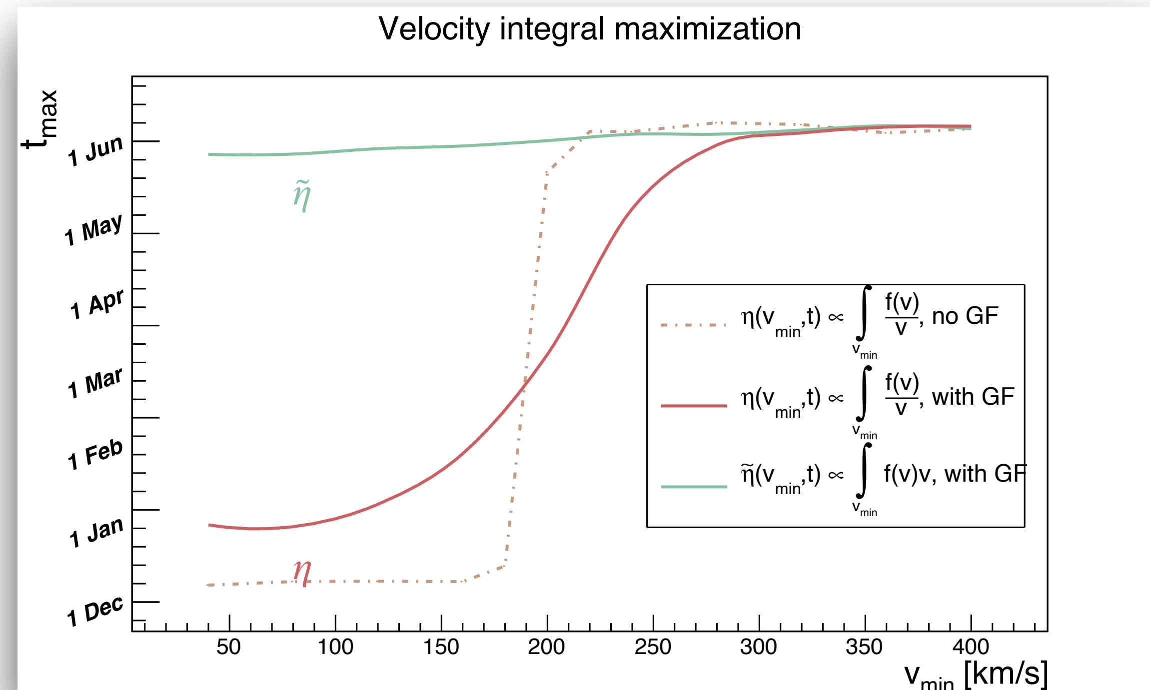

$$\frac{dR}{dE}(v_{min}, t) \propto \left[A(v_{min})\, \eta(v_{min}, t) + B(v_{min})\, \tilde{\eta}(v_{min}, t)\right]$$

Magnetic Dipole Dark Matter (MDDM)

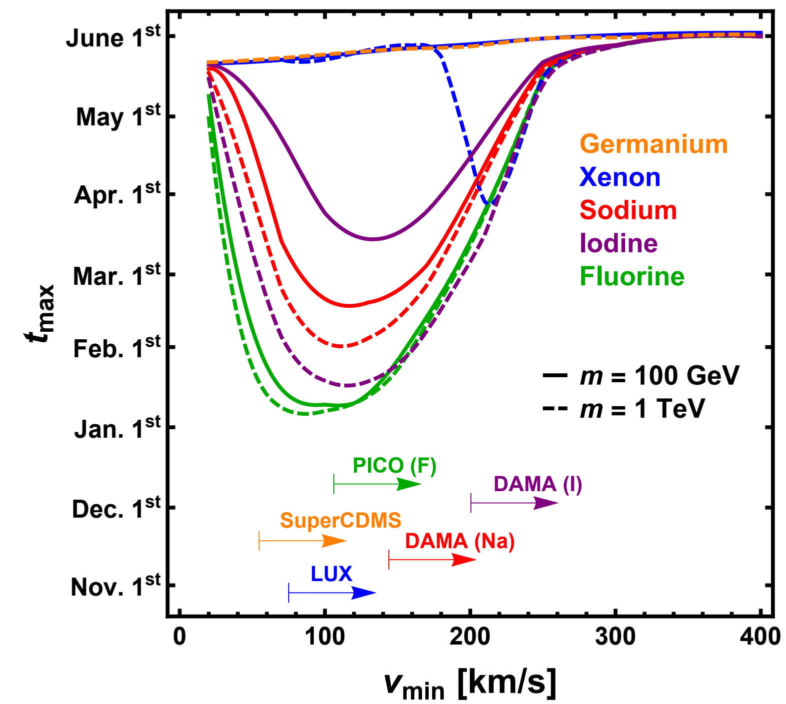

$$\mathscr{L}_{MDDM} = -\lambda_\chi\, \bar{\chi}\sigma^{\mu\nu}\chi\, F_{\mu\nu}$$

Eugenio Del Nobile, Graciela B. Gelmini, and Samuel J. Witte. Target dependence of the annual modulation in direct dark matter searches. Phys. Rev. D, 91(12):121302, 2015

G S
S I

DM direct detection EFT: two applications

1. Annual modulation in NREFT

Results: Amplitude of modulation

$$\frac{dR(t)}{dE_R} \approx A_0 + A_1 \cos\omega(t - t_0) \longrightarrow A_1 \approx \frac{1}{2}\left[\frac{\mathrm{dR}}{\mathrm{dE_R}}(v_{min}, Jun\ 1) - \frac{\mathrm{dR}}{\mathrm{dE_R}}(v_{min}, Dec\ 1)\right]$$

Inversion of phase

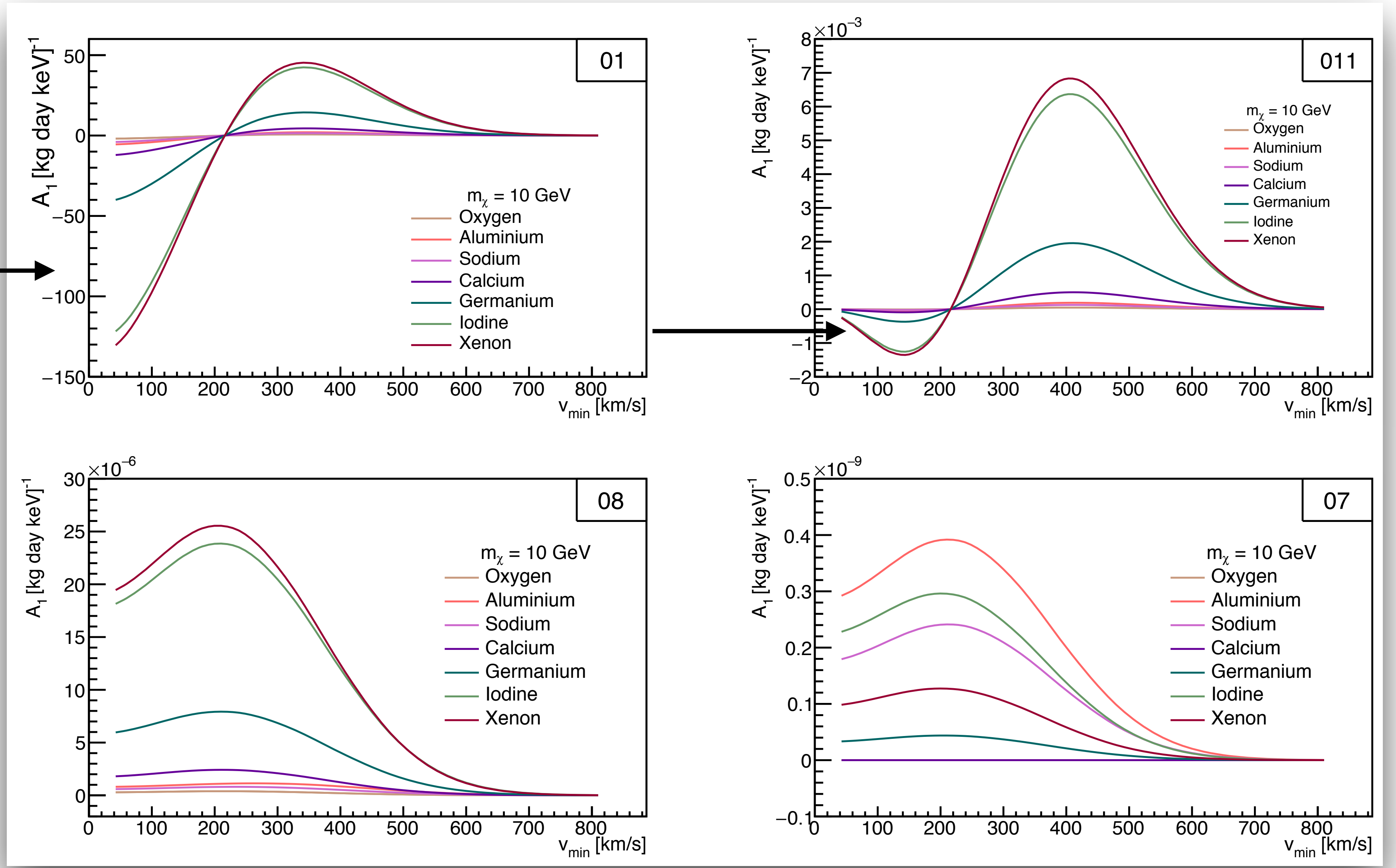

Results: Annual phase

Annual phase for different models

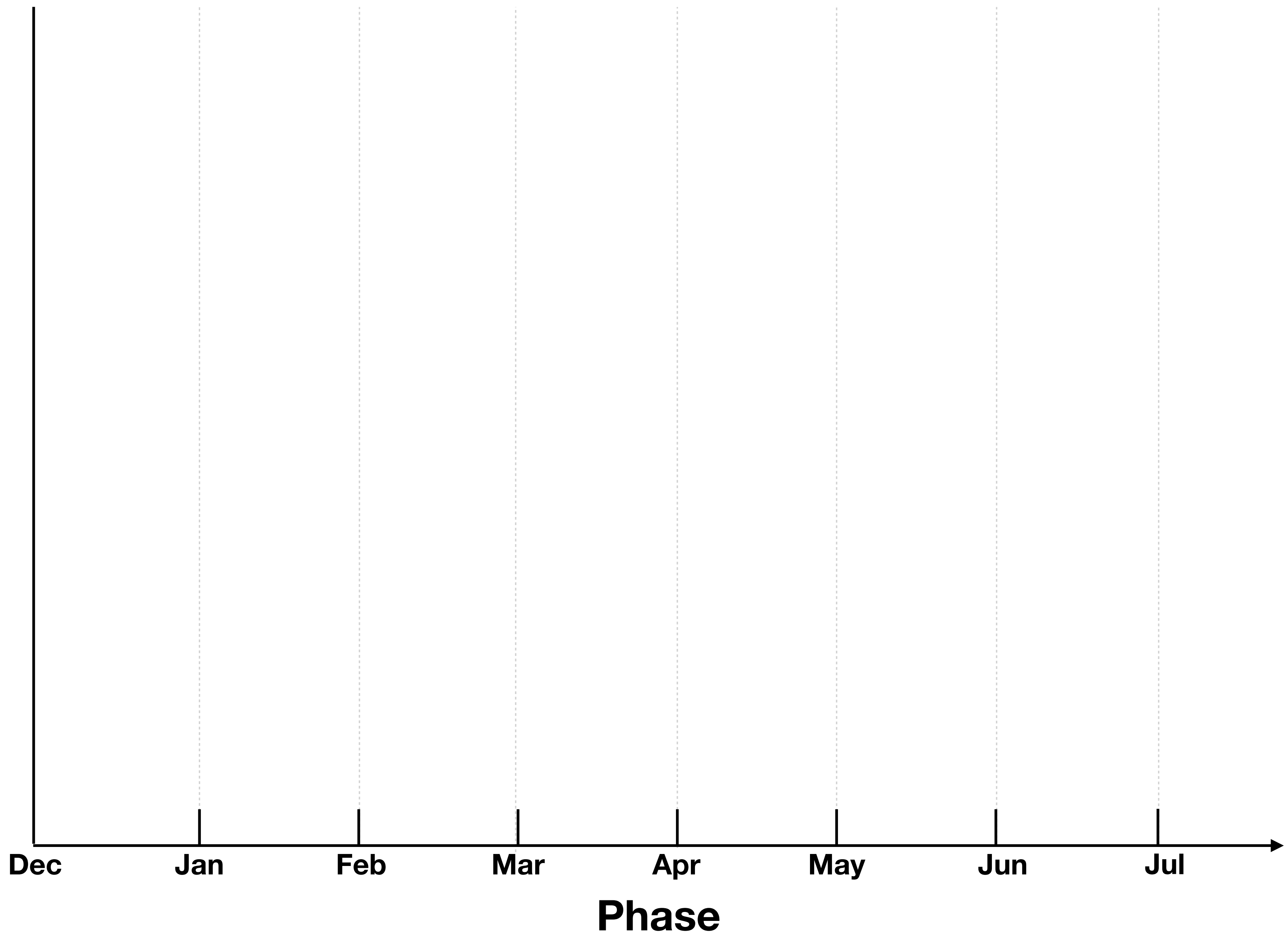

Results: Annual phase

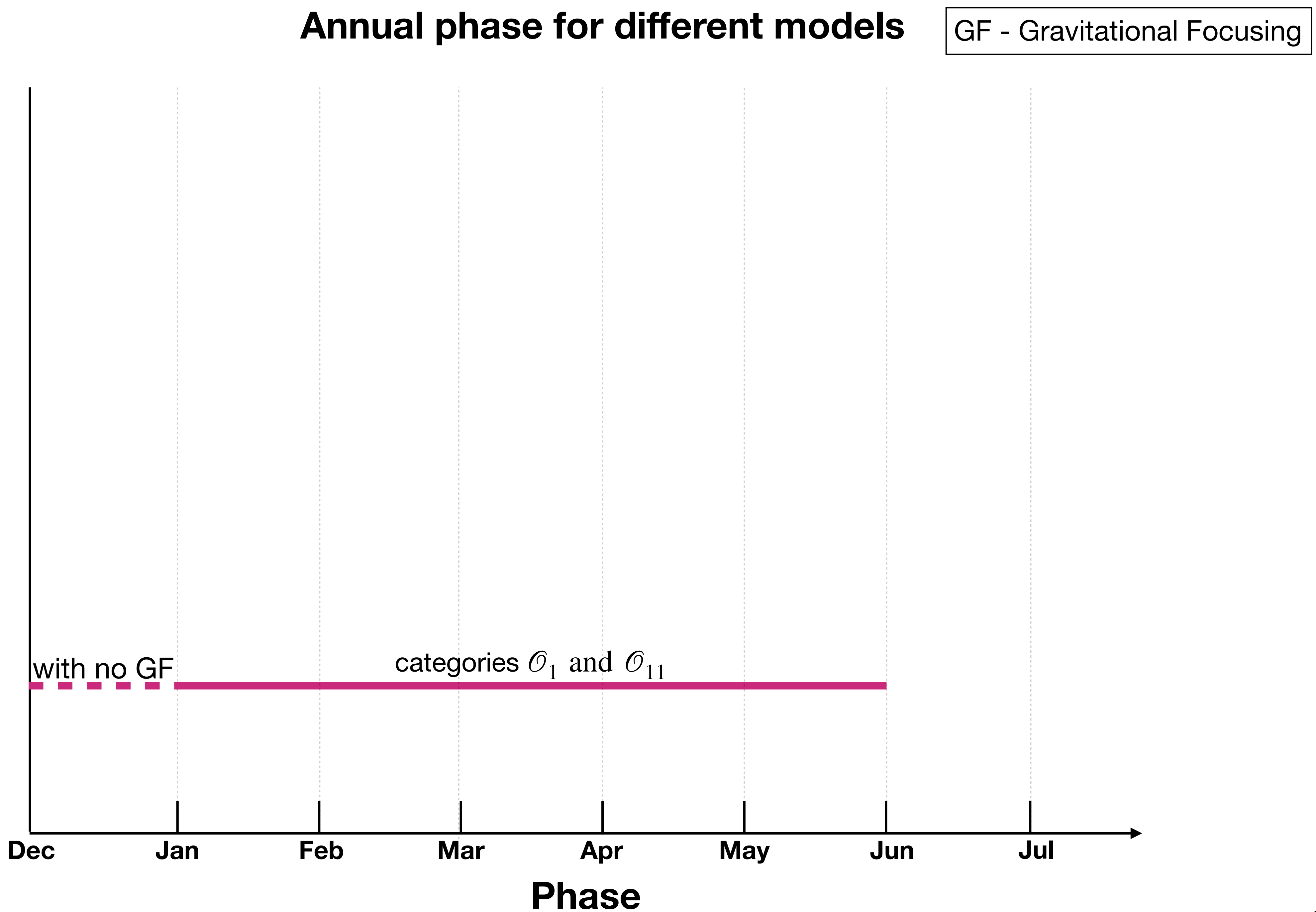

Results: Annual phase

GF - Gravitational Focusing

MDDM - Magnetic Dipole Dark Matter
ADM - Anapole Dark Matter

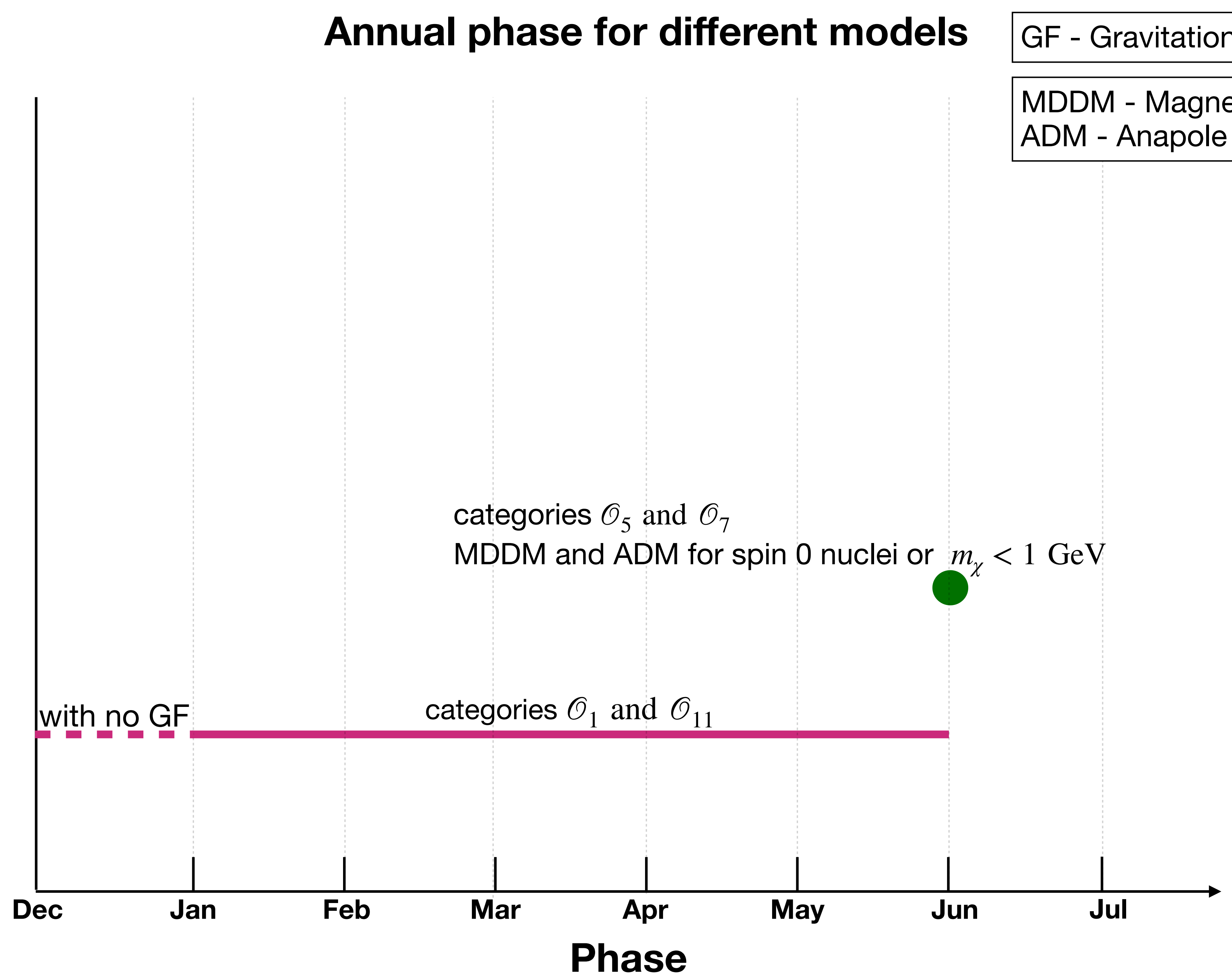

DM direct detection EFT: two applications

1. Annual modulation in NREFT

Results: Annual phase

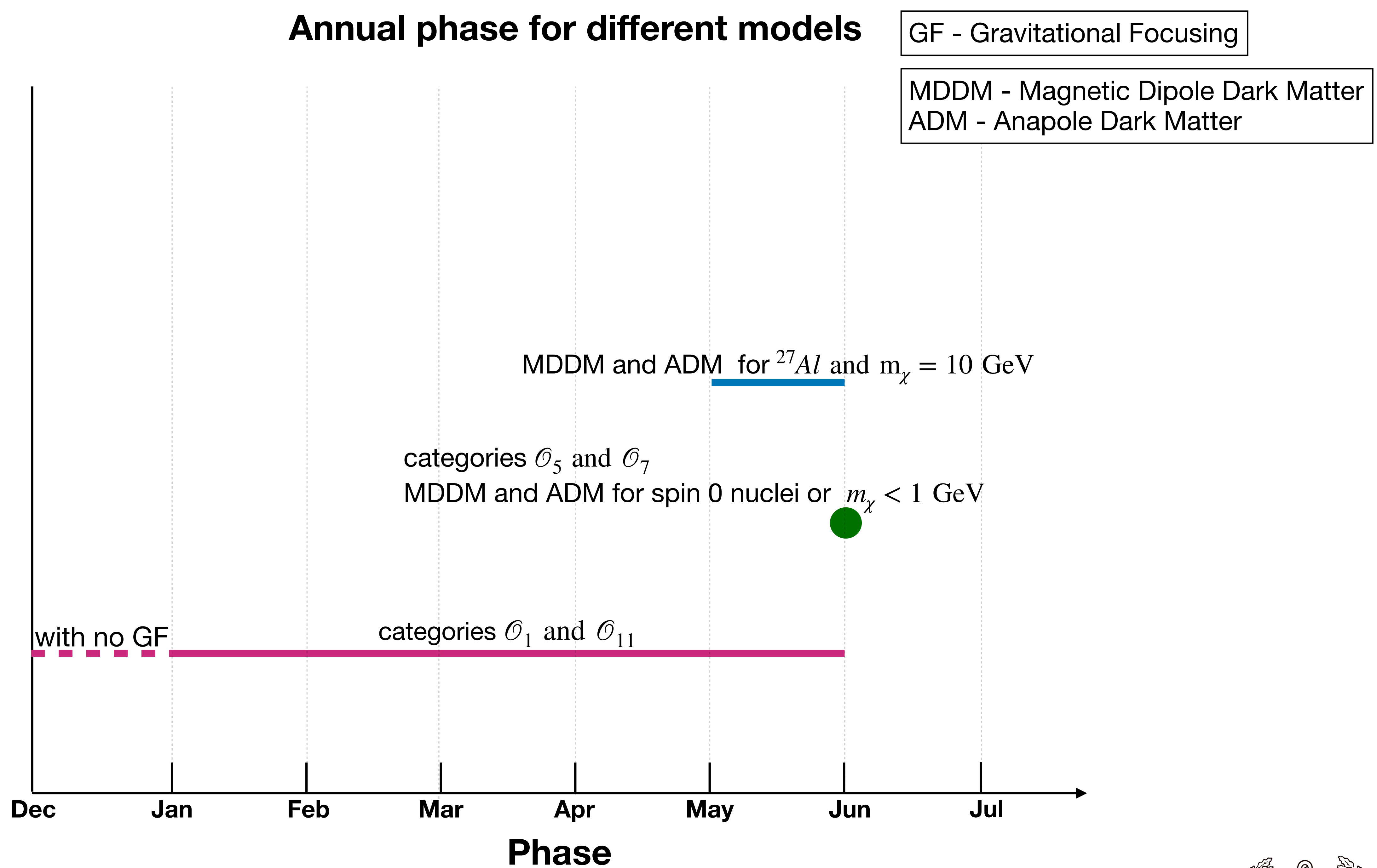

DM direct detection EFT: two applications

1. Annual modulation in NREFT

Results: Annual phase

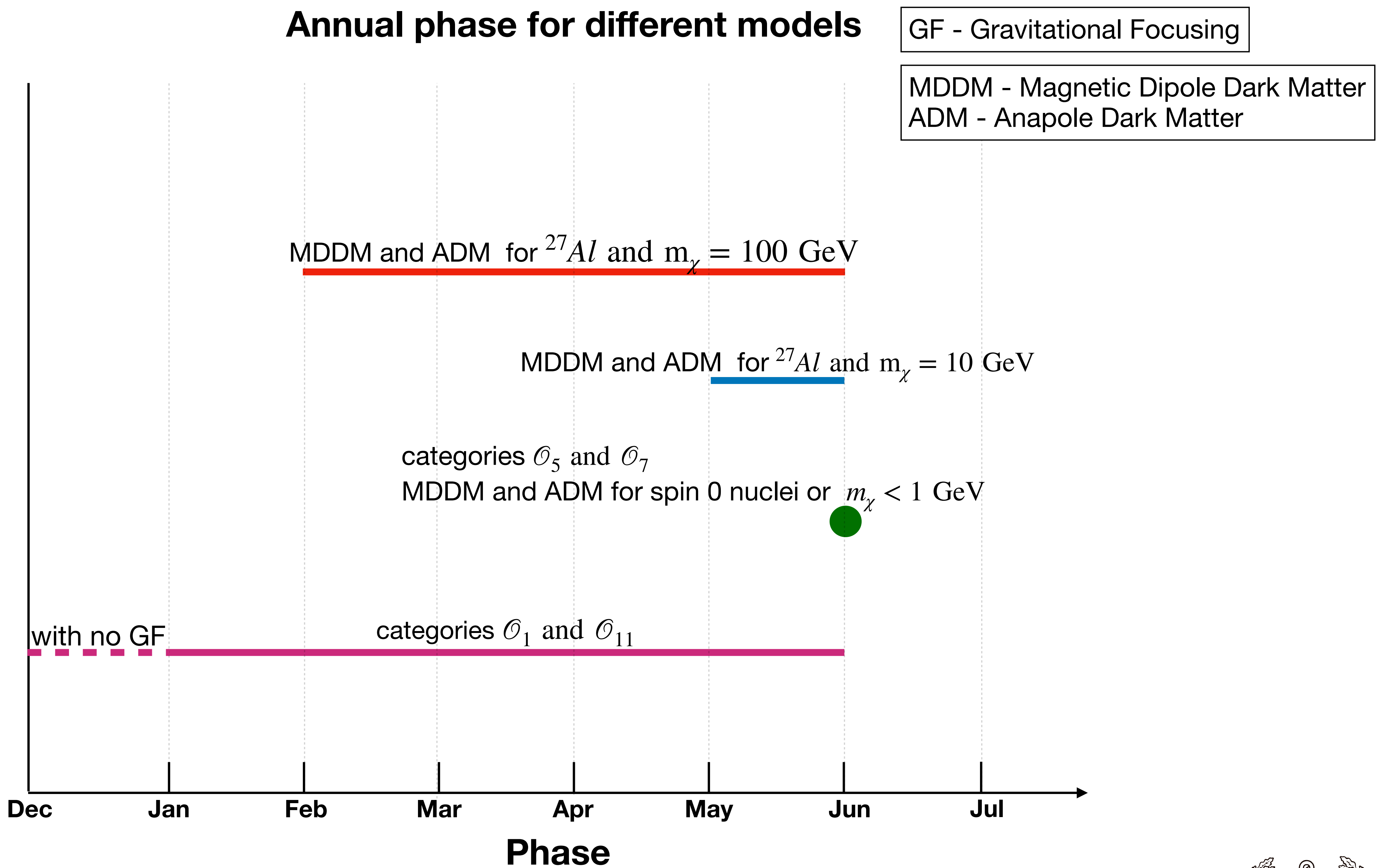

Results: Annual phase

GF - Gravitational Focusing

MDDM - Magnetic Dipole Dark Matter
ADM - Anapole Dark Matter

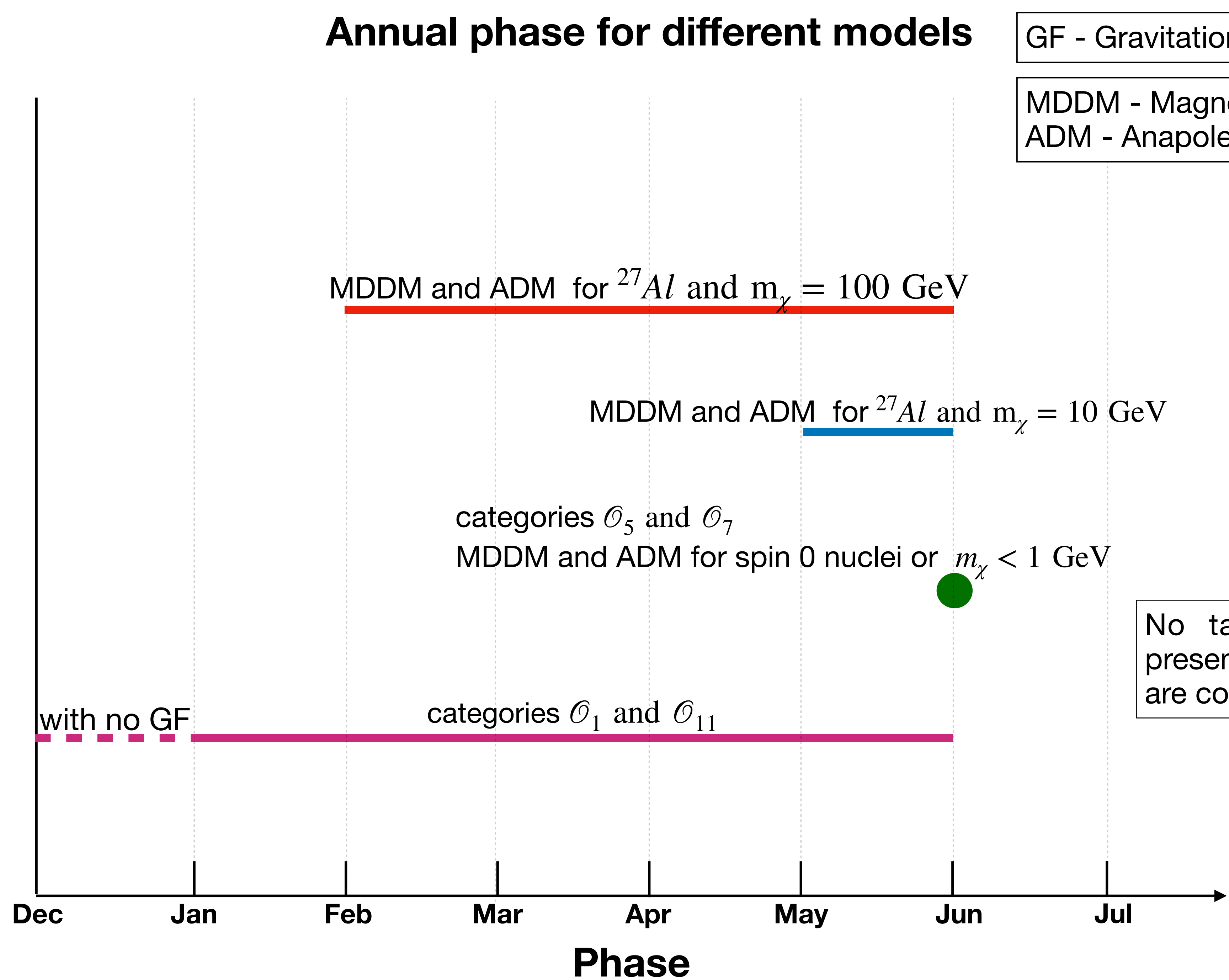

No target dependence is present if single operators are considered

Second application

Search for dark matter with polarised nuclei

Motivations

Chi-Ting Chiang, Marc Kamionkowski, and Gordan Z. Krnjaic. Dark Matter Detection with Polarized Detectors. Phys. Dark Univ., 1:109-115, 2012.

*"If WIMPs are **fermions** and participate in parity-violating interactions with ordinary matter, then the recoil-direction and recoil-energy distributions of nuclei in detectors will depend on the orientation of the initial nuclear spin with respect to the velocity of the detector through the Galactic halo."*

$$\frac{\mathrm{d}\sigma}{\mathrm{dE_R}} = A + B\,(\mathbf{v}\cdot\mathbf{S}_T) + B'\,(\mathbf{v}'\cdot\mathbf{S}_T)$$

DM direct detection EFT: two applications

2. Search for dark matter with polarised nuclei

Motivations

Chi-Ting Chiang, Marc Kamionkowski, and Gordan Z. Krnjaic. Dark Matter Detection with Polarized Detectors. Phys. Dark Univ., 1:109-115, 2012.

*"If WIMPs are **fermions** and participate in parity-violating interactions with ordinary matter, then the recoil-direction and recoil-energy distributions of nuclei in detectors will depend on the orientation of the initial nuclear spin with respect to the velocity of the detector through the Galactic halo."*

Goal

Extend previous work to spin-1 dark matter particles using EFTs in order to highlight methods to identify the dark matter spin in case of positive signal

R. Catena, K. Fridell, and **V. Zema**. Direct detection of fermionic and vector dark matter with polarised targets. JCAP, 11:018, 2018.

GS
SI

DM direct detection EFT: two applications

2. Search for dark matter with polarised nuclei

R. Catena, K. Fridell, and **V. Zema**. Direct detection of fermionic and vector dark matter with polarised targets. JCAP, 11:018, 2018

Theoretical framework

Observable: double differential rate

$$\frac{\mathrm{d}R}{\mathrm{d}E_R\mathrm{d}\Omega} = \frac{\rho_0}{m_\chi m_T} \int_{|\mathbf{v}_\chi^{det}|>v_{min}}^{|\mathbf{v}_\chi^{det}+\mathbf{v}_{det}^{gal}|<v_{esc}} d\mathbf{v}_\chi^{det}\,|\,\mathbf{v}_\chi^{det}\,|\,f(\mathbf{v}_\chi^{det}+\mathbf{v}_{det}^{gal})\; 2m_T \frac{\mathrm{d}\sigma}{\mathrm{d}q^2\mathrm{d}\Omega}$$

$$|\,\overline{\mathscr{M}}\,|^2 = \frac{1}{(2j_\chi+1)} \sum_{ss'} \sum_{r'} |\,\mathscr{M}\,|^2$$

Effective Lagrangian for fermionic DM

$$\mathscr{L}^I_{eff,\chi N} = -\frac{\lambda_3 h_3}{m_G^2}\bar{\chi}\gamma^\mu\chi\bar{N}\gamma_\mu N - \frac{\lambda_3 h_4}{m_G^2}\bar{\chi}\gamma^\mu\chi\bar{N}\gamma_\mu\gamma^5 N - \frac{\lambda_4 h_3}{m_G^2}\bar{\chi}\gamma^\mu\gamma^5\chi\bar{N}\gamma_\mu N - \frac{\lambda_4 h_4}{m_G^2}\bar{\chi}\gamma^\mu\gamma^5\chi\bar{N}\gamma_\mu\gamma^5$$

$$m_G^2 \gg q^2$$

G S
S I

DM direct detection EFT: two applications

2. Search for dark matter with polarised nuclei

R. Catena, K. Fridell, and **V. Zema**. Direct detection of fermionic and vector dark matter with polarised targets. JCAP, 11:018, 2018

Theoretical framework

Observable: double differential rate

$$\frac{\mathrm{d}R}{\mathrm{d}E_R\mathrm{d}\Omega} = \frac{\rho_0}{m_\chi m_T}\int_{|\mathbf{v}_\chi^{det}|>v_{min}}^{|\mathbf{v}_\chi^{det}+\mathbf{v}_{det}^{gal}|<v_{esc}} d\mathbf{v}_\chi^{det}\,|\mathbf{v}_\chi^{det}|\,f(\mathbf{v}_\chi^{det}+\mathbf{v}_{det}^{gal})\,2m_T\,\frac{\mathrm{d}\sigma}{\mathrm{d}q^2\mathrm{d}\Omega}$$

$$|\overline{\mathscr{M}}|^2 = \frac{1}{(2j_\chi+1)}\sum_{ss'}\sum_{r'}|\mathscr{M}|^2$$

Effective Lagrangian for vector DM

$$\mathscr{L}^I_{eff,XN} = -\frac{ib_5h_3}{m_G^2}X_\nu^\dagger\partial_\mu X^\nu\bar{N}\gamma^\mu N - \frac{ib_5h_4}{m_G^2}X_\nu^\dagger\partial_\mu X^\nu\bar{N}\gamma^\mu\gamma^5 N - \frac{b_6h_3}{m_G^2}X_\nu^\dagger\partial^\nu X_\mu\bar{N}\gamma^\mu N +$$
$$-\frac{b_6h_4}{m_G^2}X_\nu^\dagger\partial^\nu X_\mu\bar{N}\gamma^\mu\gamma^5 N - \frac{b_7h_3}{m_G^2}\epsilon_{\sigma\nu\rho\mu}(X^{\dagger\sigma}\partial^\nu X^\rho)\bar{N}\gamma^\mu N - \frac{b_7h_4}{m_G^2}\epsilon_{\sigma\nu\rho\mu}(X^{\dagger\sigma}\partial^\nu X^\rho)\bar{N}\gamma^\mu\gamma^5 N + h.c.$$

$$m_G^2 \gg q^2$$

G S
S I

2. Search for dark matter with polarised nuclei

R. Catena, K. Fridell, and **V. Zema**. Direct detection of fermionic and vector dark matter with polarised targets. JCAP, 11:018, 2018

Results

Observable: double differential rate

$$\frac{\mathrm{d}R}{\mathrm{d}E_R\mathrm{d}\Omega} = \frac{\rho_0}{m_\chi m_T}\int_{|\mathbf{v}_\chi^{det}|>v_{min}}^{|\mathbf{v}_\chi^{det}+\mathbf{v}_{det}^{gal}|<v_{esc}} d\mathbf{v}_\chi^{det}\,|\,\mathbf{v}_\chi^{det}\,|\,f(\mathbf{v}_\chi^{det}+\mathbf{v}_{det}^{gal})\;2m_T\frac{\mathrm{d}\sigma}{\mathrm{d}q^2\mathrm{d}\Omega}$$

$$|\,\overline{\mathscr{M}}\,|^2 = \frac{1}{(2j_\chi+1)}\sum_{ss'}\sum_{r'}|\,\mathscr{M}\,|^2$$

Transition amplitude for fermionic DM

$$|\,\overline{\mathscr{M}}\,|^2 = \left(16m_\chi^2 m_T^2\right)\Bigg[\left(A^2 + 3D^2\right) + \\ -2\left(\mathbf{v}\cdot\mathbf{S}_N^{rr}\right)\left(AB\left(1-\frac{m_\chi}{m_T}\right)+2BD+CD\left(1+\frac{m_\chi}{m_T}\right)\right)+ \\ -2\left(\mathbf{v}'\cdot\mathbf{S}_N^{rr}\right)\left(AB\left(1+\frac{m_\chi}{m_T}\right)-2BD+CD\left(1-\frac{m_\chi}{m_T}\right)\right)\Bigg]$$

2. Search for dark matter with polarised nuclei

R. Catena, K. Fridell, and **V. Zema**. Direct detection of fermionic and vector dark matter with polarised targets. JCAP, 11:018, 2018

Results

Observable: double differential rate

$$\frac{\mathrm{d}R}{\mathrm{d}E_R \mathrm{d}\Omega} = \frac{\rho_0}{m_\chi m_T} \int_{|\mathbf{v}_\chi^{det}|>v_{min}}^{|\mathbf{v}_\chi^{det}+\mathbf{v}_{det}^{gal}|<v_{esc}} d\mathbf{v}_\chi^{det} \, |\mathbf{v}_\chi^{det}| \, f(\mathbf{v}_\chi^{det} + \mathbf{v}_{det}^{gal}) \; 2m_T \frac{\mathrm{d}\sigma}{\mathrm{d}q^2 \mathrm{d}\Omega}$$

$$|\overline{\mathscr{M}}|^2 = \frac{1}{(2j_\chi + 1)} \sum_{ss'} \sum_{r'} |\mathscr{M}|^2$$

Transition amplitude for vector DM

$$\frac{1}{3} \sum_{r'} \sum_{ss'} |\mathscr{M}|^2 = \left(\frac{4}{m_G^4} \right) \cdot 16 \, m_\chi^2 \, m_N^2 \, [\mathscr{I} - \mathscr{J}(\mathbf{v} \cdot 2\mathbf{S}_N^{rr}) - \mathscr{K}(\mathbf{v}' \cdot 2\mathbf{S}_N^{rr})]$$

DM direct detection EFT: two applications

2. Search for dark matter with polarised nuclei

R. Catena, K. Fridell, and **V. Zema**. Direct detection of fermionic and vector dark matter with polarised targets. JCAP, 11:018, 2018

Results

Further observable: Purely polarisation dependent part of the differential scattering rate

$$\frac{\mathrm{d}\Delta \mathrm{R}}{\mathrm{d}E_R \mathrm{d}\Omega} \equiv \frac{1}{2}\left(\frac{\mathrm{d}R(\mathbf{S}_N)}{\mathrm{d}E_R \mathrm{d}\Omega} - \frac{\mathrm{d}R(-\mathbf{S}_N)}{\mathrm{d}E_R \mathrm{d}\Omega}\right)$$

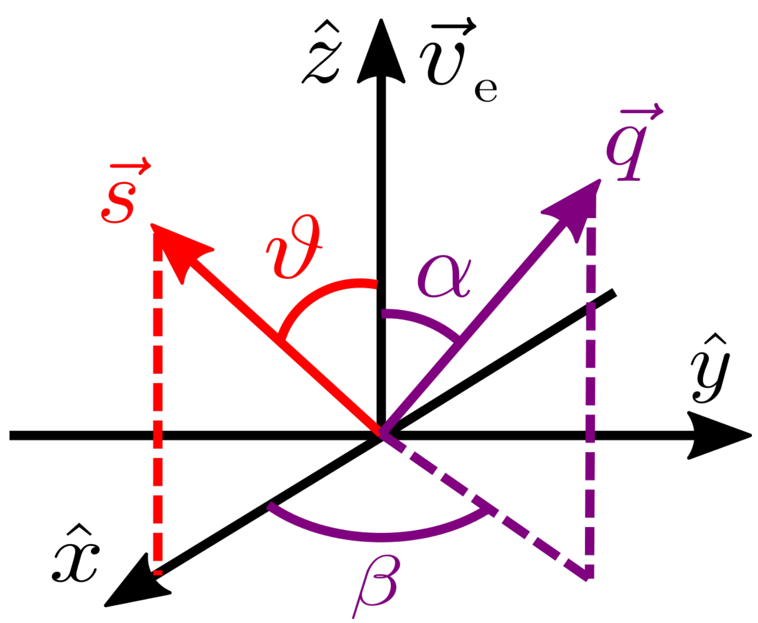

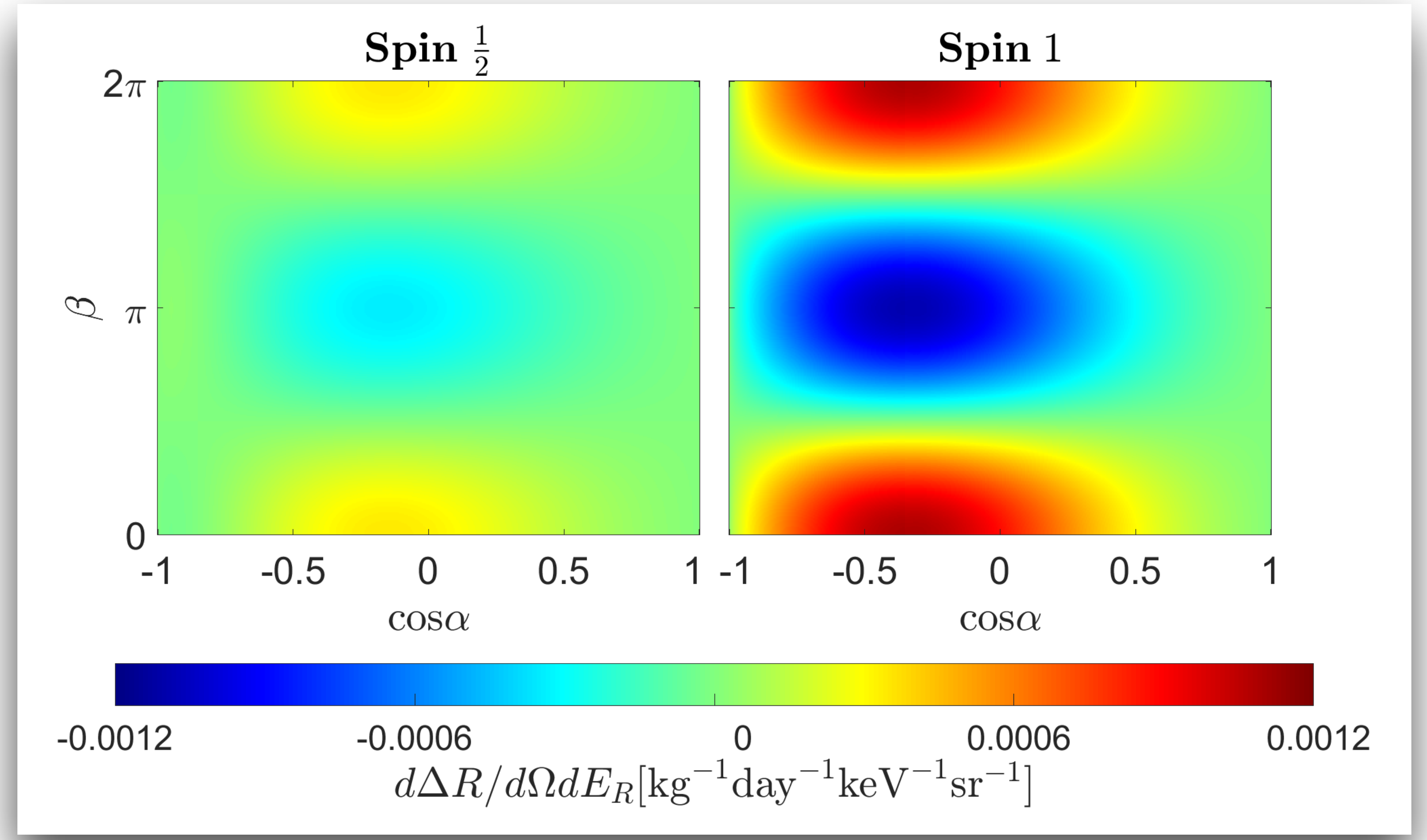

$$m_\chi = m_T = m_G = 100\ GeV$$

G S
S I

DM direct detection EFT: two applications

2. Search for dark matter with polarised nuclei

R. Catena, K. Fridell, and **V. Zema**. Direct detection of fermionic and vector dark matter with polarised targets. JCAP, 11:018, 2018

Results

Differential rate

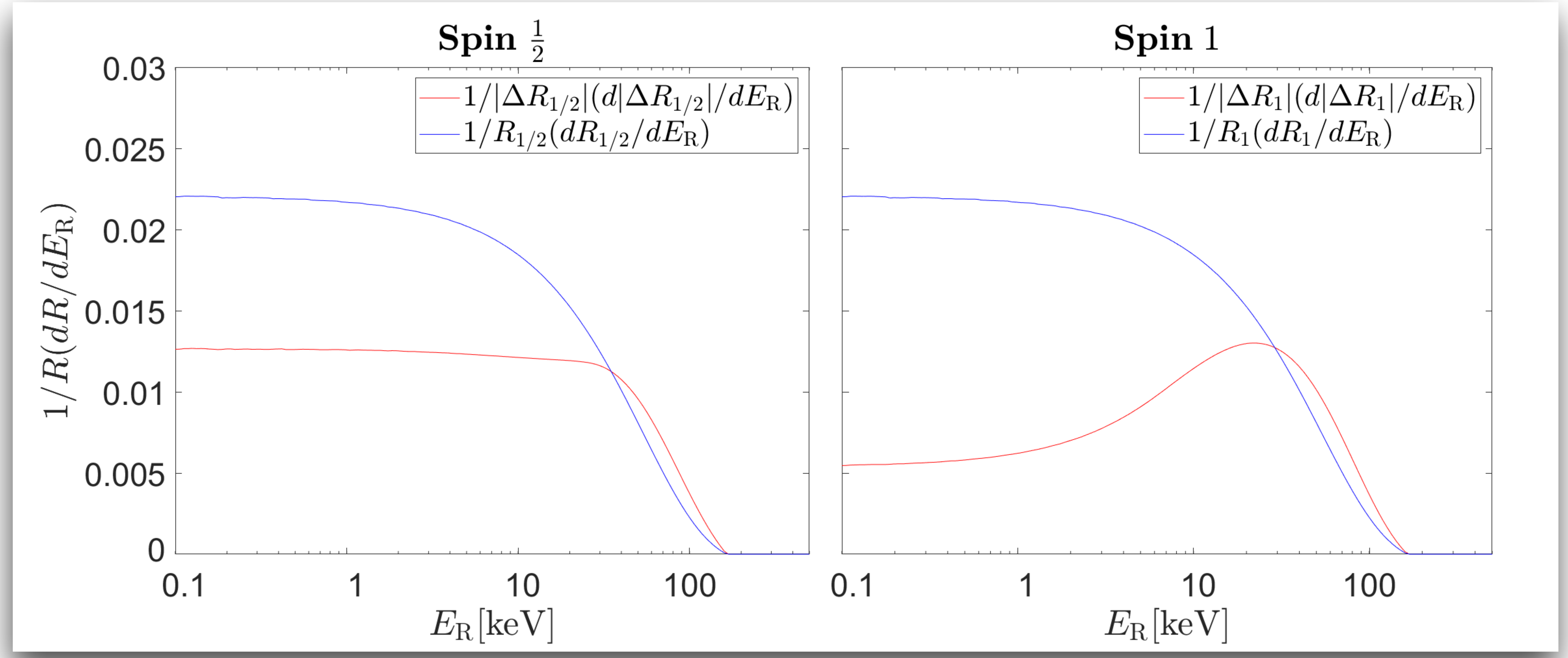

$$m_\chi = m_T = m_G = 100\ GeV$$

Dark matter search with the CRESST experiment

Cryogenic Rare Event Search with Superconducting Thermometers

GSSI

DM search with the CRESST experiment

Cryogenic Rare Event Search with Superconducting Thermometers

Istituto Nazionale di Fisica Nucleare
Laboratori Nazionali del Gran Sasso

DM search with the CRESST experiment

Cryogenic Rare Event Search with Superconducting Thermometers

Istituto Nazionale di Fisica Nucleare
Laboratori Nazionali del Gran Sasso

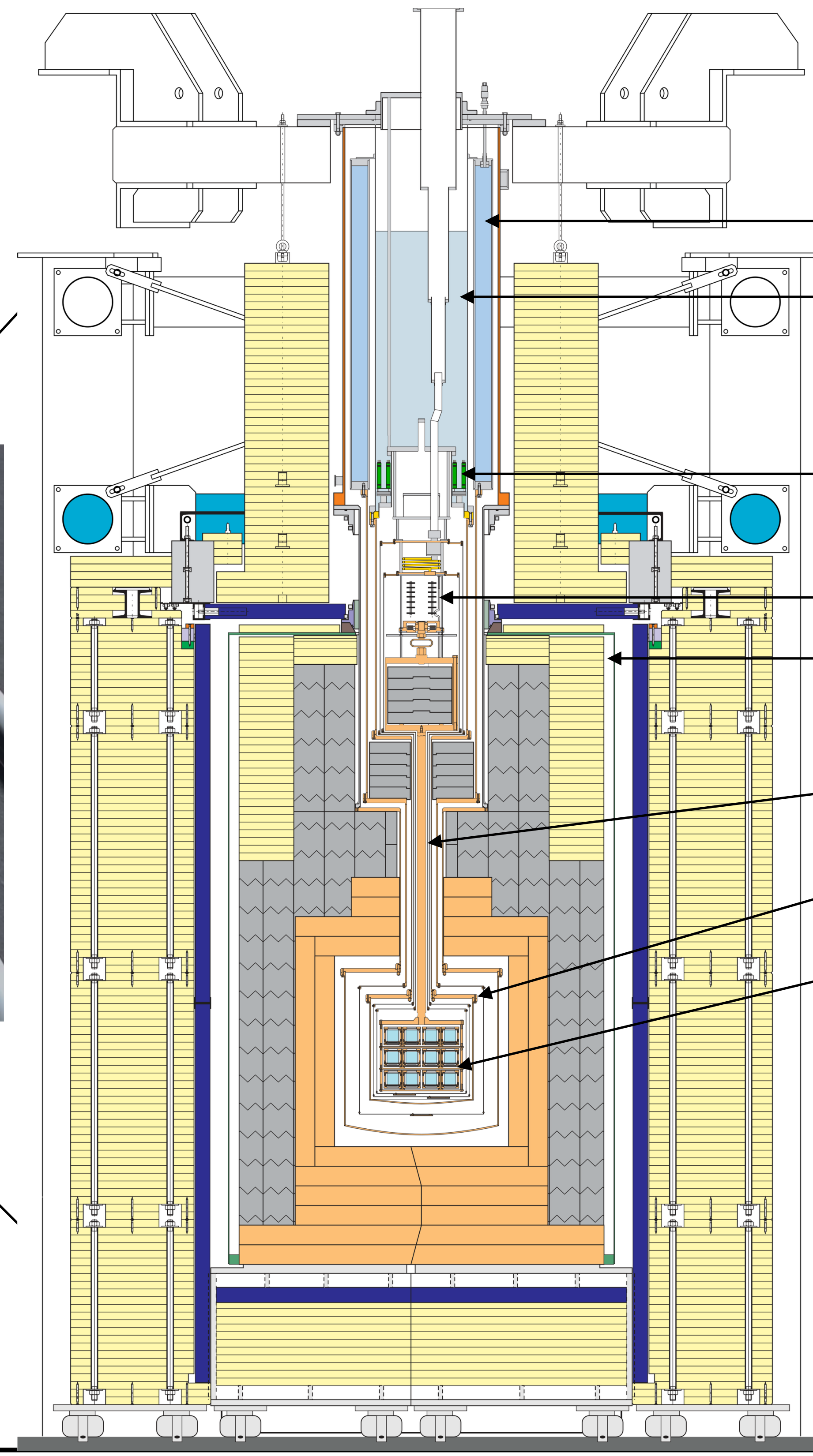

CRESST-III: the detectors

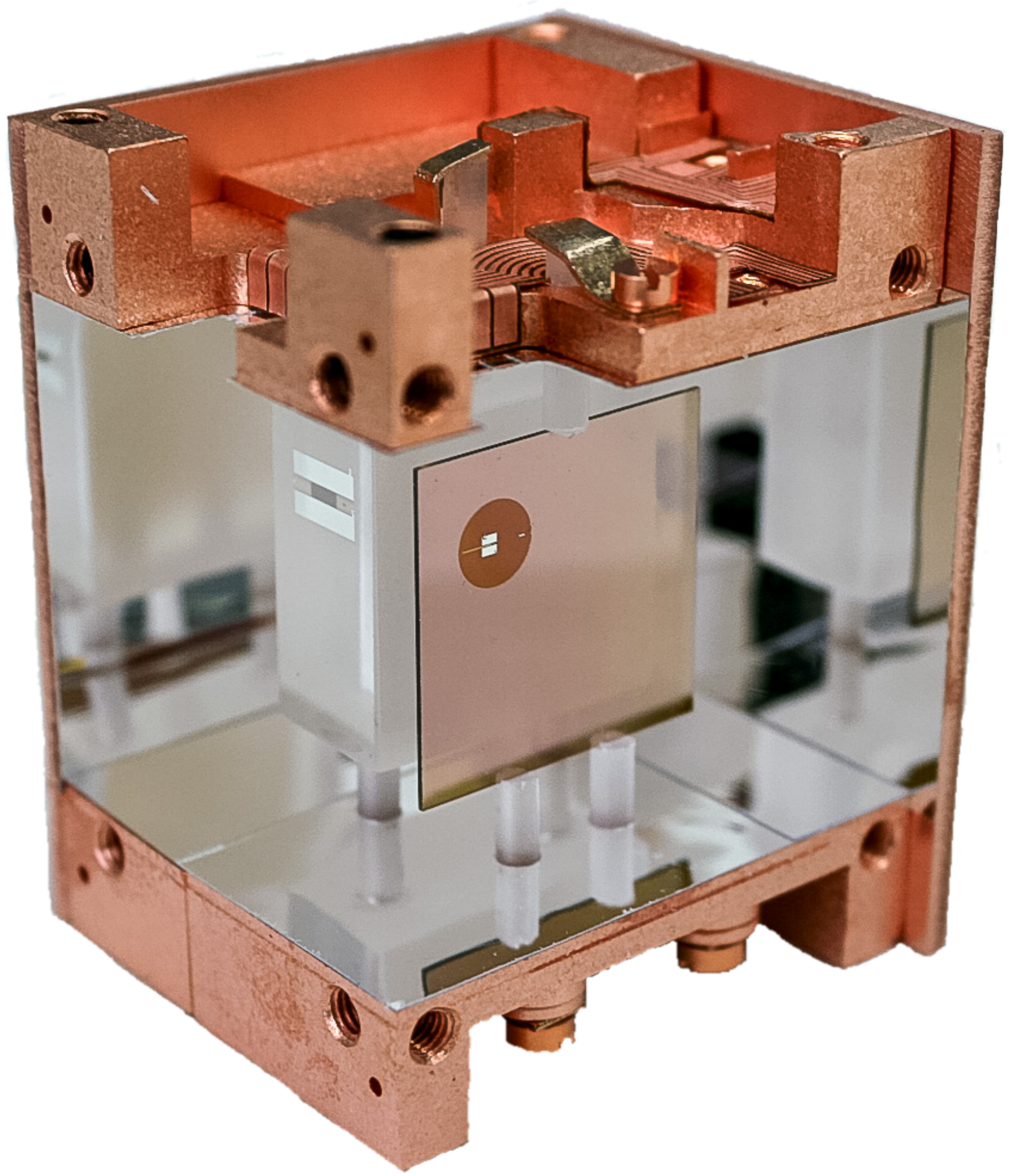

- **$CaWO_4$** scintillating crystal
- Cryogenic temperature $\sim\mathcal{O}(10\ \mathrm{mK})$

CRESST-III: the detectors

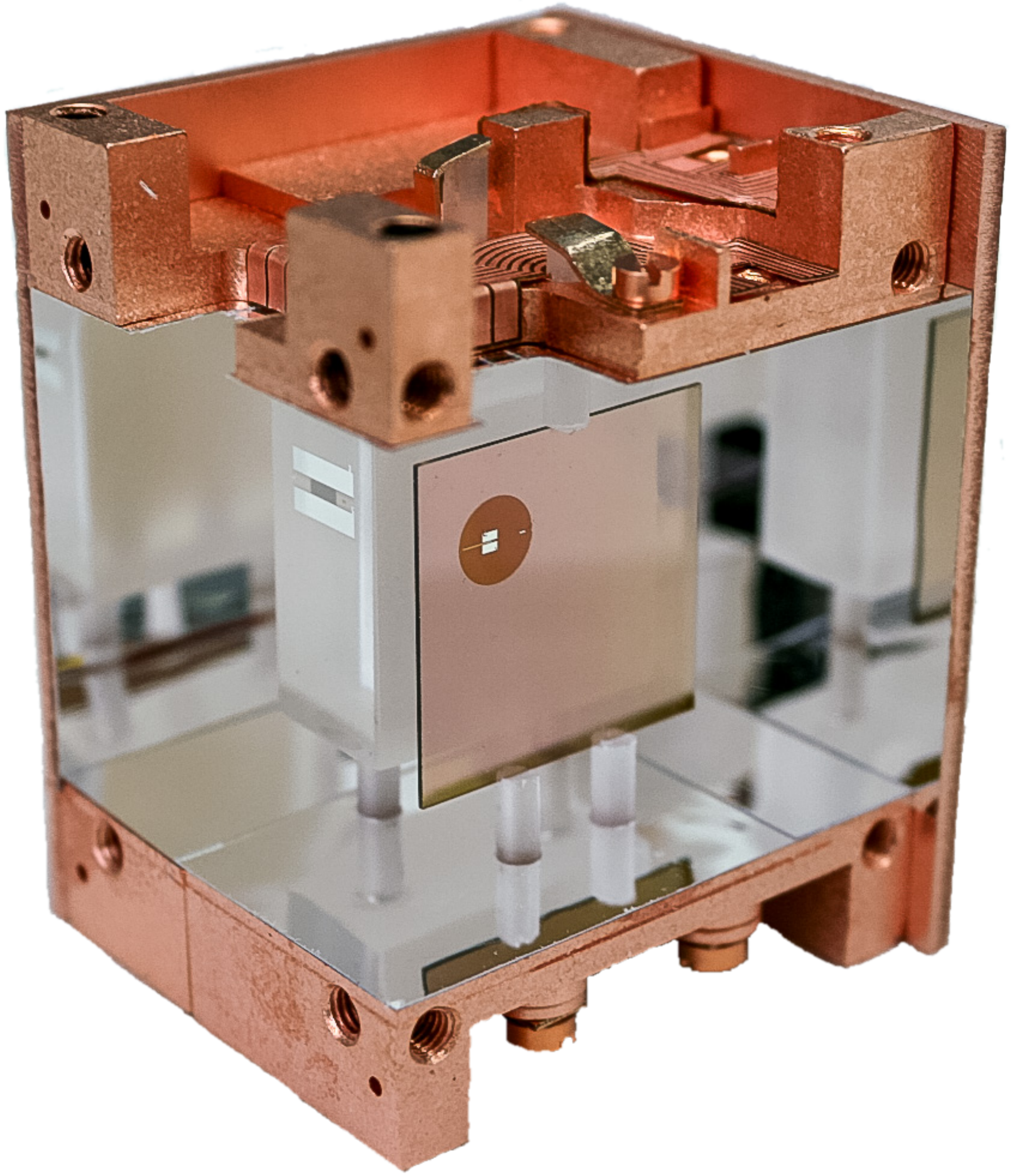

- **$CaWO_4$** scintillating crystal
- Cryogenic temperature $\sim\mathcal{O}(10\ \mathrm{mK})$

Both the energy converted in **heat** (**phonons**) and the energy converted in **scintillation light** are detected

DM search with the CRESST experiment

Cryogenic Rare Event Search with Superconducting Thermometers

CRESST-III: the detectors

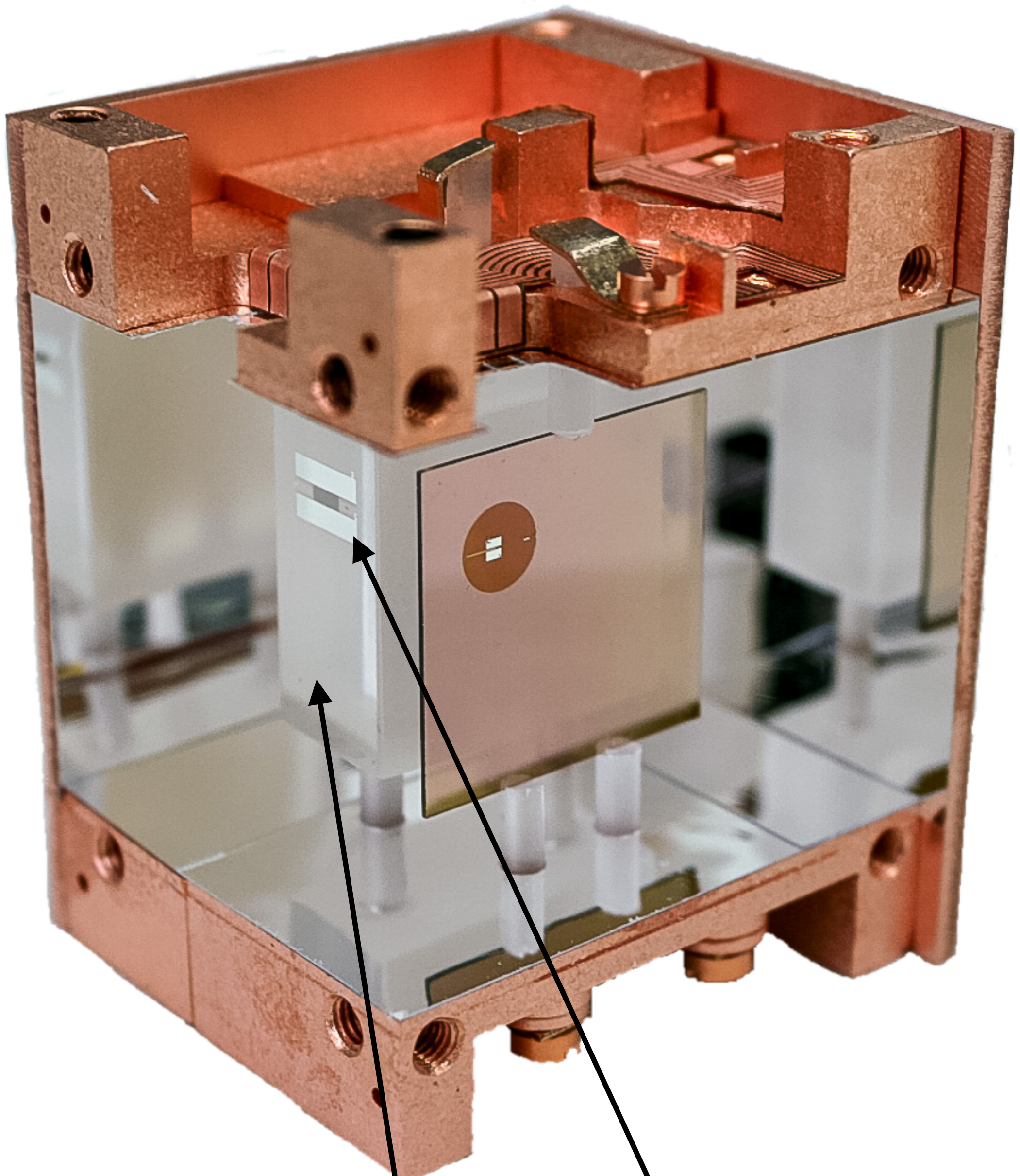

- **$CaWO_4$** scintillating crystal
- Cryogenic temperature ~$\mathcal{O}(10\ \mathrm{mK})$

Both the energy converted in **heat** (**phonons**) and the energy converted in **scintillation light** are detected

$CaWO_4$+TES is the **phonon detector**

GSSI

CRESST-III: the detectors

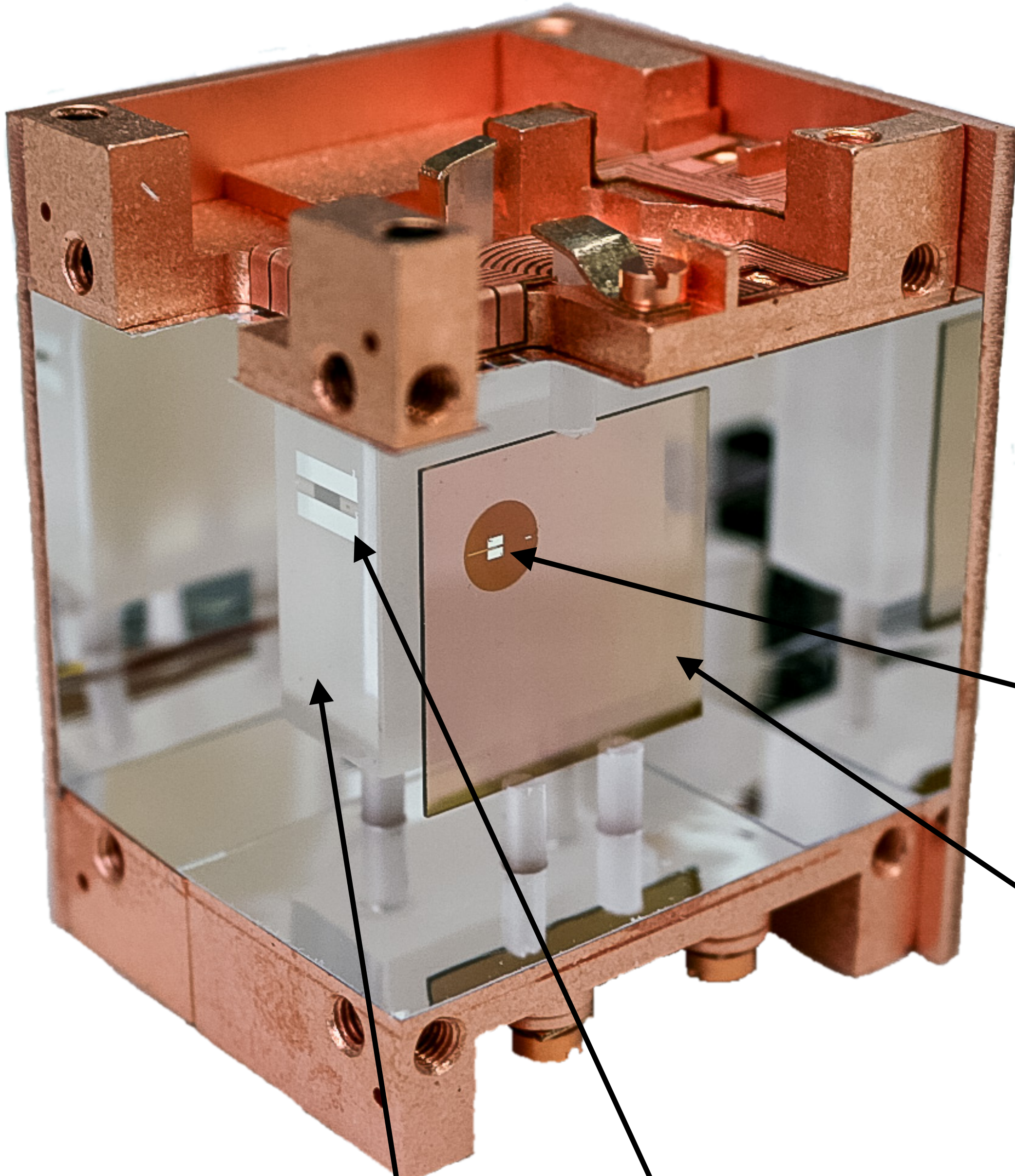

- **$CaWO_4$** scintillating crystal
- Cryogenic temperature $\sim\mathcal{O}(10\ \mathrm{mK})$

Both the energy converted in **heat** (**phonons**) and the energy converted in **scintillation light** are detected

Silicon on Sapphire (SOS)+TES is the **light detector**

$CaWO_4$+TES is the **phonon detector**

CRESST-III: working principle

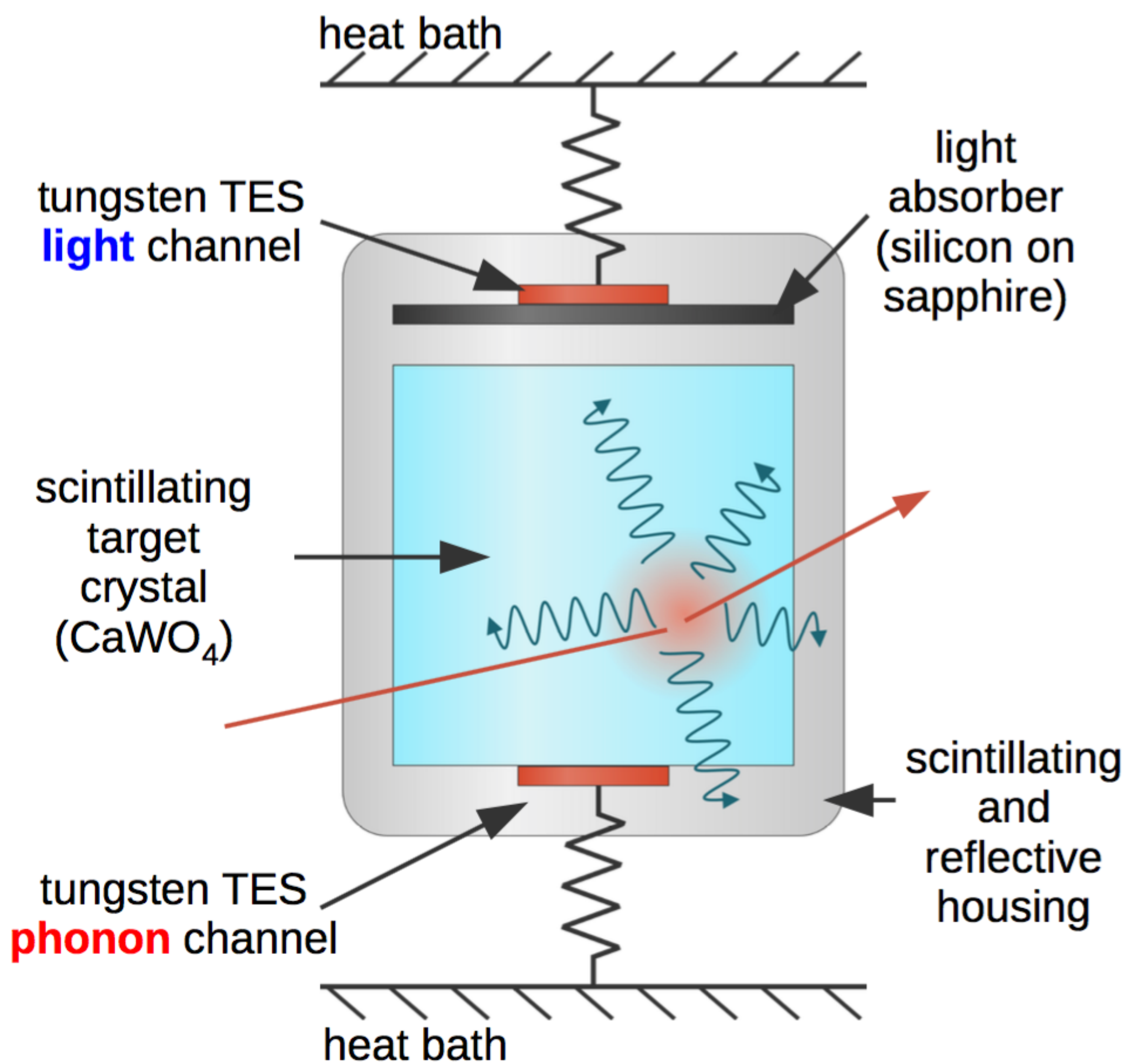

C. Strandhagen

CRESST-III: particle discrimination

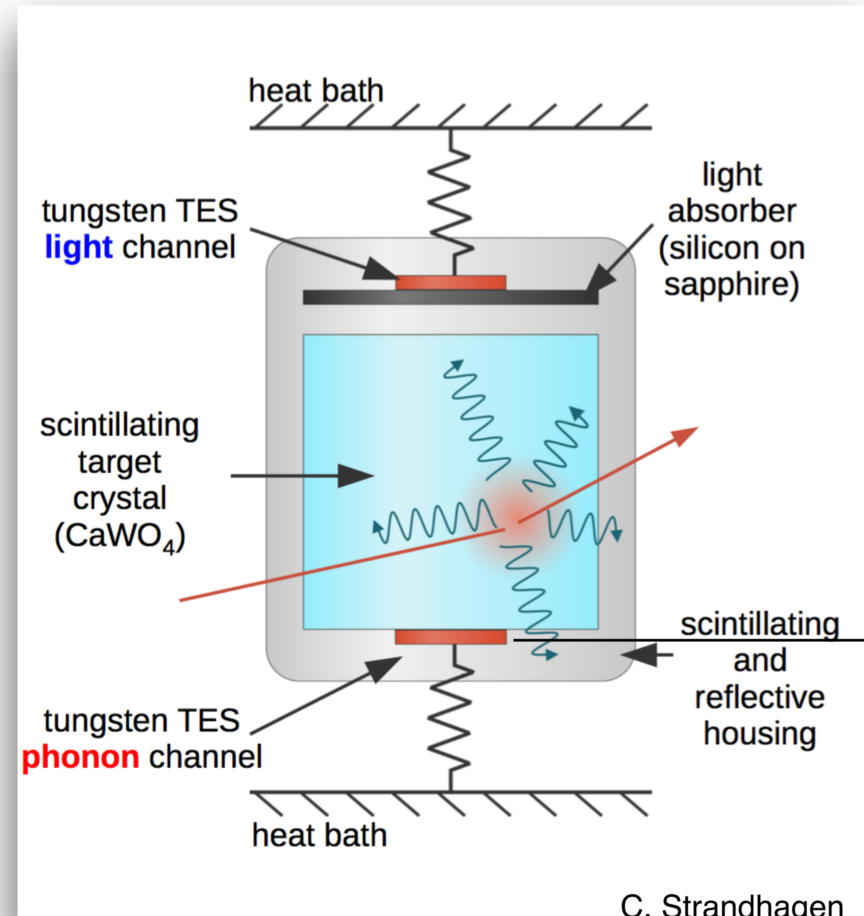

crystal + TES is the phonon-channel → **Phonon signal** (almost) independent of particle type

CRESST-III: particle discrimination

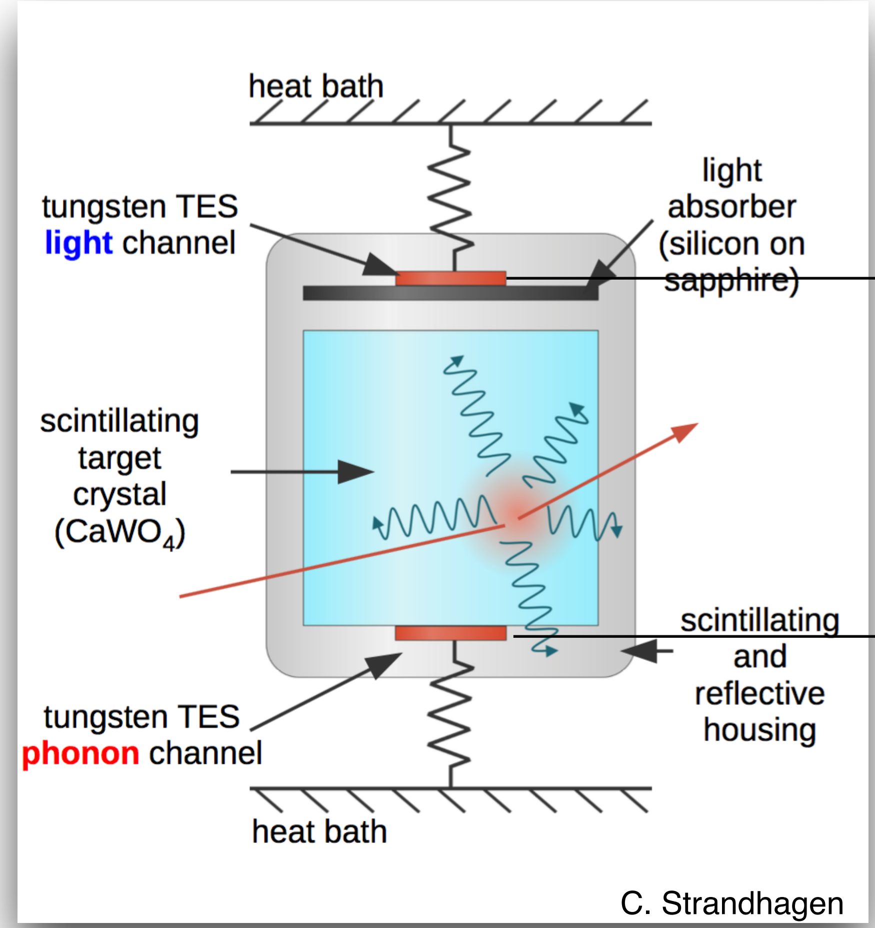

SOS + TES is the light-channel → **Scintillation light**
amount of emitted light depends on particle type
LIGHT QUENCHING

crystal + TES is the phonon-channel → **Phonon signal**
(almost) independent of particle type

CRESST-III: particle discrimination

$$\text{Light Yield } (LY) = \frac{\text{Light pulse energy}}{\text{Phonon pulse energy}}$$

CRESST-III: particle discrimination

$$Light\ Yield\ (LY) = \frac{Light\ pulse\ energy}{Phonon\ pulse\ energy}$$

The events in the LY vs Energy plane distribute along horizontal bands

CRESST-III: particle discrimination

$$Light\ Yield\ (LY) = \frac{Light\ pulse\ energy}{Phonon\ pulse\ energy}$$

The events in the LY vs Energy plane distribute along horizontal bands

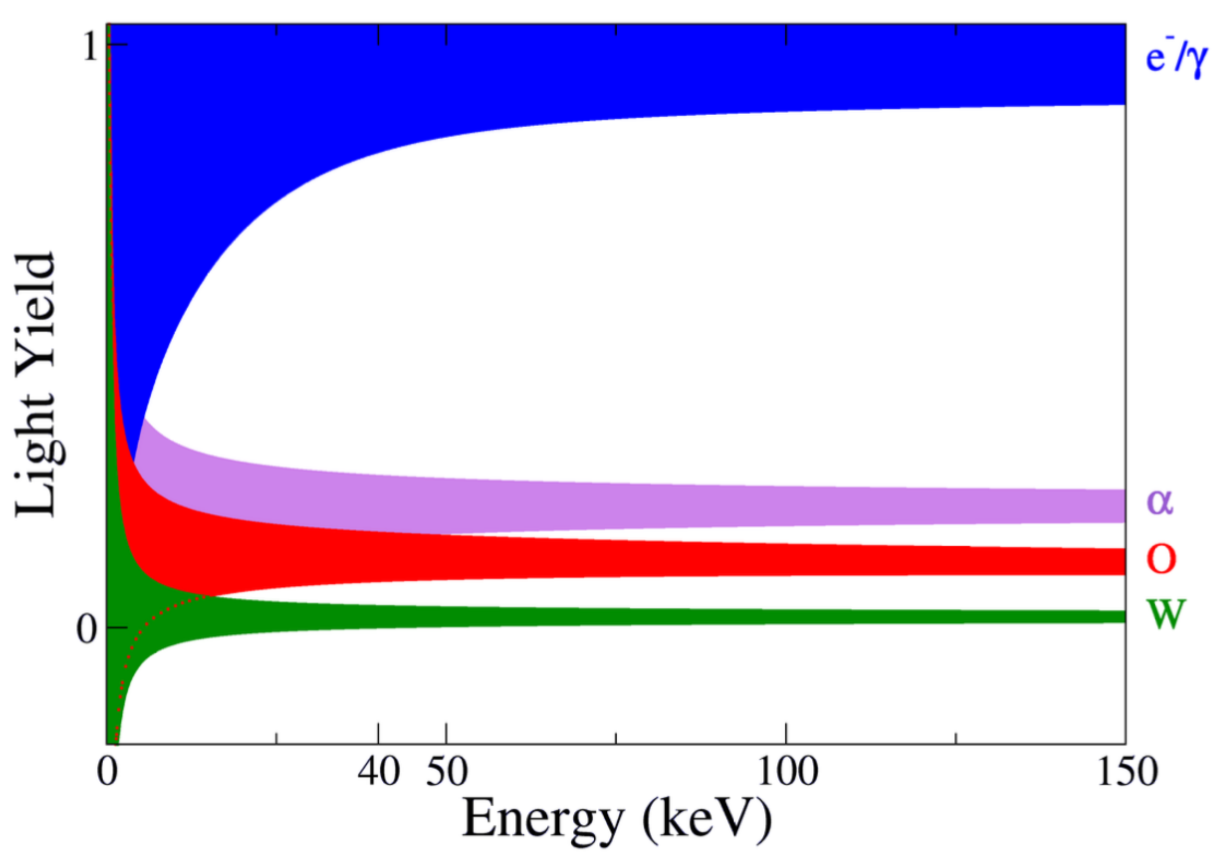

CRESST-III: particle discrimination

$$Light\ Yield\ (LY) = \frac{Light\ pulse\ energy}{Phonon\ pulse\ energy}$$

The events in the LY vs Energy plane distribute along horizontal bands

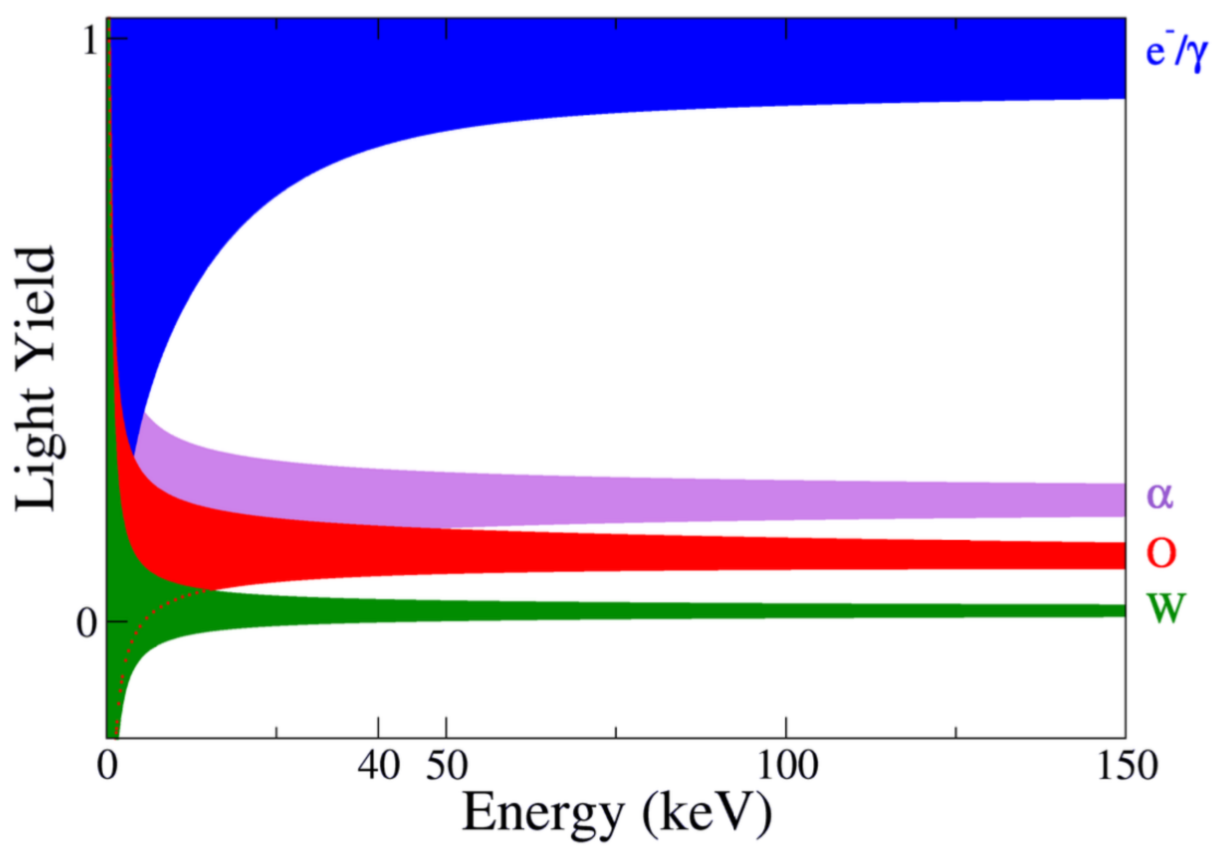

The ratio $LY(X)/LY(e^-)$ is the **Quenching Factor** of the particle X **(QF).**

The QF is smaller as heavier is X.

R. Strauss et al., Energy-Dependent Light Quenching in CaWO4 Crystals at mK Temperatures, Eur.Phys.J.C 74 (2014) 7, 2957

DM search with the CRESST experiment

Cryogenic Rare Event Search with Superconducting Thermometers

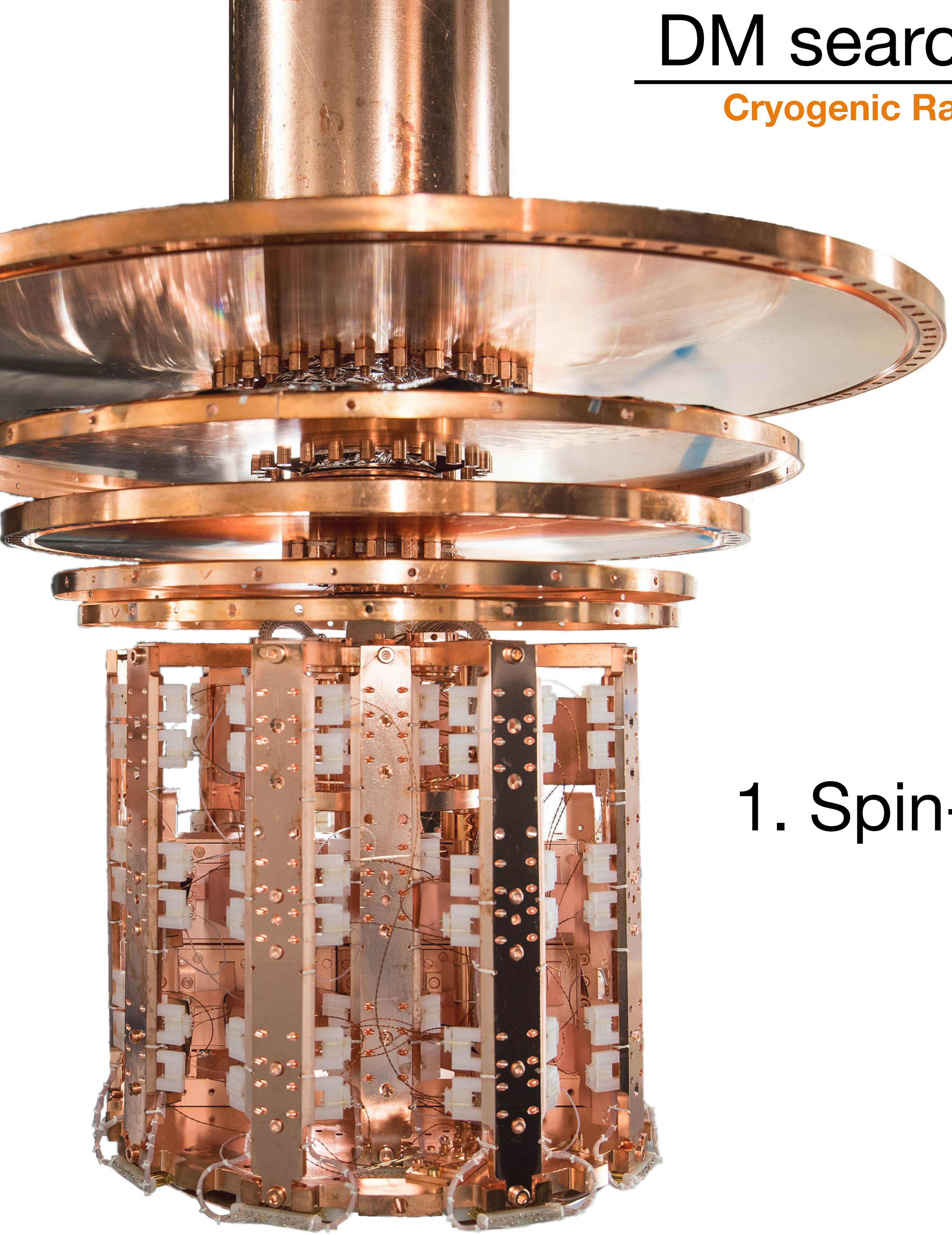

1. Spin-dependent search in ^{7}Li target

Motivation: Lithium target nucleus

1. One of the lightest targets
2. Spin matrix elements $\langle S_{p,n} \rangle \neq 0$
3. Neutron capture $^6Li + n \rightarrow \alpha +^3 H + 4.78\ MeV$

Isotope	Z	Abundance	J_T^P	$\langle S_p \rangle$	$\langle S_n \rangle$	Ref. for $\langle S_N \rangle$
^{6}Li	3	0.0759(4)	1+	0.464(3)	0.464(3)	[198]
^{7}Li	3	0.9241(4)	3/2-	0.497	0.004	[229, 230]

Alex Gnech, Michele Viviani, and Laura Elisa Marcucci. Calculation of the ^{6}Li ground state within the hyperspherical harmonic basis. 4 2020

V. A. Bednyakov and F. Simkovic. Nuclear spin structure in dark matter search: The Zero momentum transfer limit. Phys. Part. Nucl., 36:131-152, 2005. [Fiz. Elem. Chast. Atom. Yadra36,257(2005)].

Goal

Demonstrate the advantage of Li-based target materials for the DM search

A.H. Abdelhameed et al. First results on sub-GeV spin-dependent dark matter interactions with ^{7}Li. Eur. Phys. J. C, 79(7):630, 2019

Motivation: Lithium target nucleus

1. One of the lightest targets
2. Spin matrix elements $\langle S_{p,n} \rangle \neq 0$
3. Neutron capture $^6Li + n \rightarrow \alpha +^3 H + 4.78\ MeV$

Isotope	Z	Abundance	J_T^P	$\langle S_p \rangle$	$\langle S_n \rangle$	Ref. for $\langle S_N \rangle$
^{6}Li	3	0.0759(4)	1+	0.464(3)	0.464(3)	[198]
^{7}Li	3	0.9241(4)	3/2-	0.497	0.004	[229, 230]

[198] Alex Gnech, Michele Viviani, and Laura Elisa Marcucci. Calculation of the ^{6}Li ground state within the hyperspherical harmonic basis. 4 2020

[229, 230] V. A. Bednyakov and F. Simkovic. Nuclear spin structure in dark matter search: The Zero momentum transfer limit. Phys. Part. Nucl., 36:131-152, 2005. [Fiz. Elem. Chast. Atom. Yadra36,257(2005)].

Theoretical framework: conventional SD interactions

$$\frac{\mathrm{d}R}{\mathrm{d}E_R} = \left[\frac{\mathrm{d}R}{\mathrm{d}E_R}\right] \xi \frac{2m_T\ [GeV]}{m_\chi\ [GeV]} \left(\frac{J_T+1}{3J_T}\right) \left(\frac{\mu_T}{\mu_{p/n}}\right)^2 (2\langle S_{p/n}\rangle)^2 \frac{\sigma_{SD}^{p/n}\ [cm^2]}{4\mu_T^2\ [GeV^2]} \cdot \mathcal{I}_{halo} \left[\frac{GeV}{cm^3}\frac{cm}{s}\right]$$

A.H. Abdelhameed et al. First results on sub-GeV spin-dependent dark matter interactions with ^{7}Li. Eur. Phys. J. C, 79(7):630, 2019

DM search with the CRESST experiment

Cryogenic Rare Event Search with Superconducting Thermometers

1. Spin-dependent search in ^{7}Li target

Results

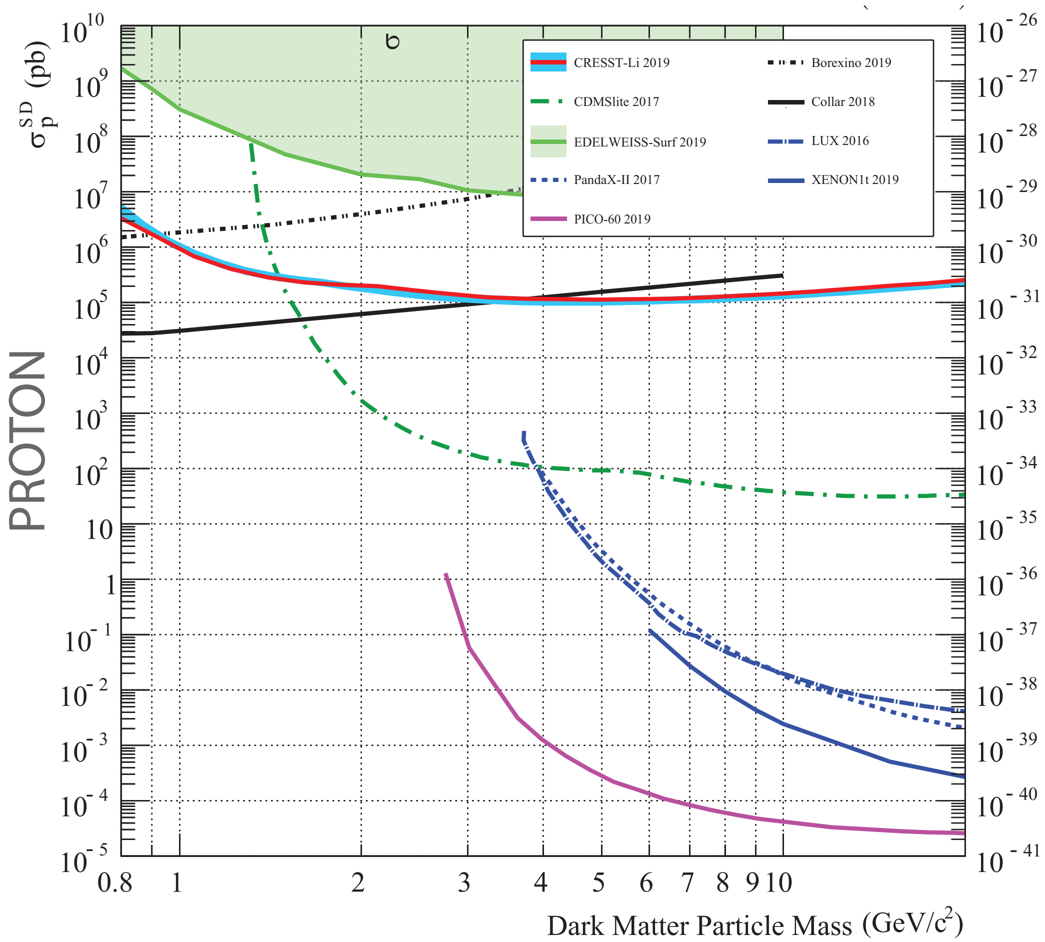

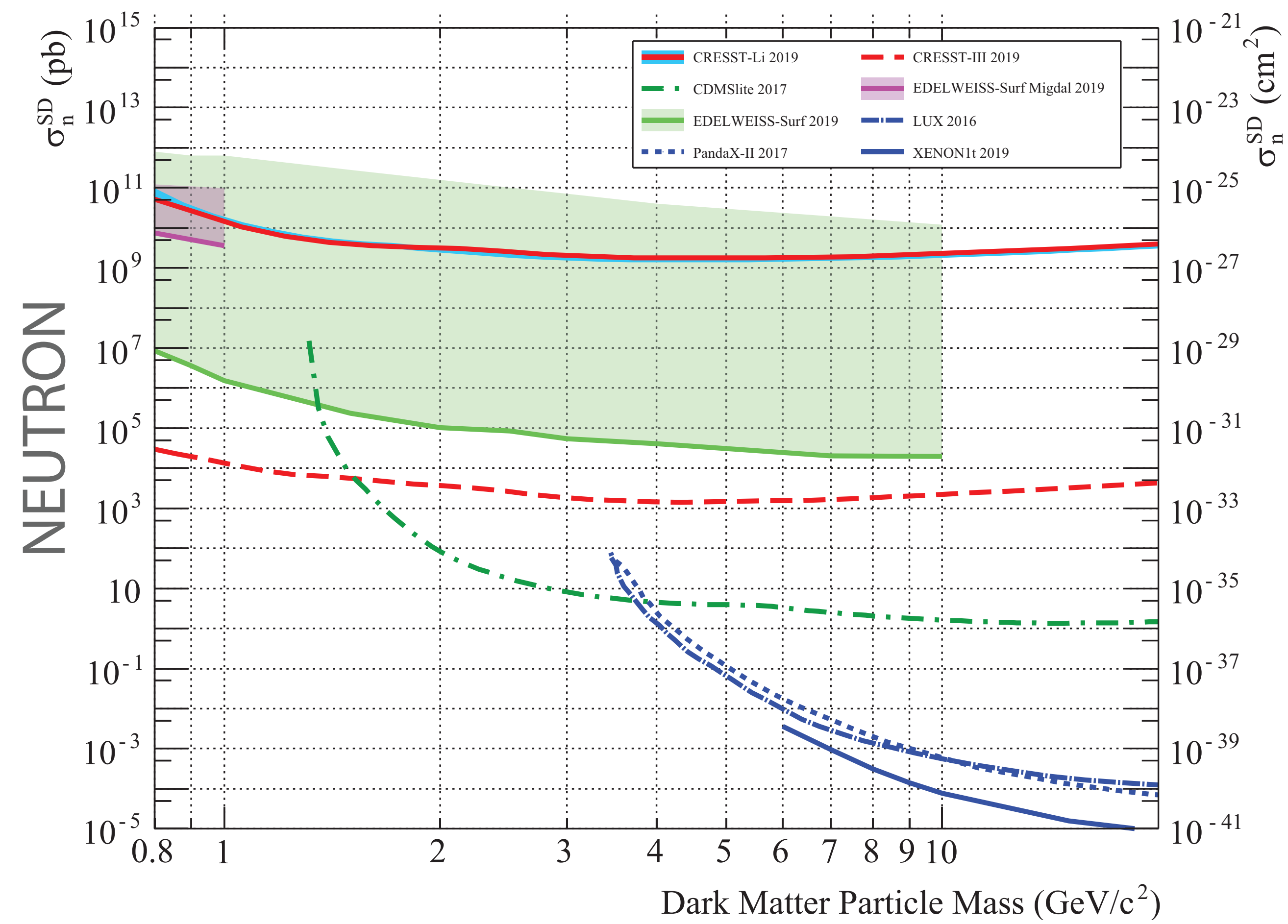

- Small cubic **Li_2MoO_4** (1 cm side)
- Above ground laboratory
- Effective time of 9.68 hours
- Energy threshold of $0.932 \pm 0.012\ keV$

A.H. Abdelhameed et al. First results on sub-GeV spin-dependent dark matter interactions with ^{7}Li. Eur. Phys. J. C, 79(7):630, 2019

GSSI

2. Annual modulation phenomenology in CRESST-III

GSSI

Motivation: CRESST-III data release

2. Annual modulation phenomenology in CRESST-III

A.H. Abdelhameed et al. First results from the CRESST-III low-mass dark matter program. Phys. Rev. D, 100(10):102002, 2019

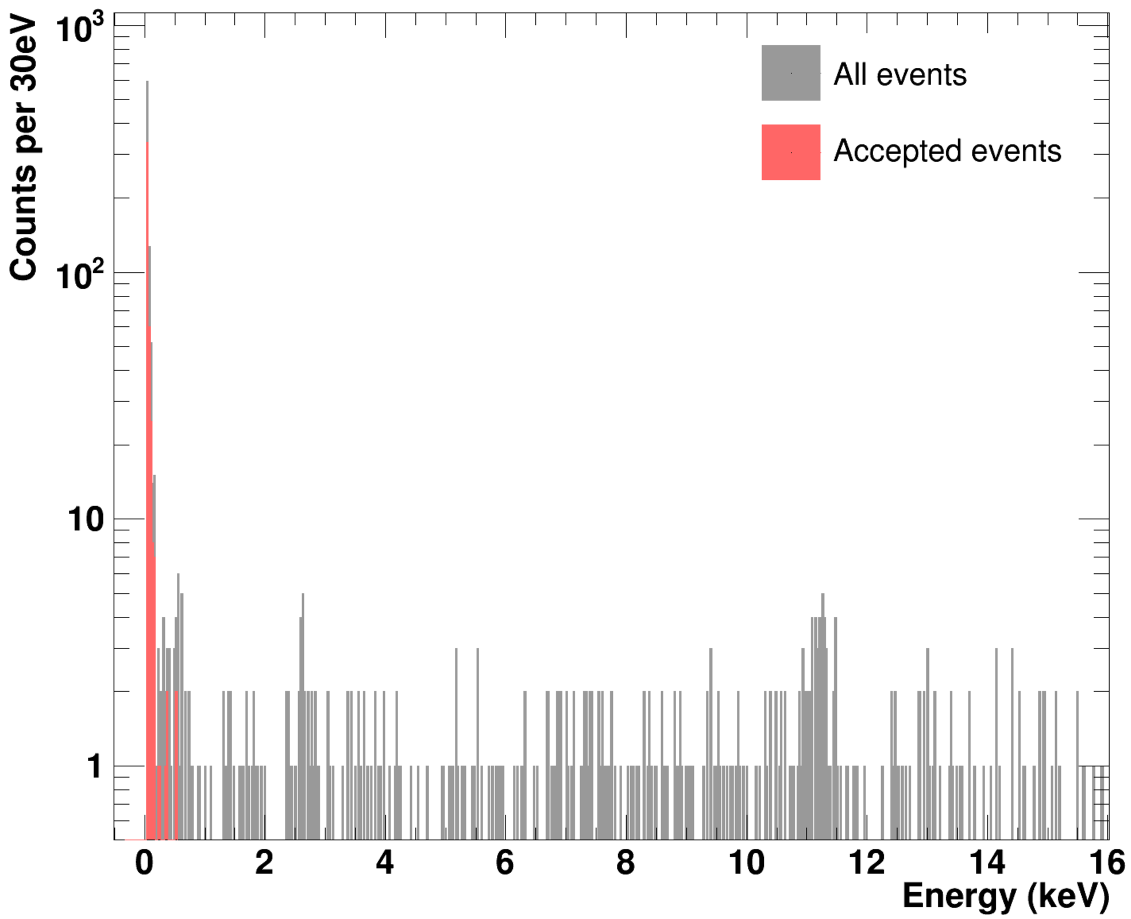

Motivation: CRESST-III data release

2. Annual modulation phenomenology in CRESST-III

A.H. Abdelhameed et al. First results from the CRESST-III low-mass dark matter program. Phys. Rev. D, 100(10):102002, 2019

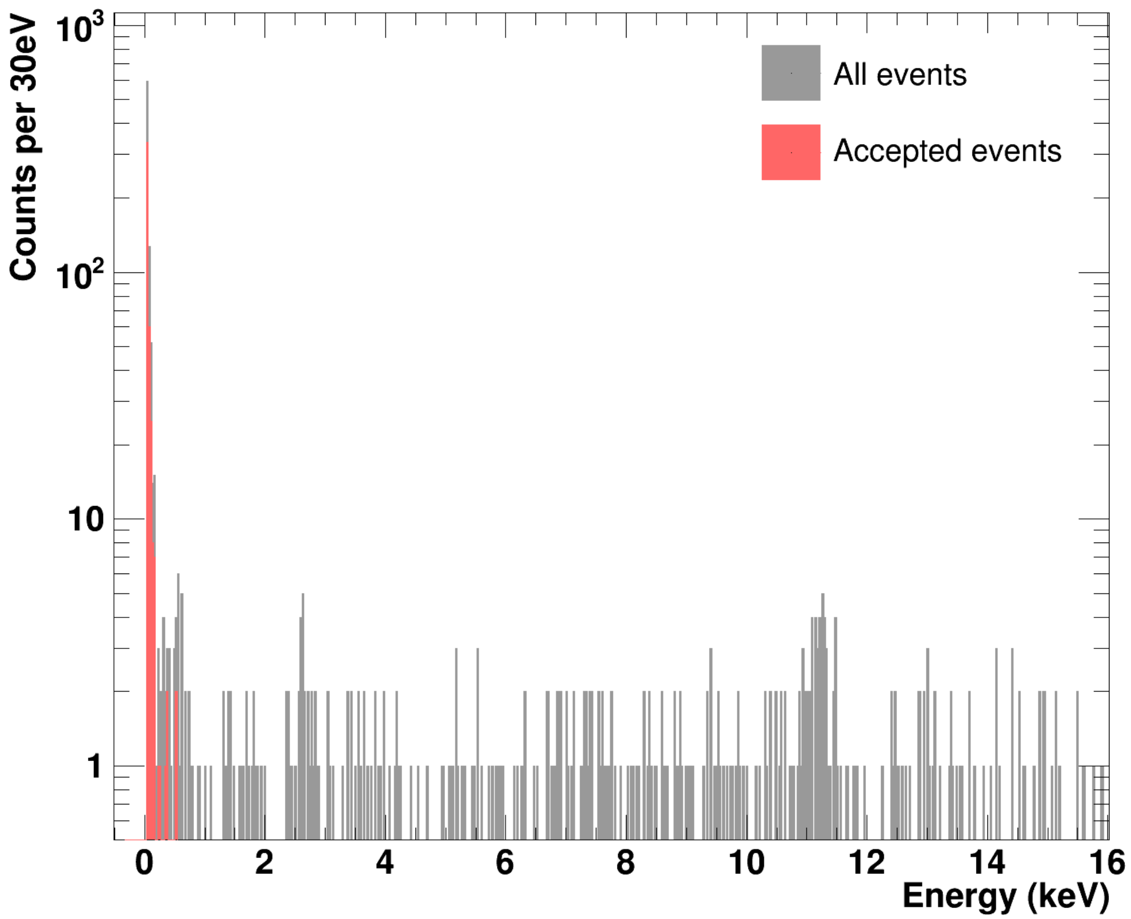

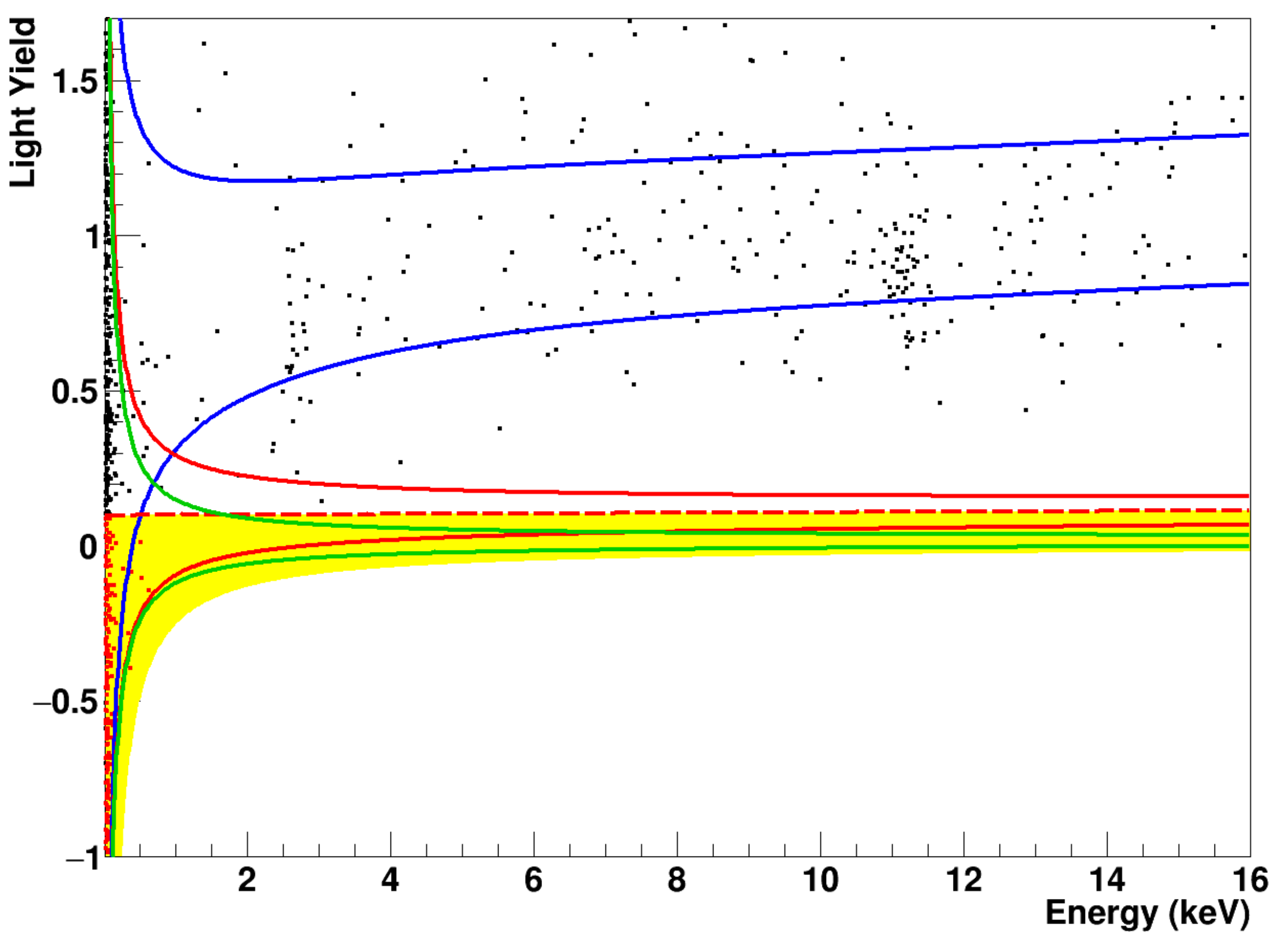

DM search with the CRESST experiment

Cryogenic Rare Event Search with Superconducting Thermometers

Motivation: CRESST-III data release

2. Annual modulation phenomenology in CRESST-III

A.H. Abdelhameed et al. First results from the CRESST-III low-mass dark matter program. Phys. Rev. D, 100(10):102002, 2019

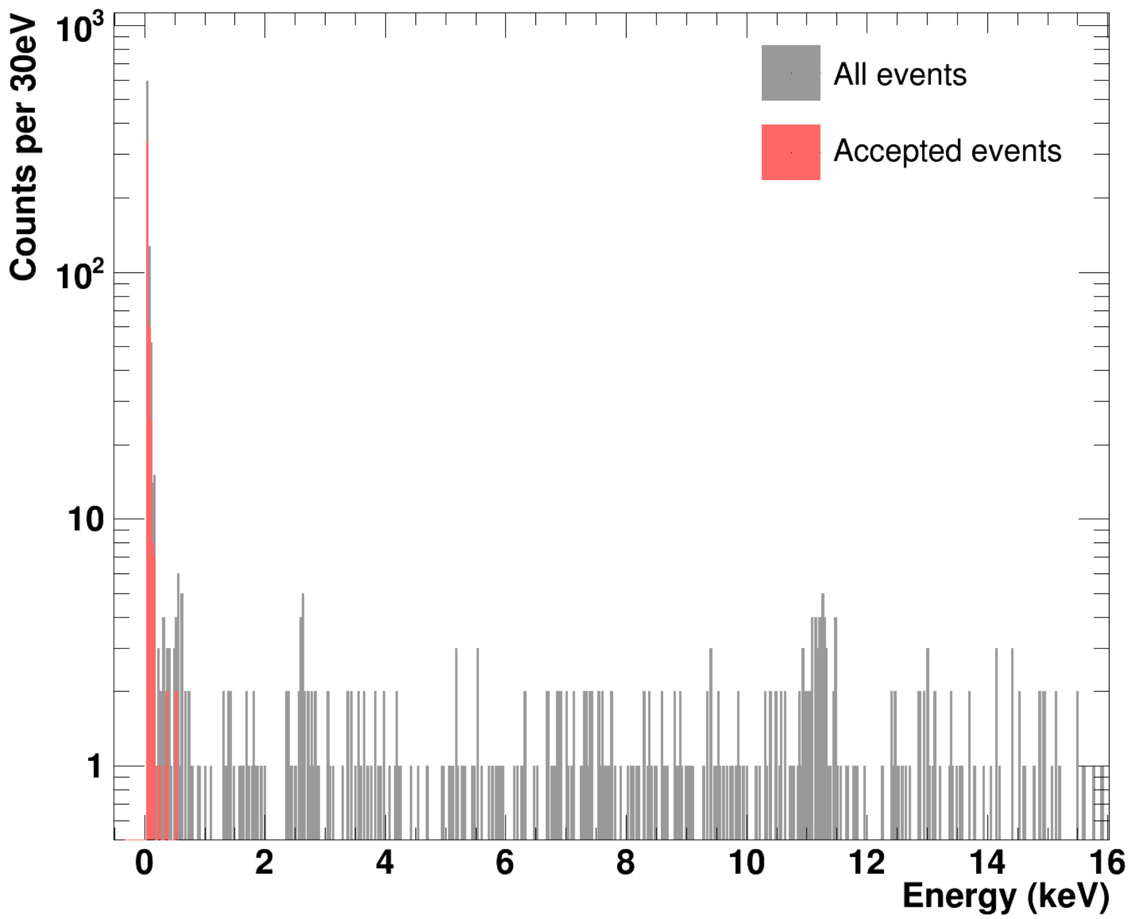

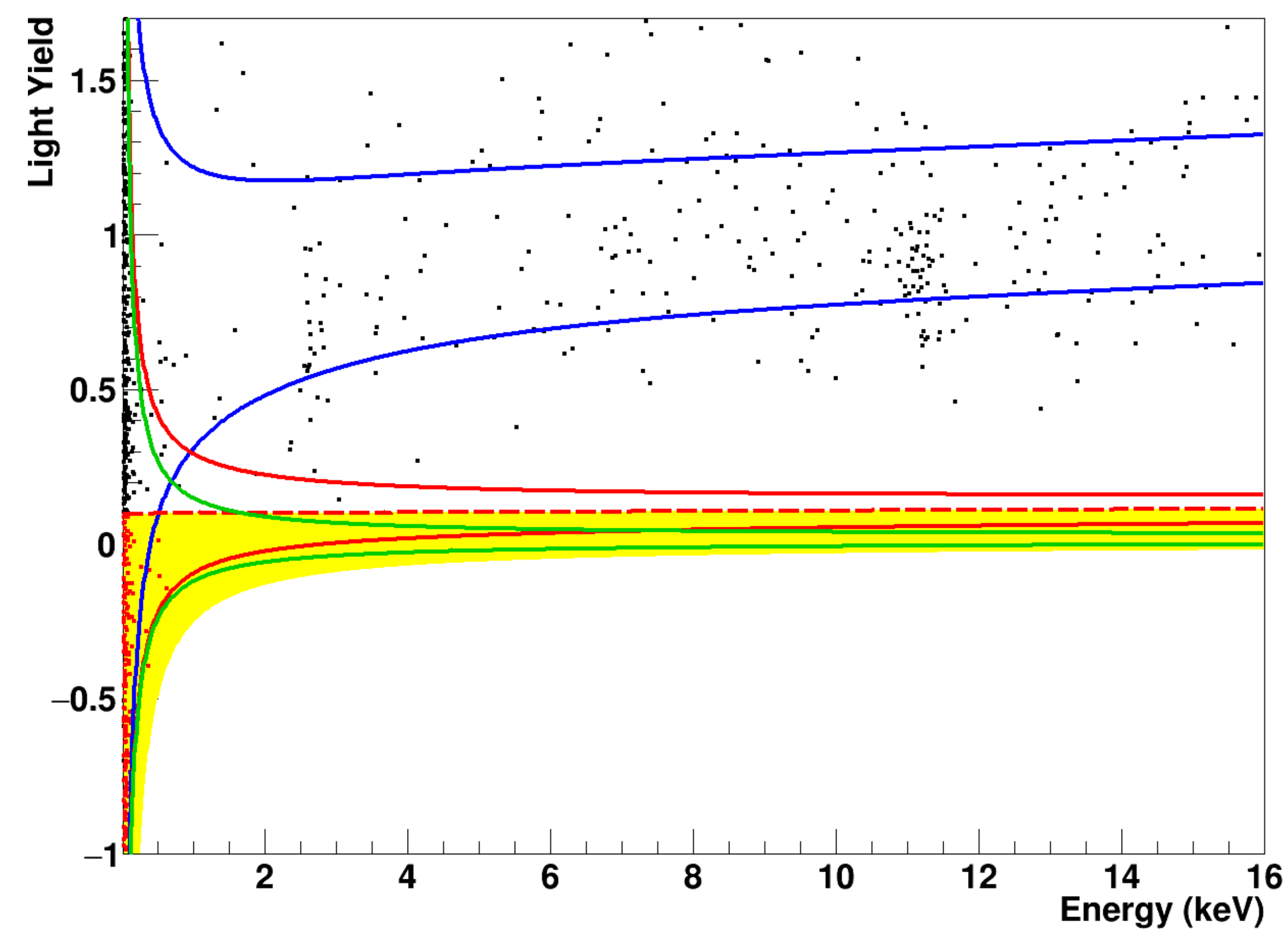

Does time information help DM signal identification,
when a background similar to the excess observed in CRESST-III is present?

Statistical theory

2. Annual modulation phenomenology in CRESST-III

1. The problem of signal discovery

2. The problem of model selection

Statistical theory

2. Annual modulation phenomenology in CRESST-III

1. The problem of signal discovery

$\mathscr{H}_b$

$\mathscr{H}_{b+s}$

Statistical theory

2. Annual modulation phenomenology in CRESST-III

1. The problem of signal discovery

$$\mathscr{H}_b \qquad\qquad \mathscr{H}_{b+s}$$

$$\mathscr{L}(\mathscr{H}_b | b) \qquad \mathscr{L}(\mathscr{H}_b | b + s)$$

Statistical theory

1. The problem of signal discovery

$$
\begin{tikzcd}[column sep=small]
& \mathscr{H}_b \arrow[dl] \arrow[dr] & \\
\mathscr{L}(\mathscr{H}_b | b) & & \mathscr{L}(\mathscr{H}_b | b+s)
\end{tikzcd}
\qquad
\begin{tikzcd}[column sep=small]
& \mathscr{H}_{b+s} \arrow[dl] \arrow[dr] & \\
\mathscr{L}(\mathscr{H}_{b+s} | b) & & \mathscr{L}(\mathscr{H}_{b+s} | b+s)
\end{tikzcd}
$$

Statistical theory

1. The problem of signal discovery

$$\mathcal{H}_b \rightarrow \mathcal{L}(\mathcal{H}_b | b), \quad \mathcal{L}(\mathcal{H}_b | b+s)$$

$$\mathcal{H}_{b+s} \rightarrow \mathcal{L}(\mathcal{H}_{b+s} | b), \quad \mathcal{L}(\mathcal{H}_{b+s} | b+s)$$

$$q_b = -2\, log \left(\frac{\mathcal{L}(\mathcal{H}_b | b)}{\mathcal{L}(\mathcal{H}_b | s+b)} \right)$$

$$q_{b+s} = -2\, log \left(\frac{\mathcal{L}(\mathcal{H}_{b+s} | b)}{\mathcal{L}(\mathcal{H}_{b+s} | s+b)} \right)$$

Statistical theory

1. The problem of signal discovery

$$
\begin{tikzcd}[column sep=small]
 & \mathscr{H}_b \arrow[dl] \arrow[dr] & \\
\mathscr{L}(\mathscr{H}_b | b) & & \mathscr{L}(\mathscr{H}_b | b+s)
\end{tikzcd}
\qquad
\begin{tikzcd}[column sep=small]
 & \mathscr{H}_{b+s} \arrow[dl] \arrow[dr] & \\
\mathscr{L}(\mathscr{H}_{b+s} | b) & & \mathscr{L}(\mathscr{H}_{b+s} | b+s)
\end{tikzcd}
$$

$$q_b = -2\, log \left(\frac{\mathscr{L}(\mathscr{H}_b | b)}{\mathscr{L}(\mathscr{H}_b | s+b)} \right) \qquad q_{b+s} = -2\, log \left(\frac{\mathscr{L}(\mathscr{H}_{b+s} | b)}{\mathscr{L}(\mathscr{H}_{b+s} | s+b)} \right)$$

$$f(q_b) \qquad f(q_{b+s})$$

Statistical theory

1. The problem of signal discovery

$$\mathcal{H}_b \qquad\qquad \mathcal{H}_{b+s}$$

$$\mathcal{L}(\mathcal{H}_b | b) \quad \mathcal{L}(\mathcal{H}_b | b+s) \quad \mathcal{L}(\mathcal{H}_{b+s} | b) \quad \mathcal{L}(\mathcal{H}_{b+s} | b+s)$$

$$q_b = -2\,log\left(\frac{\mathcal{L}(\mathcal{H}_b | b)}{\mathcal{L}(\mathcal{H}_b | s+b)}\right) \qquad q_{b+s} = -2\,log\left(\frac{\mathcal{L}(\mathcal{H}_{b+s} | b)}{\mathcal{L}(\mathcal{H}_{b+s} | s+b)}\right)$$

$$f(q_b) \qquad\qquad f(q_{b+s})$$

p-value

Statistical theory

2. Annual modulation phenomenology in CRESST-III

1. The problem of signal discovery

- The Neyman-Pearson's lemma

$$q = -2\,log\left(\frac{\mathscr{L}(\mathscr{H}\,|\,b)}{\mathscr{L}(\mathscr{H}\,|\,s+b)}\right)$$

Statistical theory

1. The problem of signal discovery

- The Neyman-Pearson's lemma

$$q = -2\ log\left(\frac{\mathcal{L}(\mathcal{H}\,|\,b)}{\mathcal{L}(\mathcal{H}\,|\,s+b)}\right)$$

- The profile-likelihood method

$$q = -2\ log\left(\frac{\mathcal{L}(\mathcal{H}\,|\,b(\hat{\hat{\theta}}))}{\mathcal{L}(\mathcal{H}\,|\,\hat{\mu}s+b(\hat{\theta}))}\right)$$

Statistical theory

1. The problem of signal discovery

- The Neyman-Pearson's lemma

$$q = -2\,log\left(\frac{\mathcal{L}(\mathcal{H}\,|\,b)}{\mathcal{L}(\mathcal{H}\,|\,s+b)}\right)$$

- The profile-likelihood method

$$q = -2\,log\left(\frac{\mathcal{L}(\mathcal{H}\,|\,b(\hat{\hat{\theta}}))}{\mathcal{L}(\mathcal{H}\,|\,\hat{\mu}s+b(\hat{\theta}))}\right)$$

2. The problem of model discrimination

Statistical theory

2. Annual modulation phenomenology in CRESST-III

1. The problem of signal discovery

- The Neyman-Pearson's lemma

$$q = -2\ log \left(\frac{\mathscr{L}(\mathscr{H}\,|\,b)}{\mathscr{L}(\mathscr{H}\,|\,s+b)} \right)$$

- The profile-likelihood method

$$q = -2\ log \left(\frac{\mathscr{L}(\mathscr{H}\,|\,b(\hat{\hat{\theta}}))}{\mathscr{L}(\mathscr{H}\,|\,\hat{\mu}s + b(\hat{\theta}))} \right)$$

2. The problem of model discrimination

- The profile-likelihood method

$$q_0 = -2\ log \frac{\mathscr{L}(\mathscr{H}_0\,|\,s_0 + b(\hat{\theta}))}{\mathscr{L}(\mathscr{H}_0\,|\,s_a + b(\hat{\theta}))}$$

$$q_a = -2\ log \frac{\mathscr{L}(\mathscr{H}_a\,|\,s_0 + b(\hat{\theta}))}{\mathscr{L}(\mathscr{H}_a\,|\,s_a + b(\hat{\theta}))}$$

Statistical theory

1. The problem of signal discovery

- The Neyman-Pearson's lemma

$$q = -2\, log \left(\frac{\mathcal{L}(\mathcal{H}\,|\,b)}{\mathcal{L}(\mathcal{H}\,|\,s+b)} \right)$$

- The profile-likelihood method

$$q = -2\, log \left(\frac{\mathcal{L}(\mathcal{H}\,|\,b(\hat{\hat{\theta}}))}{\mathcal{L}(\mathcal{H}\,|\,\hat{\mu}s+b(\hat{\theta}))} \right)$$

2. The problem of model discrimination

- The profile-likelihood method

$$q_0 = -2\, log \frac{\mathcal{L}(\mathcal{H}_0\,|\,s_0+b(\hat{\theta}))}{\mathcal{L}(\mathcal{H}_0\,|\,s_a+b(\hat{\theta}))}$$

$$q_a = -2\, log \frac{\mathcal{L}(\mathcal{H}_a\,|\,s_0+b(\hat{\theta}))}{\mathcal{L}(\mathcal{H}_a\,|\,s_a+b(\hat{\theta}))}$$

$s_0 \rightarrow$ SI-model

$s_a \rightarrow$ MDDM-model

Background simulation

$$\frac{dN_b}{dE} = p_0 + p_1\, E + p_2\, e^{-E/p_3} + N_M\ \mathrm{Gauss}(E, E_M, \sigma_M) + N_L\ \mathrm{Gauss}(E, E_L, \sigma_L)$$

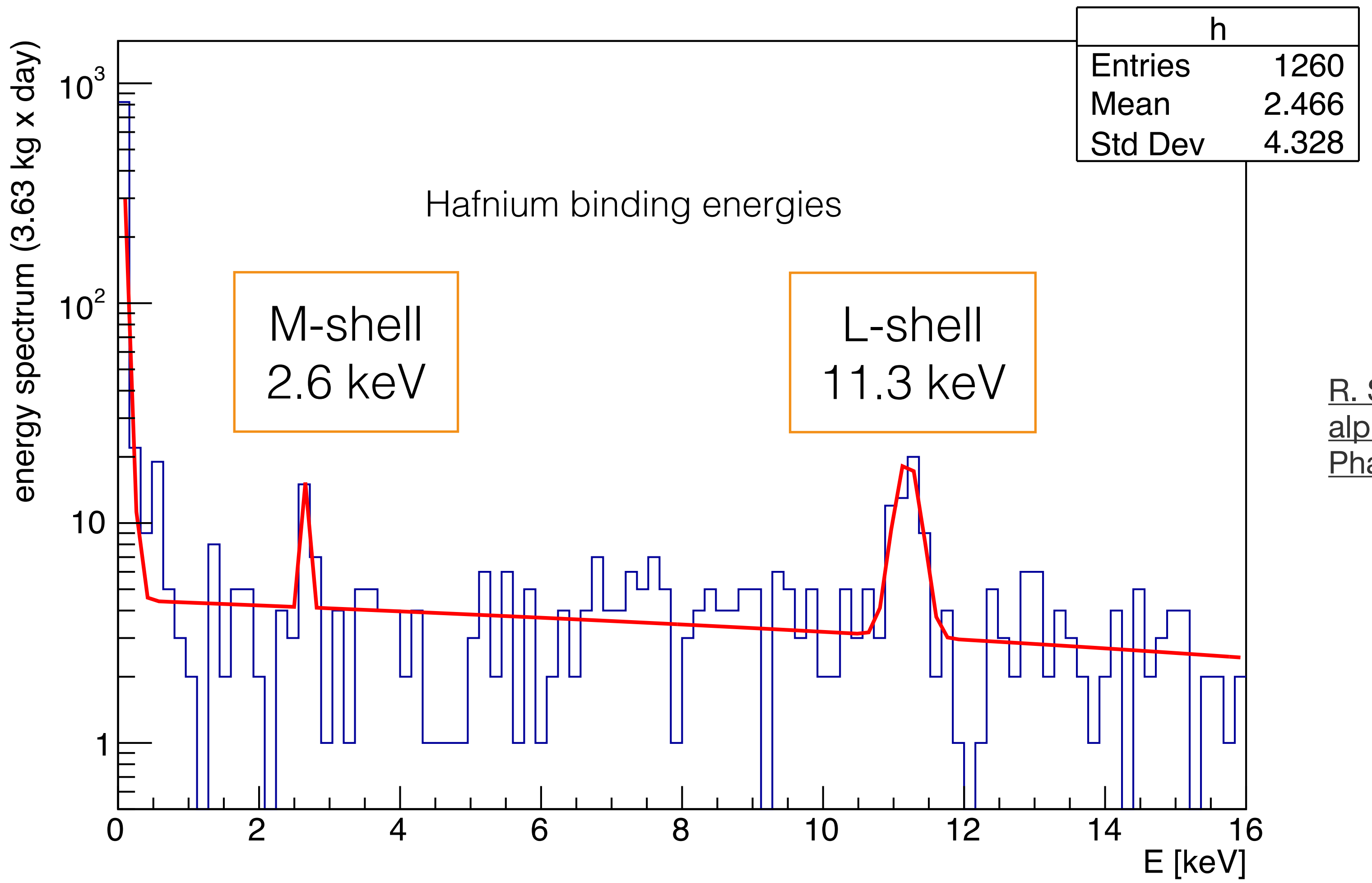

R. Strauss et al., Beta/gamma and alpha backgrounds in CRESST-II Phase 2 JCAP06(2015)030

$$\boxed{\frac{dN_b}{dE} = \bar{p}_0 + \bar{p}_1\, E + \bar{p}_2\, e^{-E/\bar{p}_3}}$$

2019 D. Schmiedmayer
Master thesis

Signal simulation

1. Problem of signal discovery

Benchmarks

$$m_\chi = 11.7\ \text{GeV/c}^2, \quad \sigma_0^p = 2.67 \cdot 10^{-38}\ \text{cm}^2 \quad \text{and} \quad r = \frac{c_1^n}{c_1^p} = -0.76$$

DAMA/LIBRA best fit parameters
PoS, ICHEP2018:353, 2019.

Signal simulation

1. Problem of signal discovery

Benchmarks

$m_\chi = 11.7$ GeV/c², $\sigma_0^p = 2.67 \cdot 10^{-38}$ cm² and $r = \frac{c_1^n}{c_1^p} = -0.76$

DAMA/LIBRA best fit parameters
PoS, ICHEP2018:353, 2019.

$m_\chi = 3.00$ GeV/c², $\sigma_0^p = 4 \cdot 10^{-42}$ cm² and $r = \frac{c_1^n}{c_1^p} = 1$

DarkSide upper limit
Phys. Rev. Lett., 121(8):081307, 2018.

Signal simulation

1. Problem of signal discovery

Benchmarks

$$m_\chi = 11.7 \text{ GeV/c}^2, \quad \sigma_0^p = 2.67 \cdot 10^{-38} \text{ cm}^2 \quad \text{and} \quad r = \frac{c_1^n}{c_1^p} = -0.76$$

DAMA/LIBRA best fit parameters
PoS, ICHEP2018:353, 2019.

$$m_\chi = 3.00 \text{ GeV/c}^2, \quad \sigma_0^p = 4 \cdot 10^{-42} \text{ cm}^2 \quad \text{and} \quad r = \frac{c_1^n}{c_1^p} = 1$$

DarkSide upper limit
Phys. Rev. Lett., 121(8):081307, 2018.

$m_\chi > 3.00 \text{ GeV/c}^2$

Target: ^{27}Al

$E_R \lesssim 200$ eV

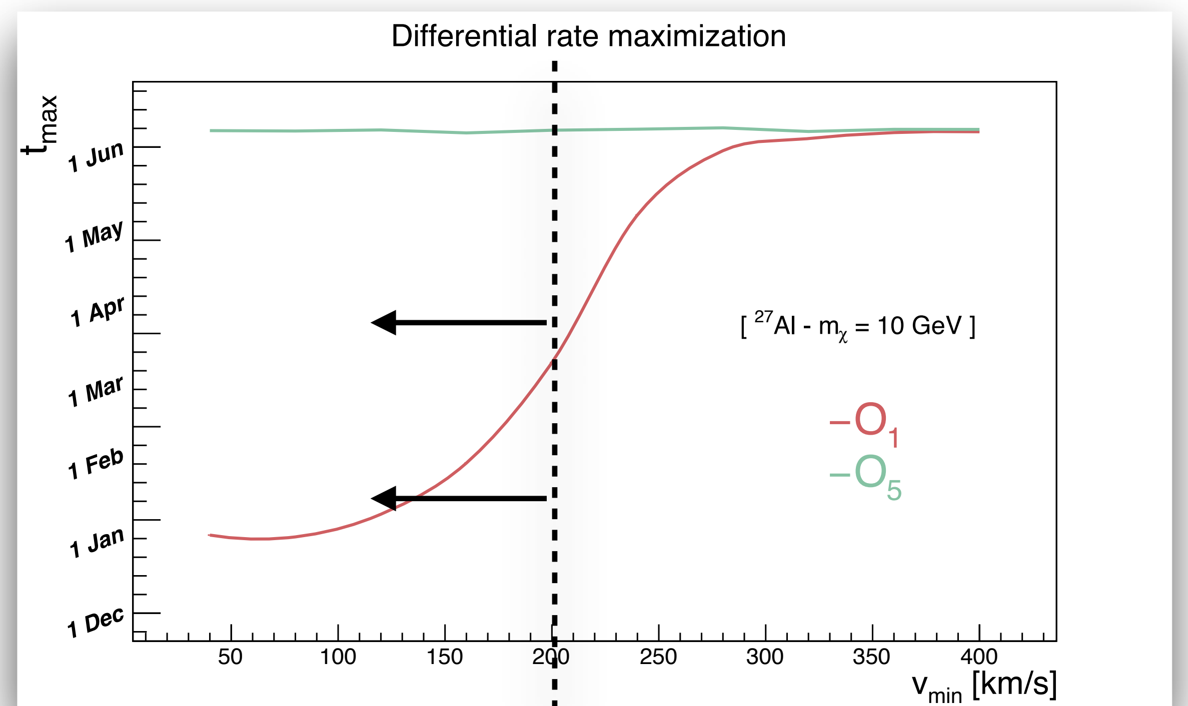

Signal simulation

1. Problem of signal discovery

Benchmarks

$m_\chi = 11.7$ GeV/c^2, $\sigma_0^p = 2.67 \cdot 10^{-38}$ cm^2 and $r = \frac{c_1^n}{c_1^p} = -0.76$

DAMA/LIBRA best fit parameters
PoS, ICHEP2018:353, 2019.

$m_\chi = 3.00$ GeV/c^2, $\sigma_0^p = 4 \cdot 10^{-42}$ cm^2 and $r = \frac{c_1^n}{c_1^p} = 1$

DarkSide upper limit
Phys. Rev. Lett., 121(8):081307, 2018.

2. Problem of model selection

$m_\chi = 3.00$ GeV/c^2, $\sigma_0^p = 4 \cdot 10^{-42}$ cm^2 and $r = \frac{c_1^n}{c_1^p} = 1$

For the SI-model

Signal simulation

1. Problem of signal discovery

Benchmarks

$m_\chi = 11.7$ GeV/c^2, $\sigma_0^p = 2.67 \cdot 10^{-38}$ cm^2 and $r = \frac{c_1^n}{c_1^p} = -0.76$

DAMA/LIBRA best fit parameters
PoS, ICHEP2018:353, 2019.

$m_\chi = 3.00$ GeV/c^2, $\sigma_0^p = 4 \cdot 10^{-42}$ cm^2 and $r = \frac{c_1^n}{c_1^p} = 1$

DarkSide upper limit
Phys. Rev. Lett., 121(8):081307, 2018.

2. Problem of model selection

$m_\chi = 3.00$ GeV/c^2, $\sigma_0^p = 4 \cdot 10^{-42}$ cm^2 and $r = \frac{c_1^n}{c_1^p} = 1$

For the SI-model

$m_\chi = 3.00$ GeV/c^2, $\sigma_{MD} = 4.72 \cdot 10^{-41}$ cm^2

corresponding MDDM benchmark

G S
S I

Results

1. Problem of signal discovery

Example for *known* background

m_T	time	λ_b	λ_s	N inter	p-value 1D	p-value 2D
23 g	1 yr	10^3	$\simeq 141$	10^3	$\simeq 0$	$\simeq 0$
"	"	10^4	"	"	0.046	0.045
"	"	10^5	"	"	0.284	0.247
2 x 23g	"	"	283	"	0.161	0.163
3 x 23g	"	"	424	"	0.055	0.077

In the conditions considered,
the annual modulation search does not improve the significance power
for the signal discovery

Results

2. Problem of model selection

$$m_\chi = 3.00 \text{ GeV/c}^2, \quad \sigma_0^p = 4 \cdot 10^{-42} \text{ cm}^2 \quad \text{and} \quad r = \frac{c_1^n}{c_1^p} = 1$$

$$m_\chi = 3.00 \text{ GeV/c}^2, \quad \sigma_{MD} = 4.72 \cdot 10^{-41} \text{ cm}^2$$ corresponding MDDM benchmark

m_χ	m_T	time	λ_b	λ_s	N inter	p-value 1D	p-value 2D
3 GeV/c^2	23 g	1 yr	10^3	$\simeq 2.2$	10^3	0.467	0.338
"	230 g	2 yr	$2 \cdot 10^3$	$\simeq 44$	"	0.101	0.145
"	"	5 yr	$5 \cdot 10^3$	$\simeq 110$	"	0.056 (0.02, 0.021)	0.024 (0.025)
"	1 kg	"	$2 \cdot 10^4$	$\simeq 478$	"	$\simeq 0$	$\simeq 0$

Results

2. Problem of model selection

$$m_\chi = 3.00\ \text{GeV/c}^2, \quad \sigma_0^p = 4 \cdot 10^{-42}\ \text{cm}^2 \quad \text{and} \quad r = \frac{c_1^n}{c_1^p} = 1$$

$$m_\chi = 3.00\ \text{GeV/c}^2, \quad \sigma_{MD} = 4.72 \cdot 10^{-41}\ \text{cm}^2$$ corresponding MDDM benchmark

Additional observation

m_χ	m_T	time	λ_b	λ_s	N inter	p-value 1D	p-value 2D
3 GeV/c^2	23 g	1 yr	10^3	$\simeq 2.2$	10^3	0.467	0.338
"	230 g	2 yr	$2 \cdot 10^3$	$\simeq 44$	"	0.101	0.145
"	"	5 yr	$5 \cdot 10^3$	$\simeq 110$	"	0.056 (0.02, 0.021)	0.024 (0.025)
"	1 kg	"	$2 \cdot 10^4$	$\simeq 478$	"	$\simeq 0$	$\simeq 0$

Results

2. Problem of model selection

$$m_\chi = 3.00 \text{ GeV/c}^2, \quad \sigma_0^p = 4 \cdot 10^{-42} \text{ cm}^2 \quad \text{and} \quad r = \frac{c_1^n}{c_1^p} = 1$$

$$m_\chi = 3.00 \text{ GeV/c}^2, \quad \sigma_{MD} = 4.72 \cdot 10^{-41} \text{ cm}^2$$ corresponding MDDM benchmark

Additional observation

m_χ	m_T	time	λ_b	λ_s	N inter	p-value 1D	p-value 2D
3 GeV/c^2	23 g	1 yr	10^3	$\simeq 2.2$	10^3	0.467	0.338
"	230 g	2 yr	$2 \cdot 10^3$	$\simeq 44$	"	0.101	0.145
"	"	5 yr	$5 \cdot 10^3$	$\simeq 110$	"	0.056 (0.02, 0.021)	0.024 (0.025)
"	1 kg	"	$2 \cdot 10^4$	$\simeq 478$	"	$\simeq 0$	$\simeq 0$

With detector efficiency of 50-70% in each bin

0.453
0.229
0.175
0.129

Results

2. Problem of model selection

$$m_\chi = 3.00\ \text{GeV/c}^2, \quad \sigma_0^p = 4 \cdot 10^{-42}\ \text{cm}^2 \quad \text{and} \quad r = \frac{c_1^n}{c_1^p} = 1$$

$$m_\chi = 3.00\ \text{GeV/c}^2, \quad \sigma_{MD} = 4.72 \cdot 10^{-41}\ \text{cm}^2$$ corresponding MDDM benchmark

Additional observation

m_χ	m_T	time	λ_b	λ_s	N inter	p-value 1D	p-value 2D
3 GeV/c^2	23 g	1 yr	10^3	$\simeq 2.2$	10^3	0.467	0.338
"	230 g	2 yr	$2 \cdot 10^3$	$\simeq 44$	"	0.101	0.145
"	"	5 yr	$5 \cdot 10^3$	$\simeq 110$	"	0.056 (0.02, 0.021)	0.024 (0.025)
"	1 kg	"	$2 \cdot 10^4$	$\simeq 478$	"	$\simeq 0$	$\simeq 0$

With detector efficiency of 50-70% in each bin

			0.453
			0.229
			0.175
			0.129
1 kg	2 yr	$5 \cdot 10^3$	0.072

COSINUS
phenomenology

G S
S I

COSINUS: Cryogenic calorimeter based on **NaI crystals**

COSINUS
phenomenology

INFN
LNGS
Istituto Nazionale di Fisica Nucleare
Laboratori Nazionali del Gran Sasso

GSSI

COSINUS: Cryogenic calorimeter based on **NaI crystals**

COSINUS phenomenology

INFN LNGS
Istituto Nazionale di Fisica Nucleare
Laboratori Nazionali del Gran Sasso

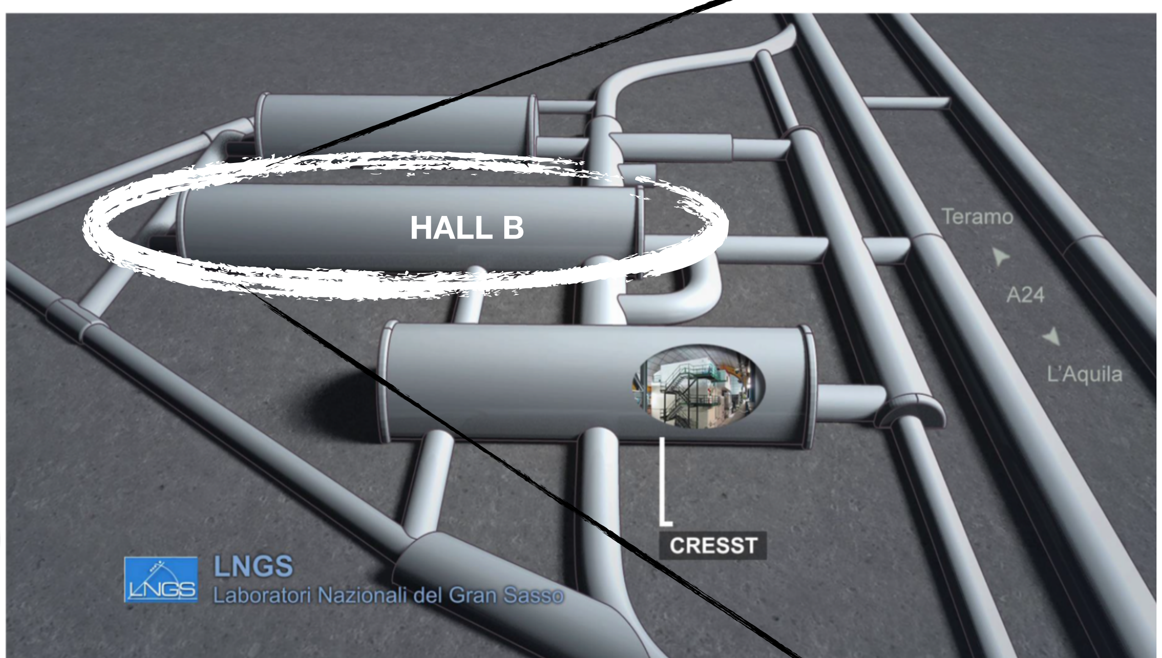

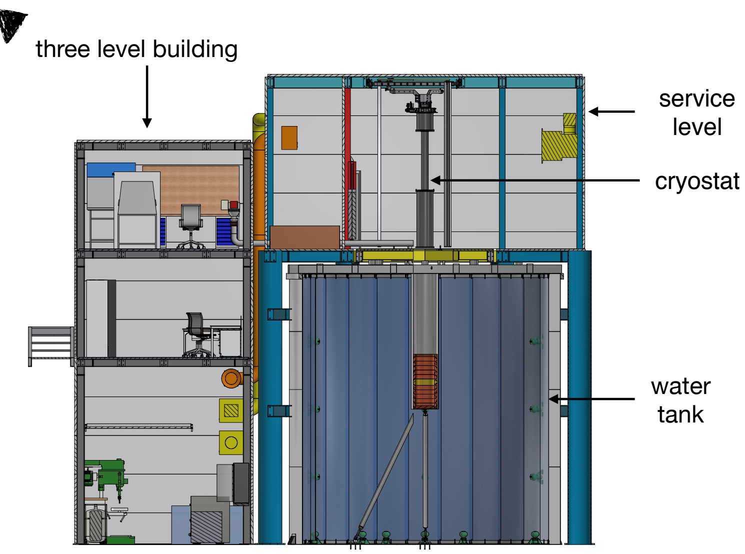

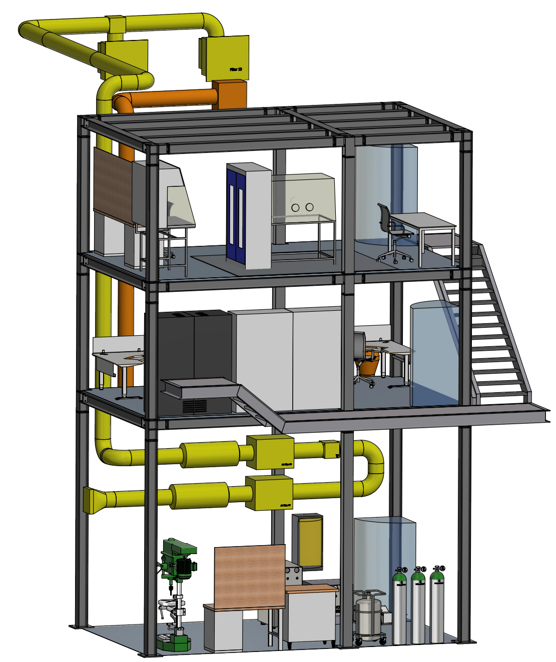

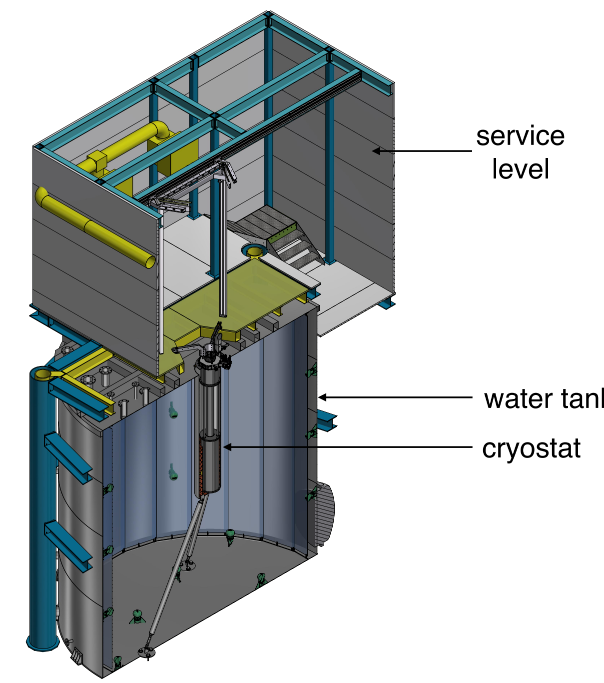

G S S I

COSINUS: Cryogenic calorimeter based on **NaI crystals**

COSINUS
phenomenology

Scientific motivation

Provide a target and model independent cross-check of DAMA/LIBRA results

G S
S I

COSINUS: Cryogenic calorimeter based on **NaI crystals**

Scientific motivation

COSINUS phenomenology

Provide a target and model independent cross-check of DAMA/LIBRA results

Single-channel

- DAMA/LIBRA
- COSINE-100
- ANAIS-112
- SABRE
- PICO-Ion

WORKING PRINCIPLE

Room temperature scintillators searching for modulation

Dual-channel

- COSINUS

WORKING PRINCIPLE

Cryogenic scintillating calorimeter which discriminates nuclear recoil events from β/γ-events

COSINUS: Cryogenic calorimeter based on **NaI crystals**

Experimental concept

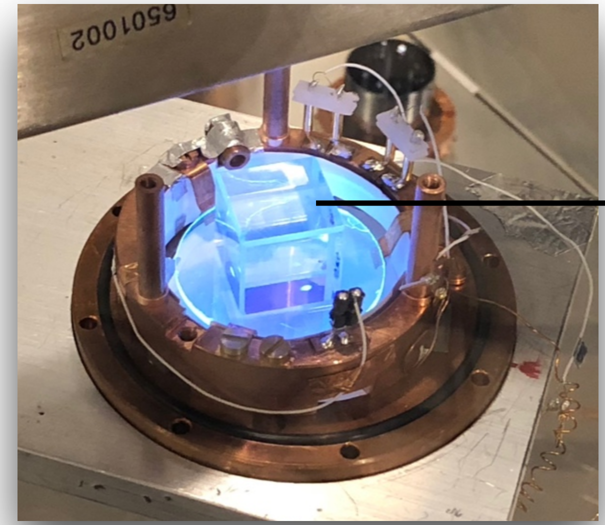

Phonon-channel

NaI crystal, "Absorber"

COSINUS: Cryogenic calorimeter based on NaI crystals

COSINUS phenomenology

Experimental concept

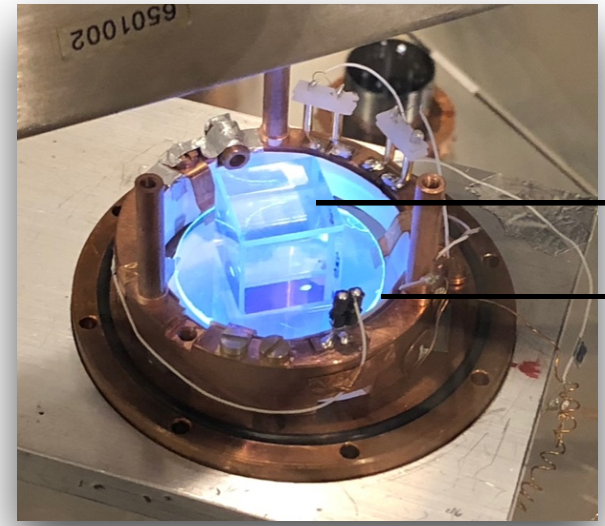

Phonon-channel

NaI crystal, "Absorber"

Crystal of harder material (e.g. $CdWO_4$) which carries the TES, "Carrier"

COSINUS: Cryogenic calorimeter based on **NaI crystals**

COSINUS phenomenology

Experimental concept

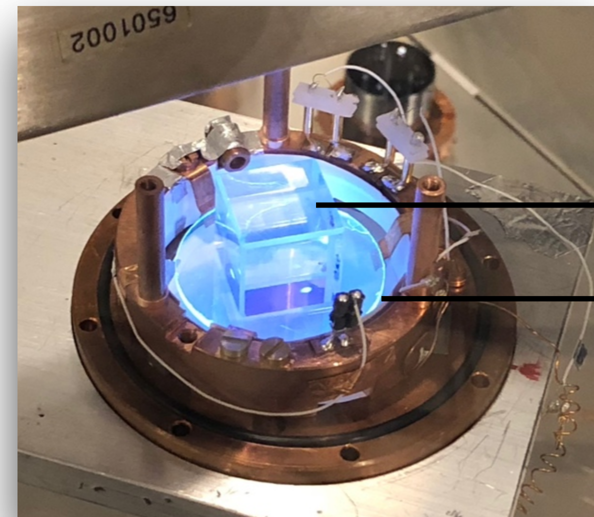

Phonon-channel

NaI crystal, "Absorber"

Crystal of harder material (e.g. $CdWO_4$) which carries the TES, "Carrier"

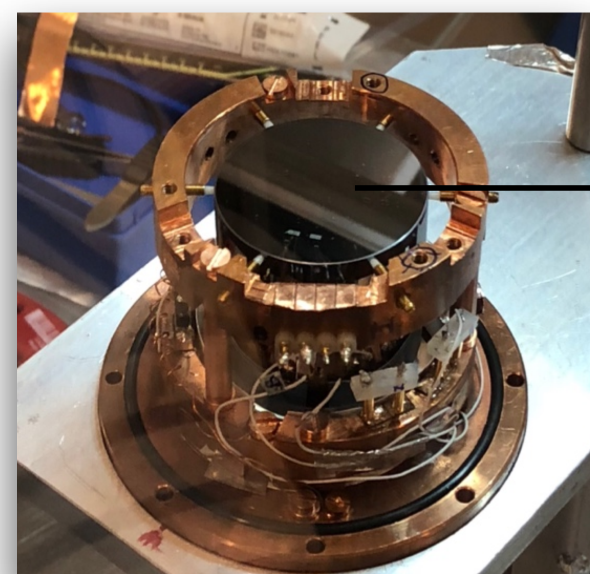

Light-channel

Silicon beaker, "Light absorber", equipped with a TES

G S S I

AVANCEZ 1829

COSINUS: Cryogenic calorimeter based on **NaI crystals**

COSINUS phenomenology

Experimental concept

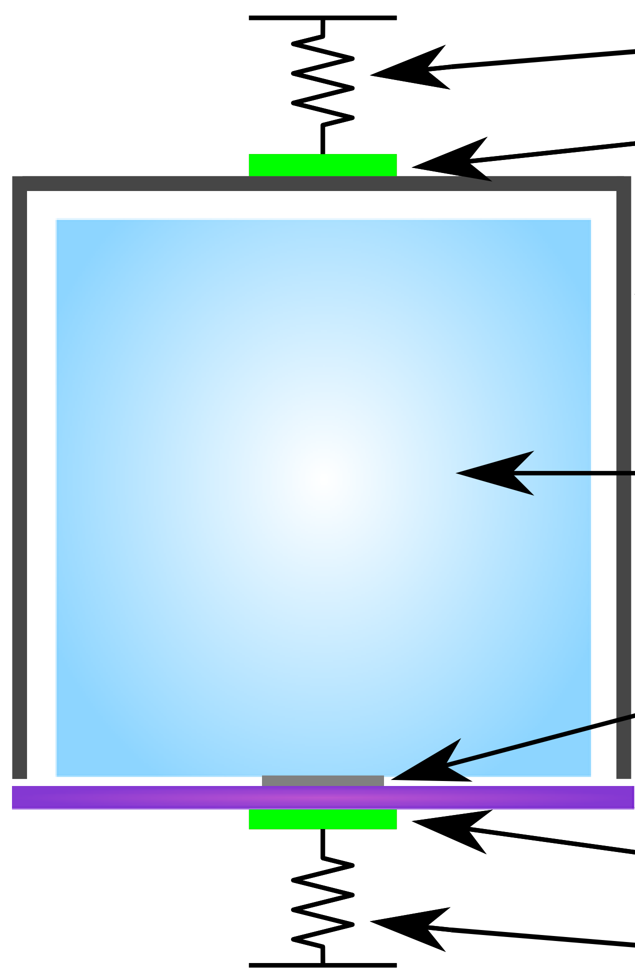

GSSI

COSINUS
phenomenology

Experimental concept

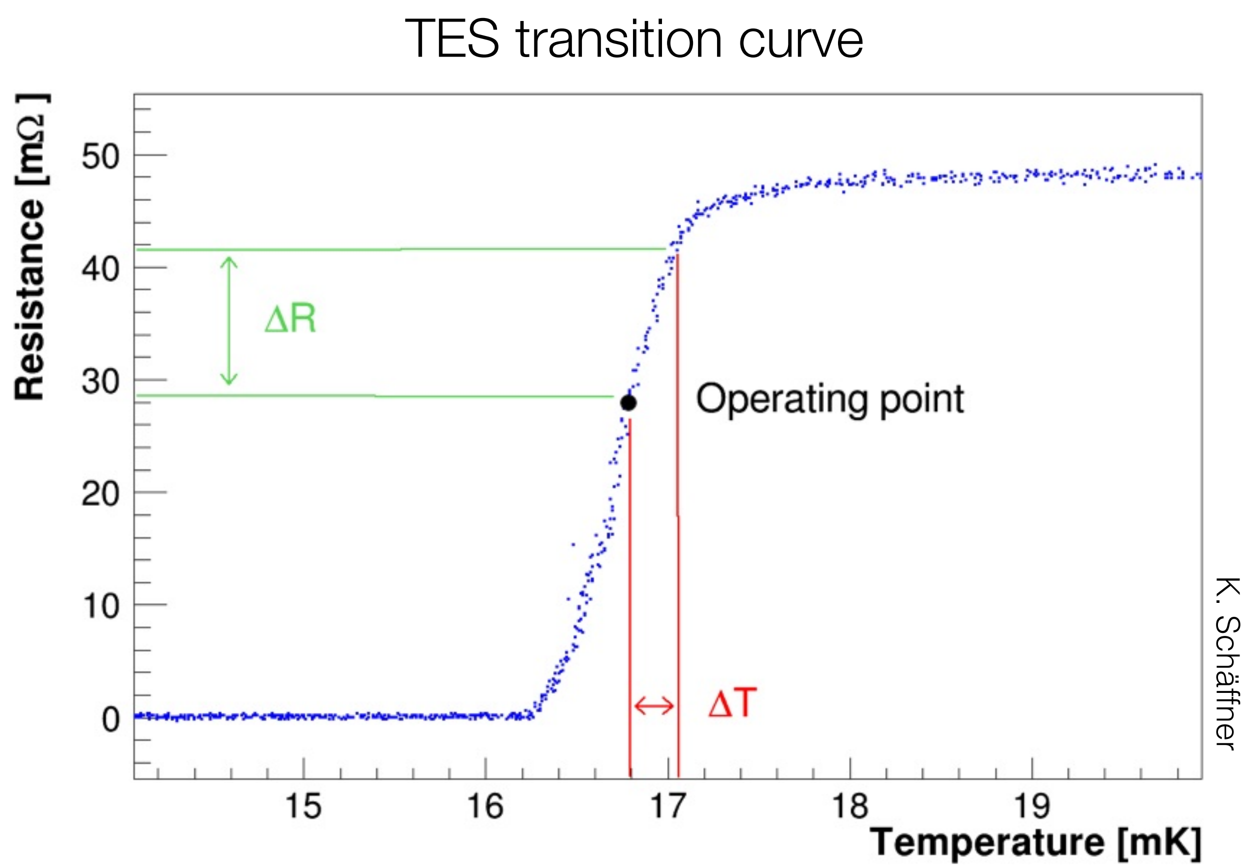

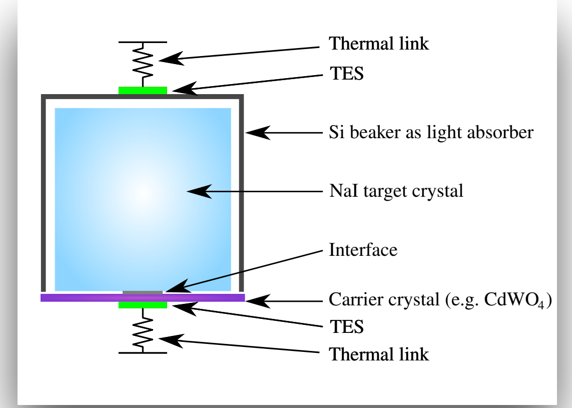

COSINUS: Cryogenic calorimeter based on NaI crystals

COSINUS phenomenology

Experimental concept

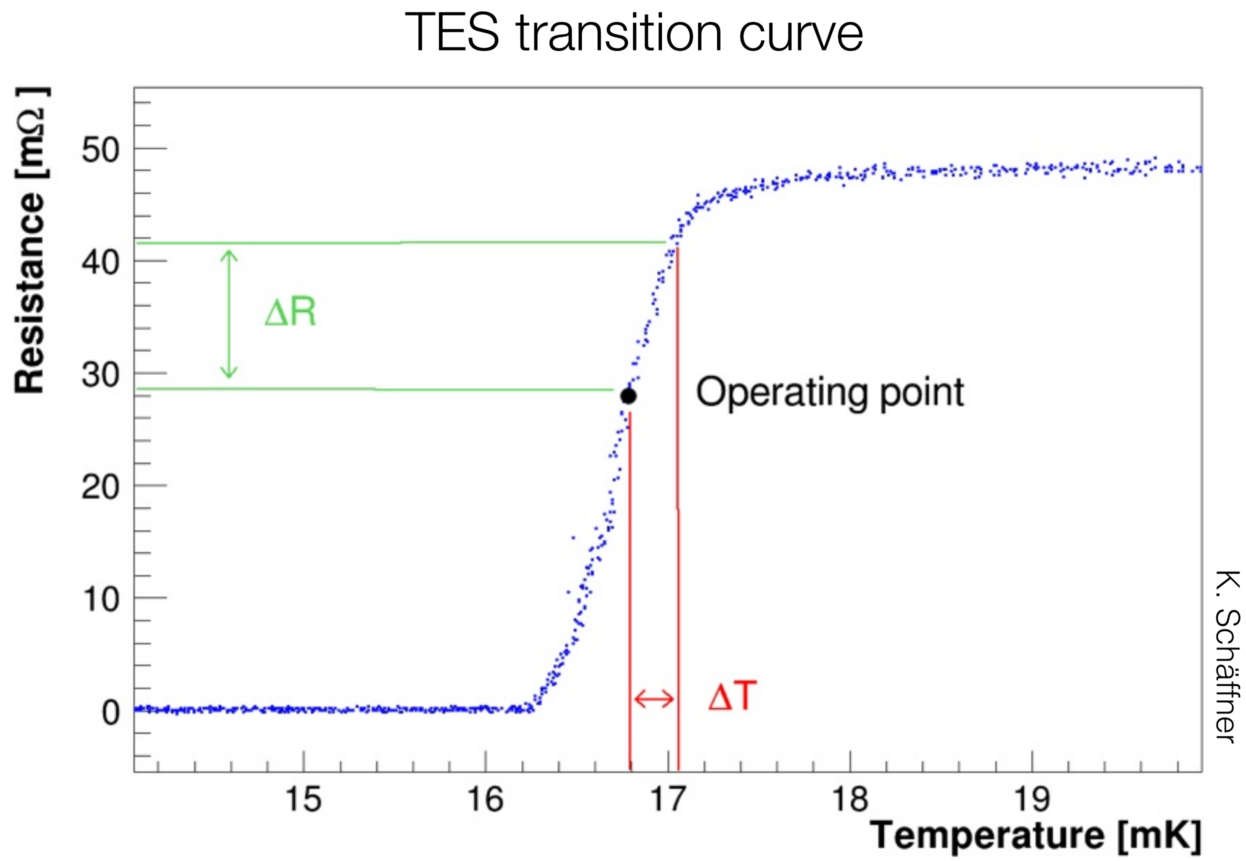

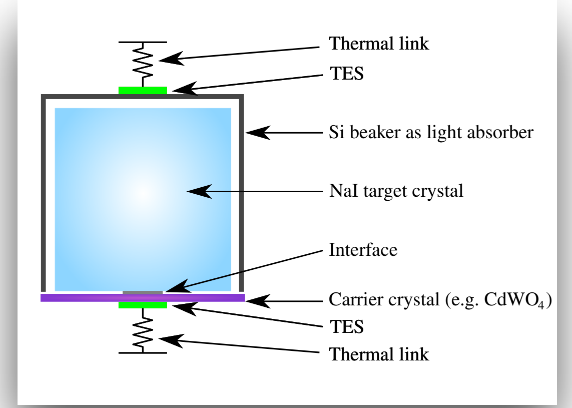

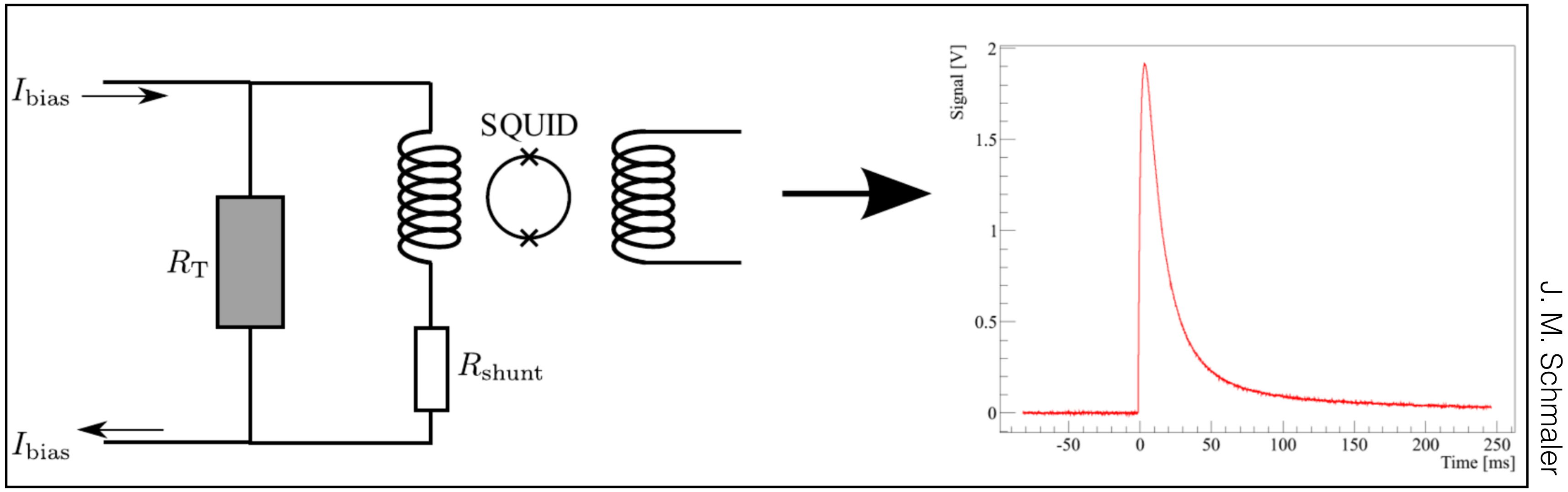

Status of prototype development

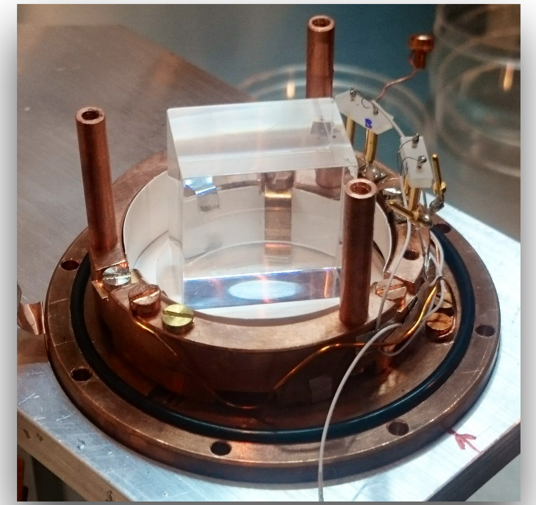

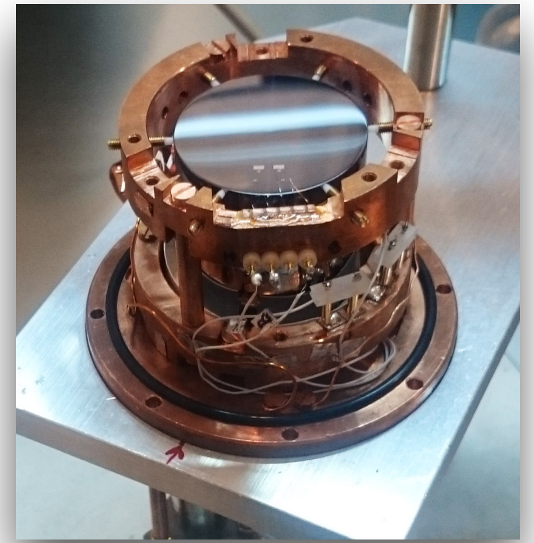

2nd COSINUS prototype performance

K. Schäffner et al. *A NaI-Based Cryogenic Scintillating Calorimeter: Results from a COSINUS Prototype Detector*. J. Low. Temp. Phys., 193(5-6):1174-1181, 2018

Mass:	$\simeq 66$ g
Exposure:	1.32 kg days
Crystal dimension:	$(20 \times 20 \times 30)$ mm^3
Interface:	Epoxy resin
Phonon detector threshold:	$[8.26 \pm 0.02$ (stat.)] keV ($\sigma_{baseline} = 1.01$ keV)
Light detector threshold:	0.6 keV$_{ee}$ ($\sigma_{baseline} = 0.015$ keV)
Energy detected in light:	$\simeq 13\%$

COSINUS phenomenology

Status of prototype development

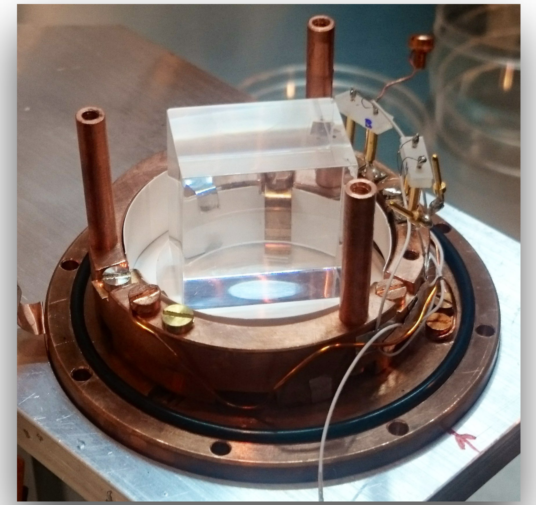

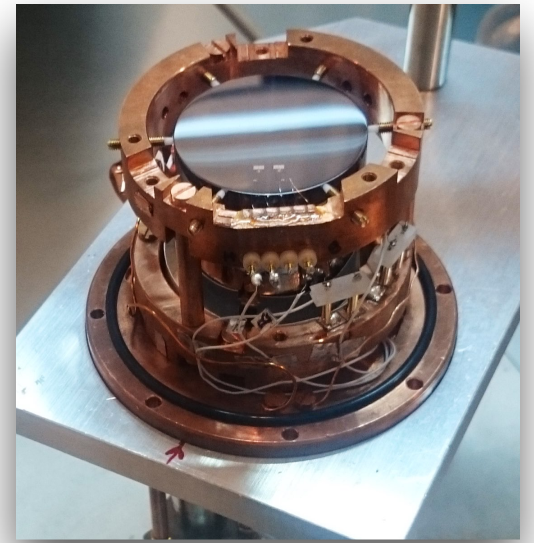

2nd COSINUS prototype performance

K. Schäffner et al. *A NaI-Based Cryogenic Scintillating Calorimeter: Results from a COSINUS Prototype Detector*. J. Low. Temp. Phys., 193(5-6):1174-1181, 2018

Mass:	$\simeq 66$ g
Exposure:	1.32 kg days
Crystal dimension:	$(20 \times 20 \times 30)$ mm^3
Interface:	Epoxy resin
Phonon detector threshold:	$[8.26 \pm 0.02$ (stat.)] keV ($\sigma_{baseline} = 1.01$ keV)
Light detector threshold:	0.6 keV$_{ee}$ ($\sigma_{baseline} = 0.015$ keV)
Energy detected in light:	$\simeq 13\%$

pure NaI ($\simeq 10\,\%$ in Tl-doped NaI)

GSSI

COSINUS: Cryogenic calorimeter based on **NaI crystals**

COSINUS
phenomenology

Status of prototype development

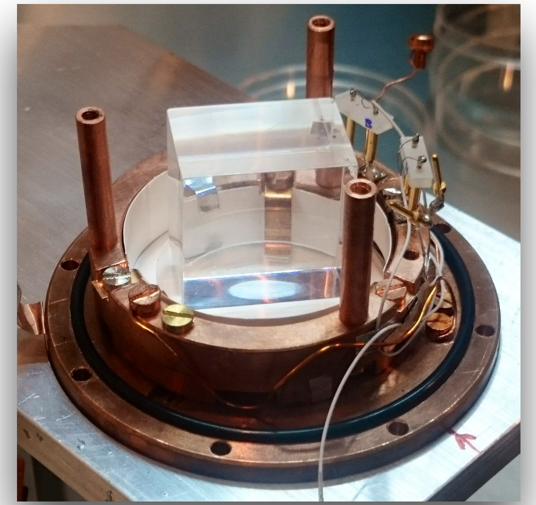

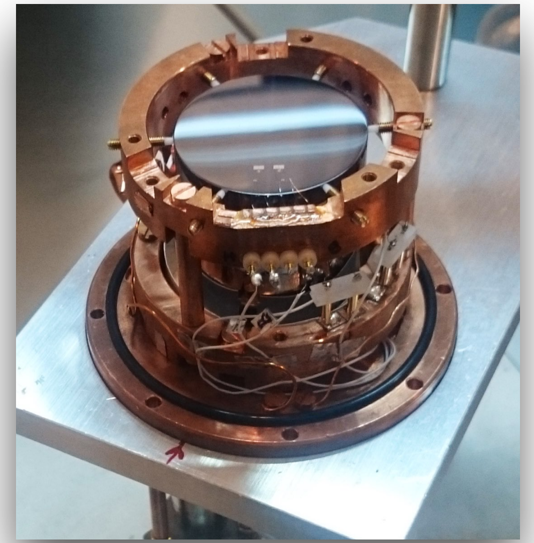

2nd COSINUS prototype performance

K. Schäffner et al. *A NaI-Based Cryogenic Scintillating Calorimeter: Results from a COSINUS Prototype Detector*. J. Low. Temp. Phys., 193(5-6):1174-1181, 2018

Mass:	$\simeq 66$ g
Exposure:	1.32 kg days
Crystal dimension:	$(20 \times 20 \times 30)$ mm^3
Interface:	Epoxy resin
Phonon detector threshold:	$[8.26 \pm 0.02$ (stat.)] keV ($\sigma_{baseline} = 1.01$ keV)
Light detector threshold:	$\boxed{0.6 \text{ keV}_{ee} \ (\sigma_{baseline} = 0.015 \text{ keV})}$
Energy detected in light:	$\simeq 13\%$

Already below the one of DAMA/LIBRA
($\simeq 1$ keV$_{ee}$)

G S
S I

COSINUS: Cryogenic calorimeter based on **NaI crystals**

COSINUS
phenomenology

Status of prototype development

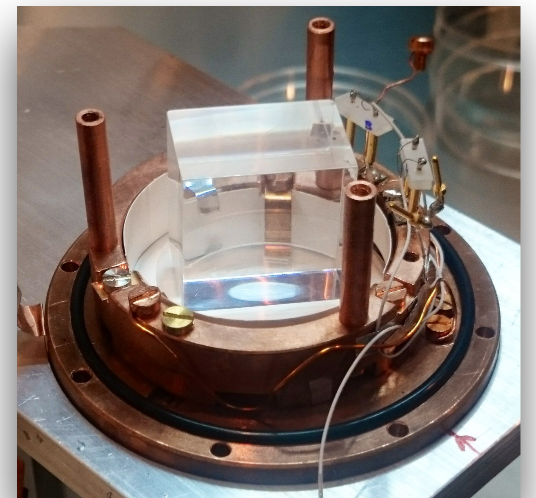

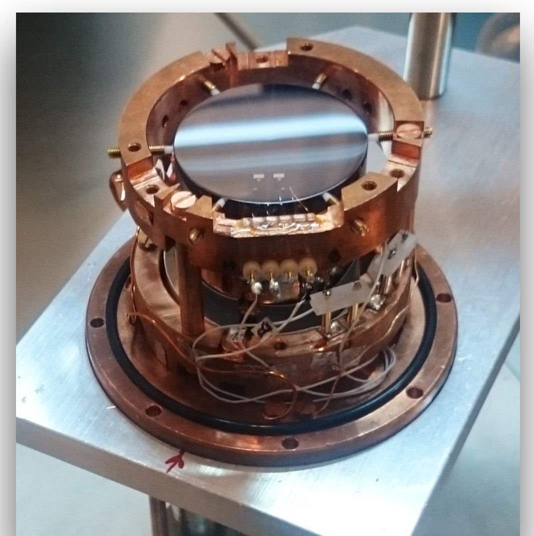

2nd COSINUS prototype performance

K. Schäffner et al. *A NaI-Based Cryogenic Scintillating Calorimeter: Results from a COSINUS Prototype Detector*. J. Low. Temp. Phys., 193(5-6):1174-1181, 2018

Mass:	$\simeq 66$ g
Exposure:	1.32 kg days
Crystal dimension:	$(20 \times 20 \times 30)$ mm^3
Interface:	Epoxy resin
Phonon detector threshold:	$\boxed{[8.26 \pm 0.02 \text{ (stat.)}] \text{ keV } (\sigma_{baseline} = 1.01 \text{ keV})}$
Light detector threshold:	0.6 keV$_{ee}$ ($\sigma_{baseline} = 0.015$ keV)
Energy detected in light:	$\simeq 13\%$

The best recent prototypes arrive at $5 - 6$ keV (the phonon detector energy threshold is not quenched).

G S
S I

COSINUS phenomenology

COSINUS pulse-shape model

G S
S I

Pulse shape model

The general model for TES-based cryogenic detectors was published by Pröbst et al. in 1995 (*F. Pröbst et al, J. Low Temp. Phys. 100,69 (1995)).*

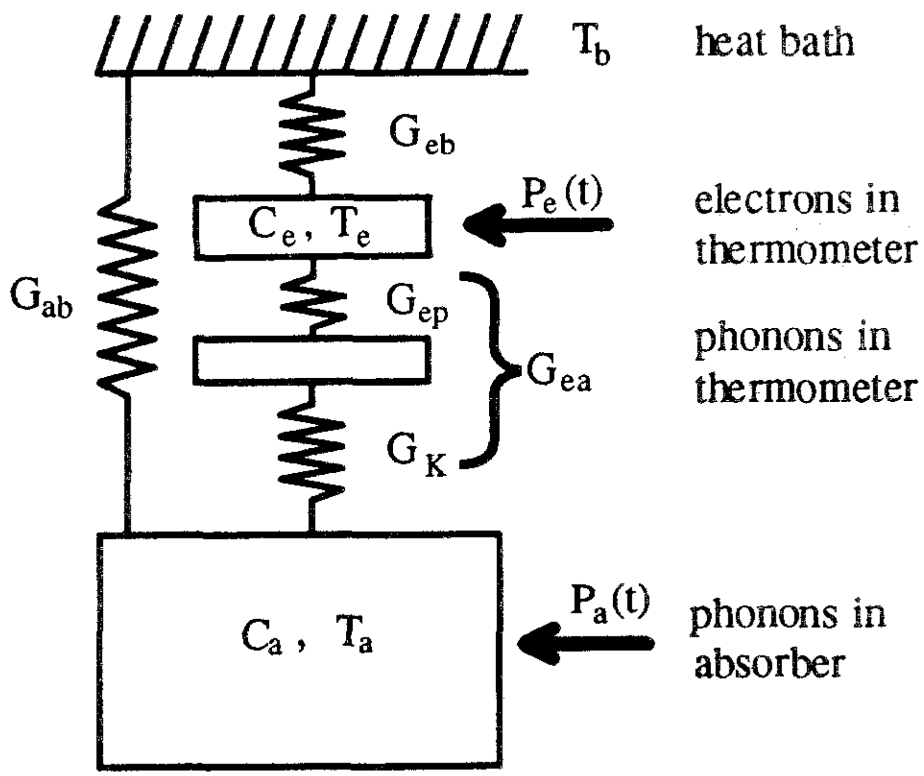

$$
\begin{cases}
C_e \dfrac{dT_e}{dt} + G_{ea}(T_e - T_a) + G_{eb}(T_e - T_b) & = P_e(t) \\
C_a \dfrac{dT_a}{dt} + G_{ea}(T_a - T_e) + G_{ab}(T_a - T_b) & = P_a(t)
\end{cases}
$$

COSINUS: Cryogenic calorimeter based on **NaI crystals**

Pulse shape model

The general model for TES-based cryogenic detectors was published by Pröbst et al. in 1995 (*F. Pröbst et al, J. Low Temp. Phys. 100,69 (1995)).*

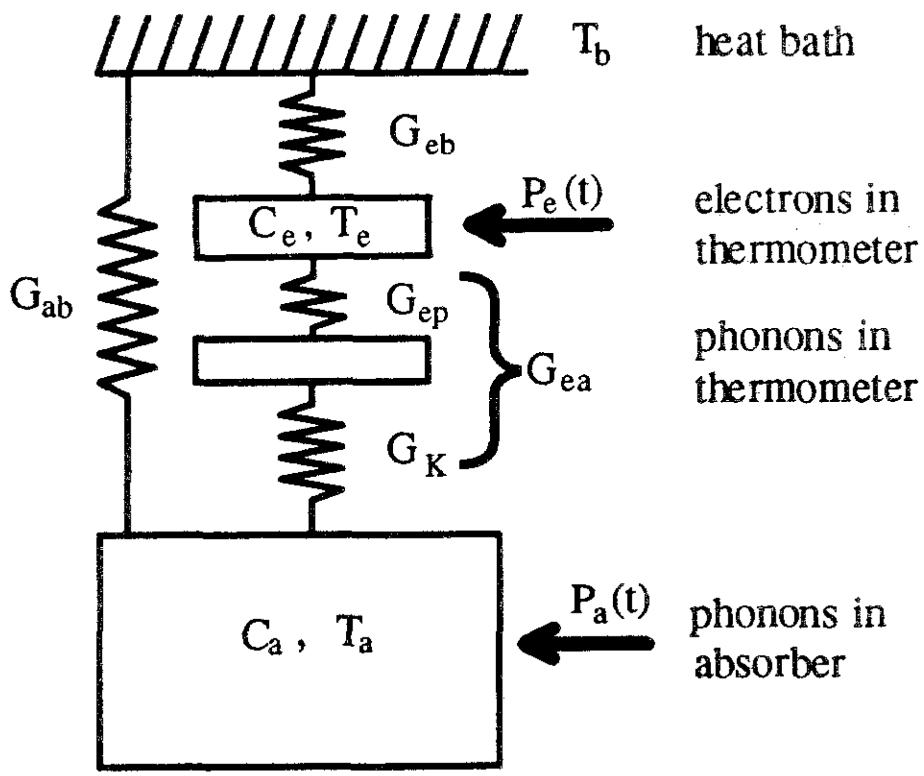

$$\begin{cases} C_e \dfrac{dT_e}{dt} + G_{ea}(T_e - T_a) + G_{eb}(T_e - T_b) & = P_e(t) \\ C_a \dfrac{dT_a}{dt} + G_{ea}(T_a - T_e) + G_{ab}(T_a - T_b) & = P_a(t) \end{cases}$$

$$\begin{cases} \dot{\mathbf{x}}(t) & = \mathbf{A}\ \mathbf{x} + \mathbf{f}(t) \\ \mathbf{x}(t=0) & = \begin{pmatrix} T_b \\ T_b \end{pmatrix} \end{cases}$$

$$\Delta T_e(t) = \theta(t)[A_n\ (e^{-t/\tau_n} - e^{-t/\tau_{in}}) + A_t\ (e^{-t/\tau_t} - e^{-t/\tau_n})]$$

COSINUS phenomenology

Pulse shape model

The general model for TES-based cryogenic detectors was published by Pröbst et al. in 1995 (*F. Pröbst et al, J. Low Temp. Phys. 100,69 (1995)).*

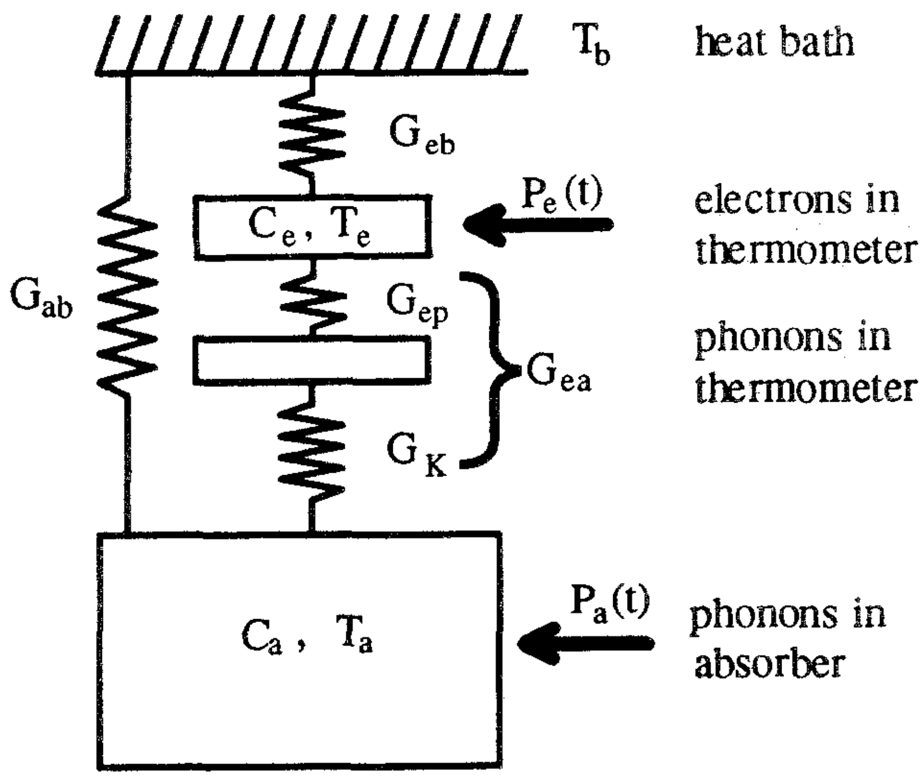

$$\begin{cases} C_e \dfrac{dT_e}{dt} + G_{ea}(T_e - T_a) + G_{eb}(T_e - T_b) & = P_e(t) \\ C_a \dfrac{dT_a}{dt} + G_{ea}(T_a - T_e) + G_{ab}(T_a - T_b) & = P_a(t) \end{cases}$$

$$\begin{cases} \dot{\mathbf{x}}(t) & = \mathbf{A}\,\mathbf{x} + \mathbf{f}(t) \\ \mathbf{x}(t=0) & = \begin{pmatrix} T_b \\ T_b \end{pmatrix} \end{cases}$$

$$\Delta T_e(t) = \theta(t)[\underbrace{A_n\,(e^{-t/\tau_n} - e^{-t/\tau_{in}})}_{Non-thermal} + \underbrace{A_t\,(e^{-t/\tau_t} - e^{-t/\tau_n})}_{Thermal}]$$

GSSI

COSINUS: Cryogenic calorimeter based on **NaI crystals**

COSINUS
phenomenology

Pulse shape model

The general model for TES-based cryogenic detectors was published by Pröbst et al. in 1995 (*F. Pröbst et al, J. Low Temp. Phys. 100,69 (1995)).*

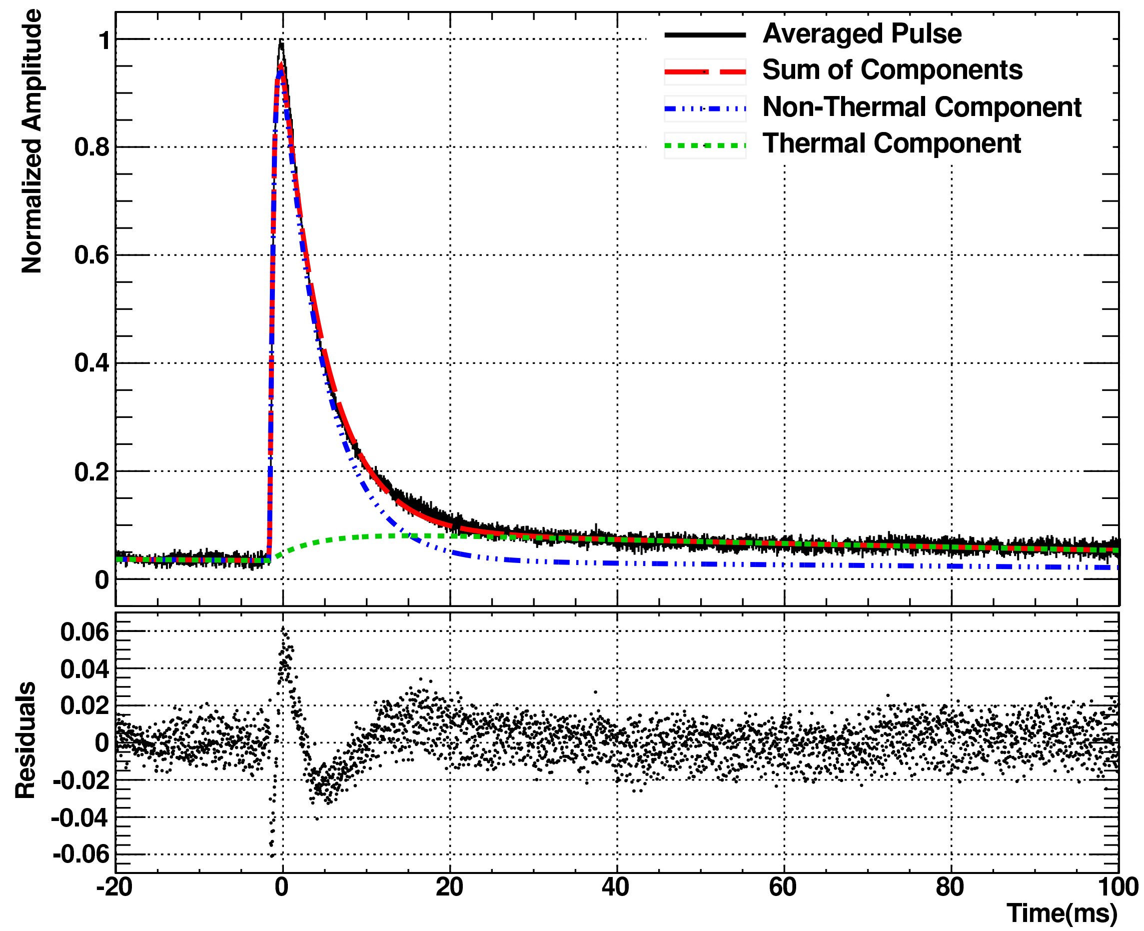

$$\Delta T_e(t) = \theta(t)[\underbrace{A_n\,(e^{-t/\tau_n} - e^{-t/\tau_{in}})}_{Non-thermal} + \underbrace{A_t\,(e^{-t/\tau_t} - e^{-t/\tau_n})}_{Thermal}]$$

GSSI

COSINUS: Cryogenic calorimeter based on **NaI crystals**

COSINUS
phenomenology

Motivation: Experimental findings

G. Angloher et al. *Results from the first cryogenic NaI detector for the COSINUS project.* JINST, 12(11):P11007, 2017.

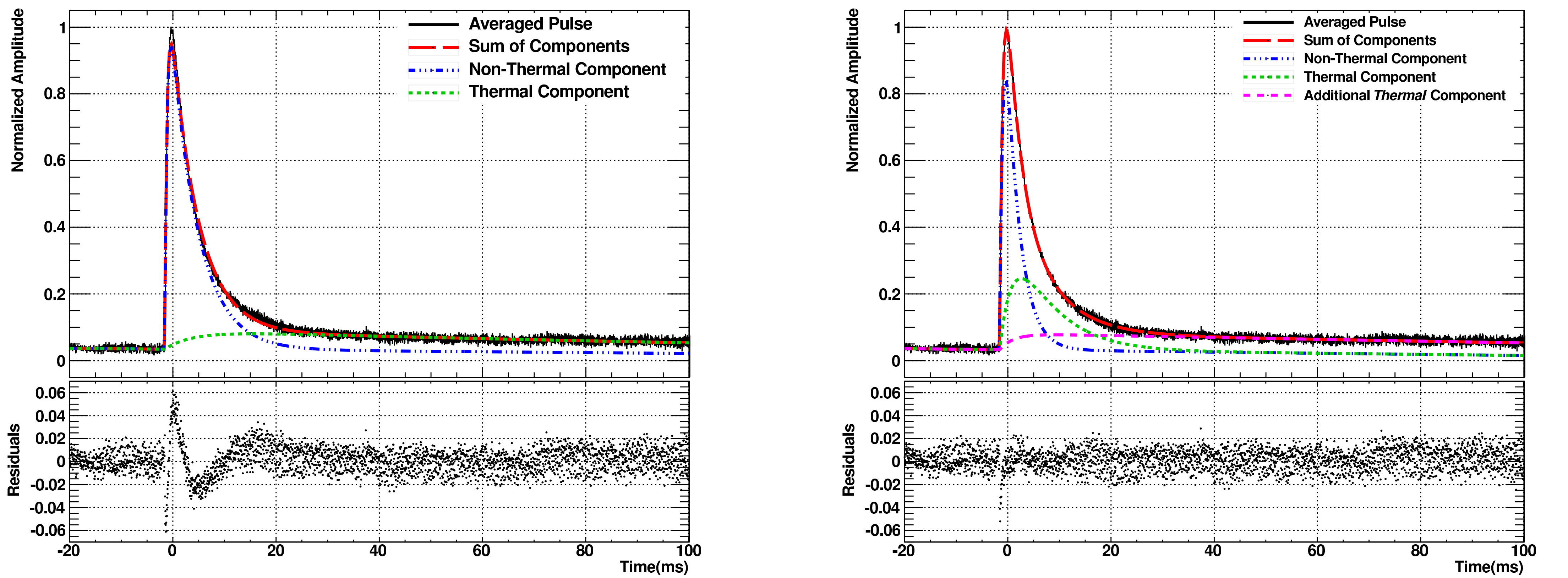

COSINUS pulses are not well described by the general model. A good fit of the model to data is achieved if an empirical additional thermal component is added.

COSINUS
phenomenology

Motivation: Experimental findings

1. **COSINUS pulse shape problem**: COSINUS pulses are not well described by the original model. A good fit of the model to data is achieved if an empirical additional thermal component is added.

G S
S I

COSINUS phenomenology

Motivation: Experimental findings

1. **COSINUS pulse shape problem**: COSINUS pulses are not well described by the original model. A good fit of the model to data is achieved if an empirical additional thermal component is added.

2. **COSINUS neutron calibration problem**: in all the prototypes except for one, the neutrons cannot be identified in the LY plot. However, when a sapphire carrier with an NTD is employed, the neutron band is visible.

G S S I

AVANCEZ 1829

Motivation: Experimental findings

COSINUS
phenomenology

1. **COSINUS pulse shape problem**: COSINUS pulses are not well described by the original model. A good fit of the model to data is achieved if an empirical additional thermal component is added.

2. **COSINUS neutron calibration problem**: in all the prototypes except for one, the neutrons cannot be identified in the LY plot. However, when a sapphire carrier with an NTD is employed, the neutron band is visible.

Hypotheses

- Peculiar phonon propagation in NaI with respect to other materials
- The presence of the carrier cannot be neglected
- The carrier is not transparent to the NaI scintillation light

COSINUS
phenomenology

Motivation: Experimental findings

1. **COSINUS pulse shape problem**: COSINUS pulses are not well described by the original model. A good fit of the model to data is achieved if an empirical additional thermal component is added.

2. **COSINUS neutron calibration problem**: in all the prototypes except for one, the neutrons cannot be identified in the LY plot. However, when a sapphire carrier with an NTD is employed, the neutron band is visible.

Hypotheses

- Peculiar phonon propagation in NaI with respect to other materials
- The presence of the carrier cannot be neglected
- The carrier is not transparent to the NaI scintillation light

→ Extension of pulse shape model

G S
S I

AVANCEZ 1829

COSINUS
phenomenology

Proposal: Extended pulse shape model

$$\begin{cases} C_e \dfrac{dT_e}{dt} + G_{ea}(T_e - T_a) + G_{eb}(T_e - T_b) & = P_e(t) \\ C_a \dfrac{dT_a}{dt} + G_{ea}(T_a - T_e) + G_{ab}(T_a - T_b) & = P_a(t) \end{cases}$$

G S
S I

Proposal: Extended pulse shape model

$$\begin{cases} C_e \dfrac{dT_e}{dt} + G_{ea}(T_e - T_c) + G_{eb}(T_e - T_b) & = \tilde{P}_e(t) \\ C_c \dfrac{dT_c}{dt} + G_{ec}(T_c - T_e) + G_{ac}(T_c - T_a) + (T_c - T_b)G_{cb} & = \tilde{P}_c(t) \\ C_a \dfrac{dT_a}{dt} + G_{ac}(T_a - T_c) + G_{ab}(T_a - T_b) & = \tilde{P}_a(t) \end{cases}$$

COSINUS: Cryogenic calorimeter based on **NaI crystals**

COSINUS
phenomenology

Proposal: Extended pulse shape model

$$
\begin{cases}
C_e \dfrac{dT_e}{dt} + G_{ea}(T_e - T_c) + G_{eb}(T_e - T_b) & = \tilde{P}_e(t) \\
C_c \dfrac{dT_c}{dt} + G_{ec}(T_c - T_e) + G_{ac}(T_c - T_a) + (T_c - T_b)G_{cb} & = \tilde{P}_c(t) \\
C_a \dfrac{dT_a}{dt} + G_{ac}(T_a - T_c) + G_{ab}(T_a - T_b) & = \tilde{P}_a(t)
\end{cases}
$$

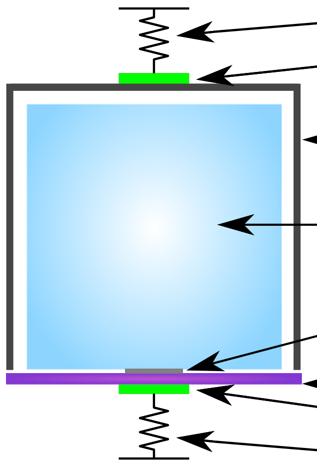

G S
S I

COSINUS: Cryogenic calorimeter based on **NaI crystals**

Proposal: Extended pulse shape model

$$\begin{cases} C_e \frac{dT_e}{dt} + G_{ea}(T_e - T_c) + G_{eb}(T_e - T_b) = \tilde{P}_e(t) \\ C_c \frac{dT_c}{dt} + G_{ec}(T_c - T_e) + G_{ac}(T_c - T_a) + (T_c - T_b)G_{cb} = \tilde{P}_c(t) \\ C_a \frac{dT_a}{dt} + G_{ac}(T_a - T_c) + G_{ab}(T_a - T_b) = \tilde{P}_a(t) \end{cases}$$

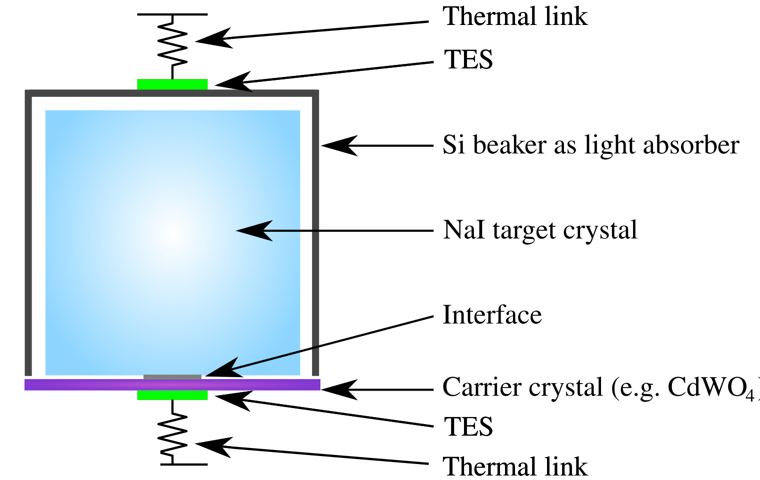

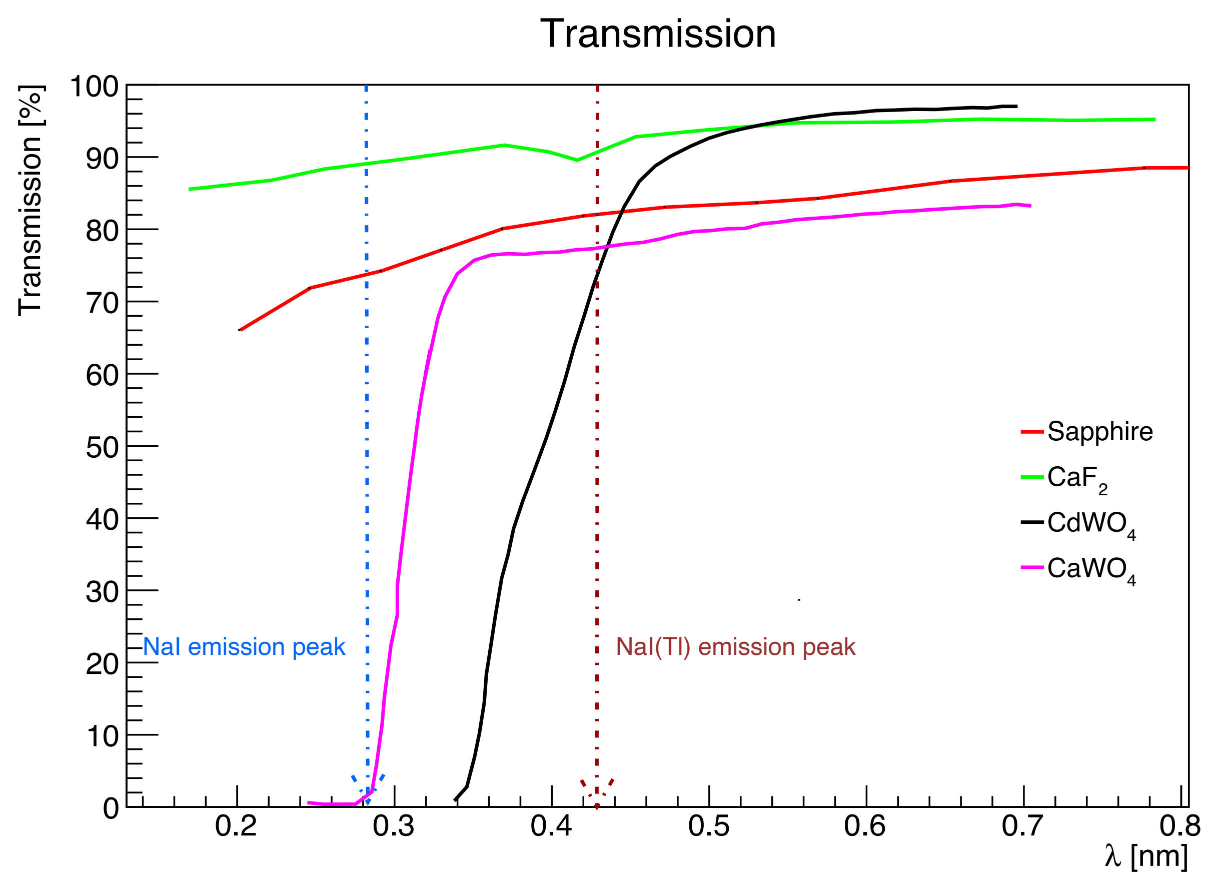

COSINUS: Cryogenic calorimeter based on **NaI crystals**

Proposal: Extended pulse shape model

$$\begin{cases} C_e \dfrac{dT_e}{dt} + G_{ea}(T_e - T_c) + G_{eb}(T_e - T_b) & = \tilde{P}_e(t) \\ C_c \dfrac{dT_c}{dt} + G_{ec}(T_c - T_e) + G_{ac}(T_c - T_a) + (T_c - T_b)G_{cb} & = \tilde{P}_c(t) \\ C_a \dfrac{dT_a}{dt} + G_{ac}(T_a - T_c) + G_{ab}(T_a - T_b) & = \tilde{P}_a(t) \end{cases}$$

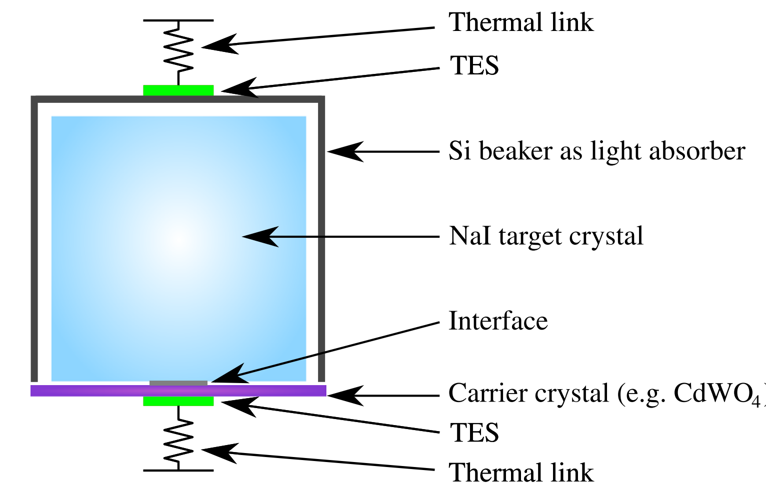

Result

$$\Delta T_e(t) = \underbrace{\sum_{i=1}^{3} A_i \, [e^{\lambda_i t} - e^{-t/\tau'_n}]}_{\textbf{Phonons in the PD}} + \underbrace{\sum_{i=1}^{3} B_i \, [e^{\lambda_i t} - e^{-t/\tau_\ell}]}_{\textbf{Light in PD}}$$

COSINUS
phenomenology

Why the EPSM could explain COSINUS experimental findings

1. **COSINUS pulse shape problem**: COSINUS pulses are not well described by the original model. A good fit of the model to data is achieved if an empirical additional thermal component is added.

$$\Delta T_e(t) = \sum_{i=1}^{3} A_i \, [e^{\lambda_i \, t} - e^{-t/\tau'_n}] + \cancel{\sum_{i=1}^{3} B_i \, [e^{\lambda_i \, t} - e^{-t/\tau_\ell}]}$$

G S
S I

COSINUS
phenomenology

Why the EPSM could explain COSINUS experimental findings

1. **COSINUS pulse shape problem**: COSINUS pulses are not well described by the original model. A good fit of the model to data is achieved if an empirical additional thermal component is added.

$$\Delta T_e(t) = \sum_{i=1}^{3} A_i\,[e^{\lambda_i\,t} - e^{-t/\tau_n'}] + \sum_{i=1}^{3} \cancel{B_i\,[e^{\lambda_i\,t} - e^{-t/\tau_\ell}]}$$

2. **COSINUS neutron calibration problem**: in all the prototypes except for one, the neutrons cannot be identified in the LY plot. However, when a sapphire carrier with an NTD is employed, the neutron band is visible.

possible explanation

G S
S I

Why the EPSM could explain COSINUS experimental findings

1. **COSINUS pulse shape problem**: COSINUS pulses are not well described by the original model. A good fit of the model to data is achieved if an empirical additional thermal component is added.

$$\Delta T_e(t) = \sum_{i=1}^{3} A_i \,[e^{\lambda_i\, t} - e^{-t/\tau'_n}] + \sum_{i=1}^{3} \cancel{B_i\,[e^{\lambda_i\, t} - e^{-t/\tau_\ell}]}$$

2. **COSINUS neutron calibration problem**: in all the prototypes except for one, the neutrons cannot be identified in the LY plot. However, when a sapphire carrier with an NTD is employed, the neutron band is visible.

possible explanation

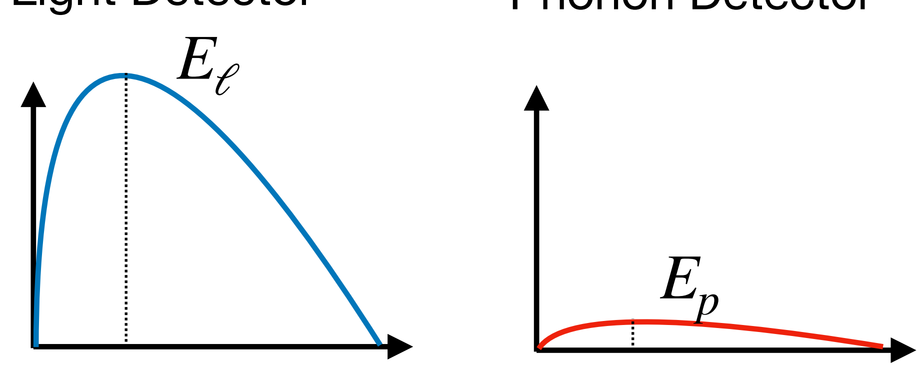

$$LY = \frac{E_\ell}{E_p}$$

COSINUS: Cryogenic calorimeter based on NaI crystals

COSINUS phenomenology

Why the EPSM could explain COSINUS experimental findings

1. **COSINUS pulse shape problem**: COSINUS pulses are not well described by the original model. A good fit of the model to data is achieved if an empirical additional thermal component is added.

$$\Delta T_e(t) = \sum_{i=1}^{3} A_i \, [e^{\lambda_i t} - e^{-t/\tau'_n}] + \sum_{i=1}^{3} \cancel{B_i \, [e^{\lambda_i t} - e^{-t/\tau_\ell}]}$$

2. **COSINUS neutron calibration problem**: in all the prototypes except for one, the neutrons cannot be identified in the LY plot. However, when a sapphire carrier with an NTD is employed, the neutron band is visible.

possible explanation

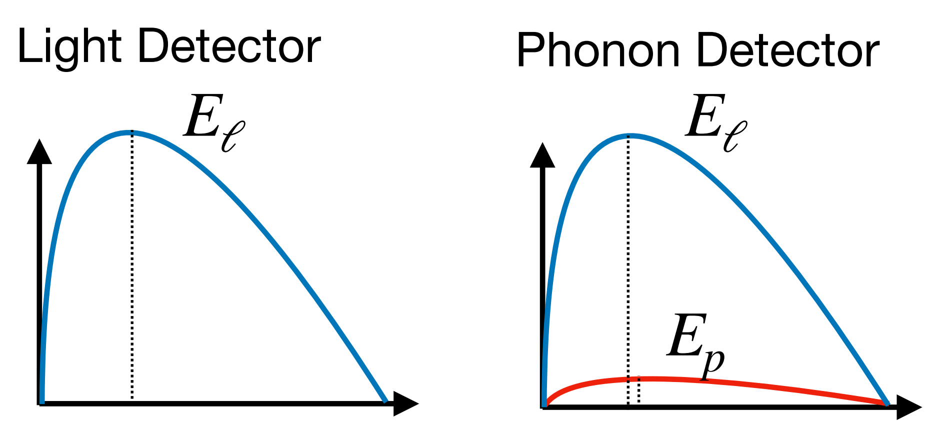

$$LY = \frac{E_\ell}{E_p + E_\ell}$$

COSINUS
phenomenology

Why the EPSM could explain COSINUS experimental findings

1. **COSINUS pulse shape problem**: COSINUS pulses are not well described by the original model. A good fit of the model to data is achieved if an empirical additional thermal component is added.

$$\Delta T_e(t) = \sum_{i=1}^{3} A_i \, [e^{\lambda_i \, t} - e^{-t/\tau'_n}] + \sum_{i=1}^{3} \cancel{B_i \, [e^{\lambda_i \, t} - e^{-t/\tau_\ell}]}$$

2. **COSINUS neutron calibration problem**: in all the prototypes except for one, the neutrons cannot be identified in the LY plot. However, when a sapphire carrier with an NTD is employed, the neutron band is visible.

possible explanation

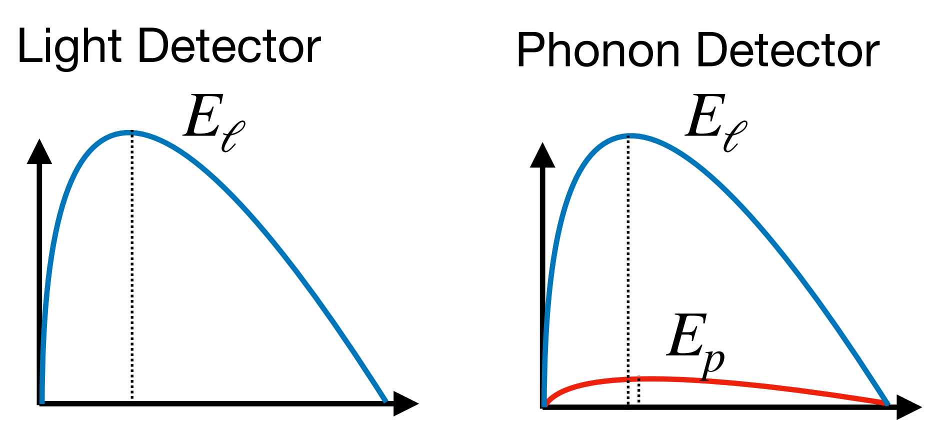

$$LY = \frac{E_\ell}{E_p + E_\ell} \approx 1$$

$$\text{if } E_p \ll E_\ell$$

G S
S I

COSINUS phenomenology

Why the EPSM could explain COSINUS experimental findings

1. **COSINUS pulse shape problem**: COSINUS pulses are not well described by the original model. A good fit of the model to data is achieved if an empirical additional thermal component is added.

$$\Delta T_e(t) = \sum_{i=1}^{3} A_i\,[e^{\lambda_i\,t} - e^{-t/\tau_n'}] + \sum_{i=1}^{3} \cancel{B_i\,[e^{\lambda_i\,t} - e^{-t/\tau_\ell}]}$$

2. **COSINUS neutron calibration problem**: in all the prototypes except for one, the neutrons cannot be identified in the LY plot. However, when a sapphire carrier with an NTD is employed, the neutron band is visible.

possible explanation

Using this energy reconstruction method neutrons cannot be discriminated from β/γ-events!

COSINUS phenomenology

Why the EPSM could explain COSINUS experimental findings

1. **COSINUS pulse shape problem**: COSINUS pulses are not well described by the original model. A good fit of the model to data is achieved if an empirical additional thermal component is added.

$$\Delta T_e(t) = \sum_{i=1}^{3} A_i \, [e^{\lambda_i t} - e^{-t/\tau'_n}] + \sum_{i=1}^{3} \cancel{B_i \, [e^{\lambda_i t} - e^{-t/\tau_\ell}]}$$

2. **COSINUS neutron calibration problem**: in all the prototypes except for one, the neutrons cannot be identified in the LY plot. However, when a sapphire carrier with an NTD is employed, the neutron band is visible.

Proposal: New energy reconstruction method based on EPSM

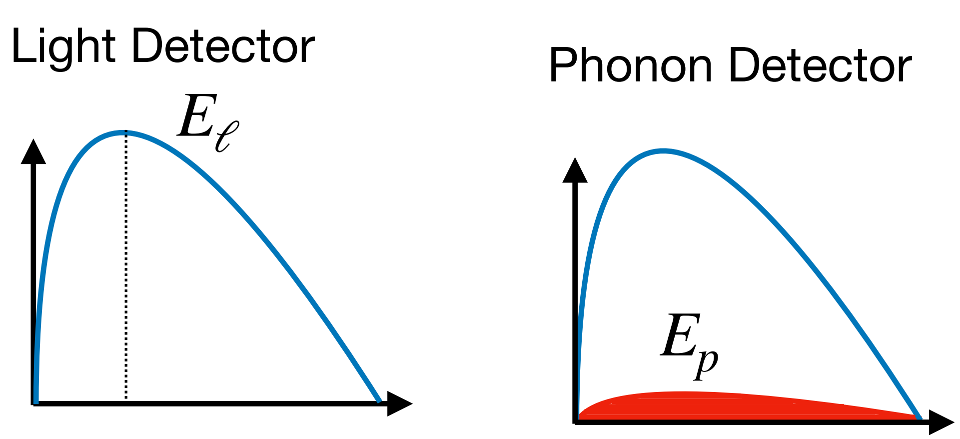

COSINUS
phenomenology

Validation of the EPSM with experimental data

Implementation by M. Stahlberg

1. **COSINUS pulse shape problem**: COSINUS pulses are not well described by the original model. A good fit of the model to data is achieved if an empirical additional thermal component is added.

COSINUS phenomenology

Validation of the EPSM with experimental data

Implementation by M. Stahlberg

1. **COSINUS pulse shape problem**: COSINUS pulses are not well described by the original model. A good fit of the model to data is achieved if an empirical additional thermal component is added.

Original model

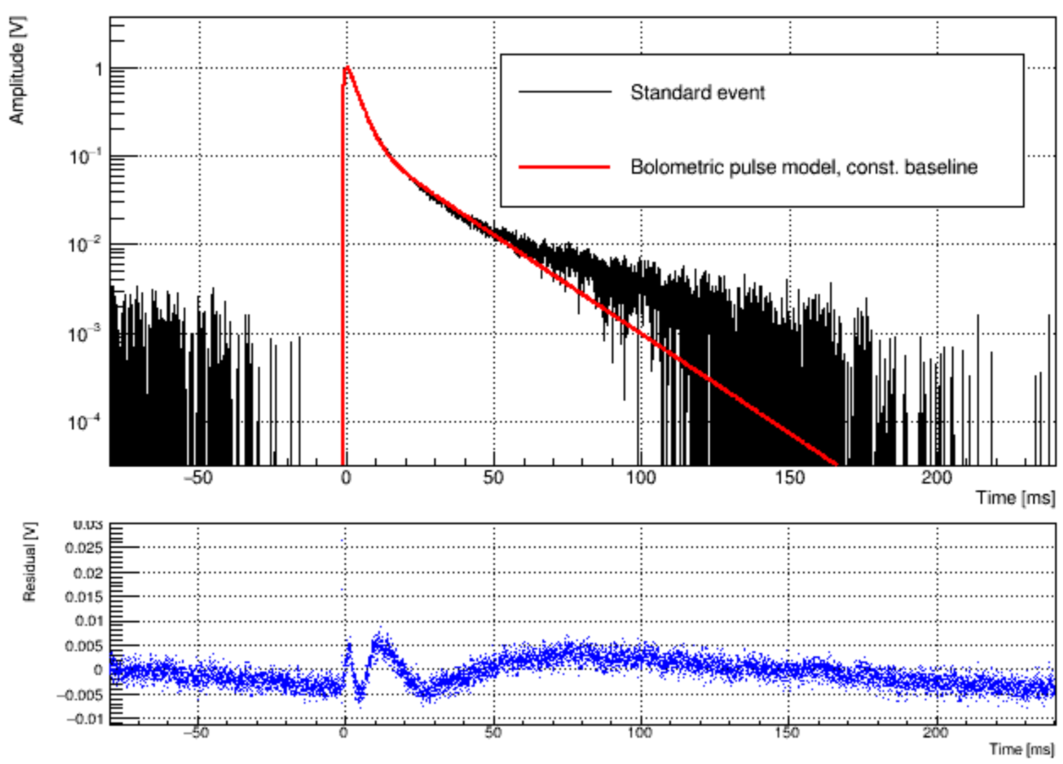

EPSM

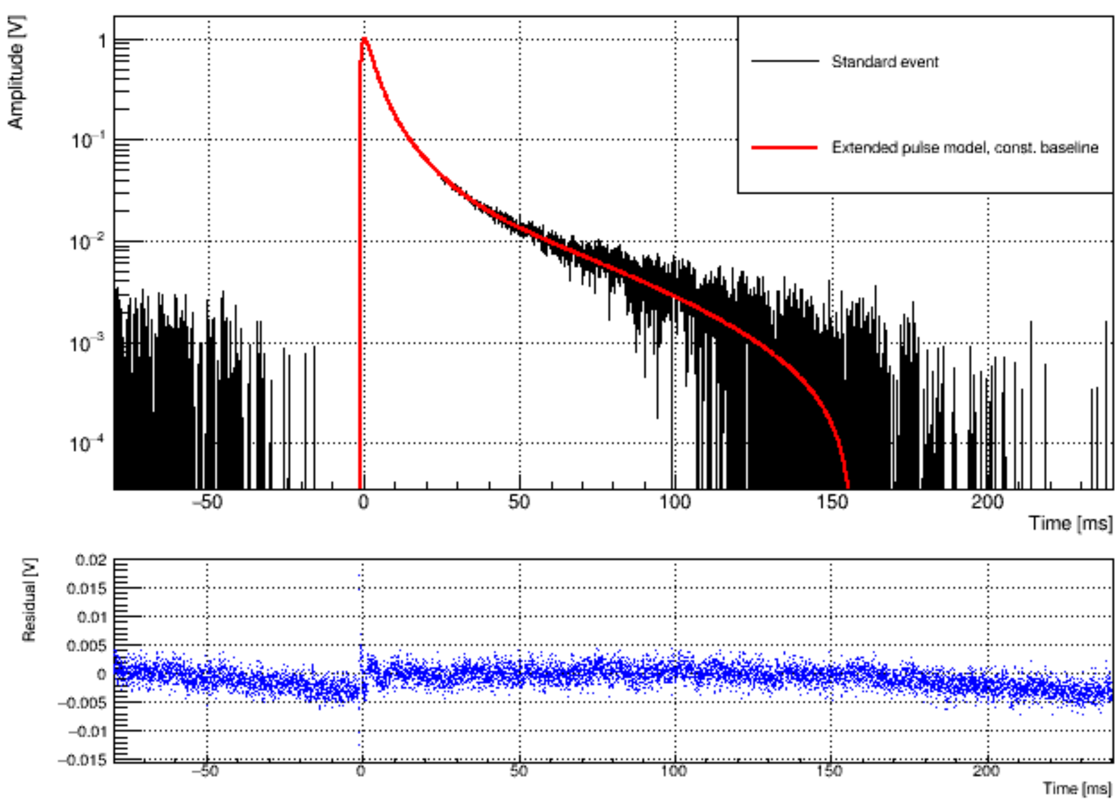

Tail well fitted using EPSM

COSINUS
phenomenology

Validation of the EPSM with experimental data

Implementation by M. Stahlberg

2. **COSINUS neutron calibration problem**: in all the prototypes except for one, the neutrons cannot be identified in the LY plot. However, when a sapphire carrier with an NTD is employed, the neutron band is visible.

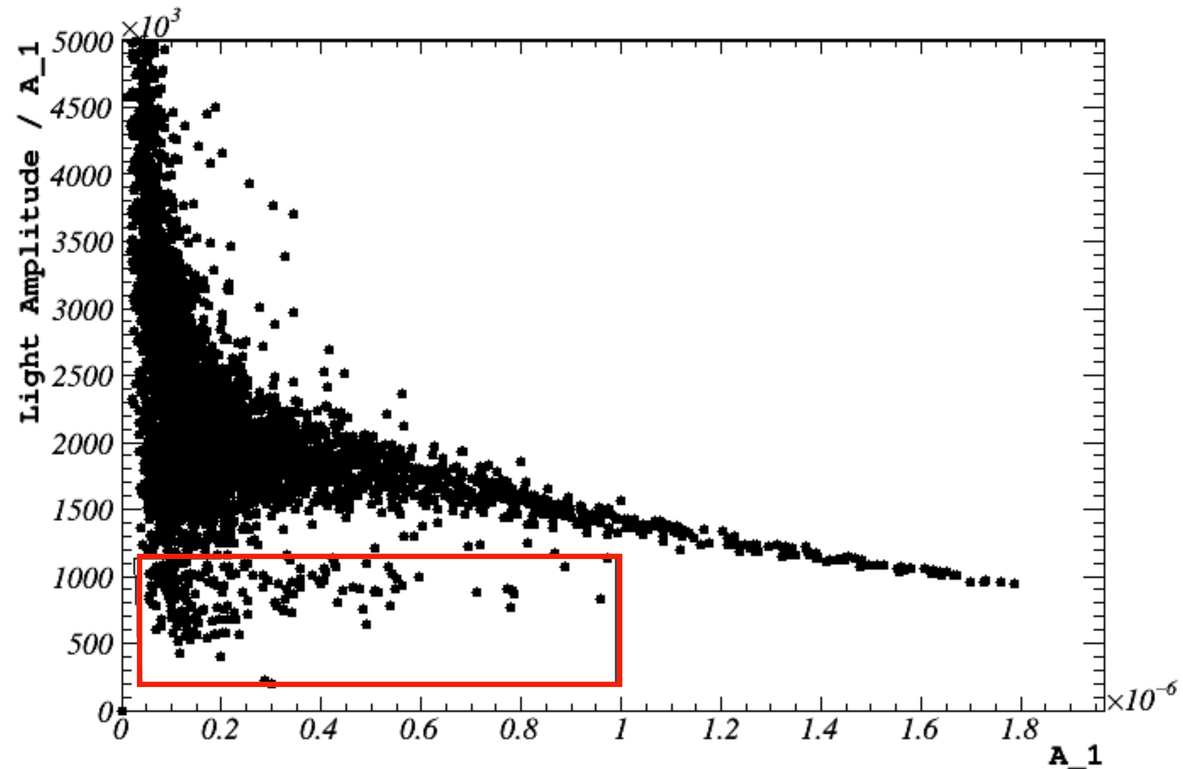

LY with energy reconstructed with the new integrated method based on EPSM

G S
S I

COSINUS phenomenology

Phonon propagation in NaI

COSINUS phenomenology

Molecular Dynamics Simulations

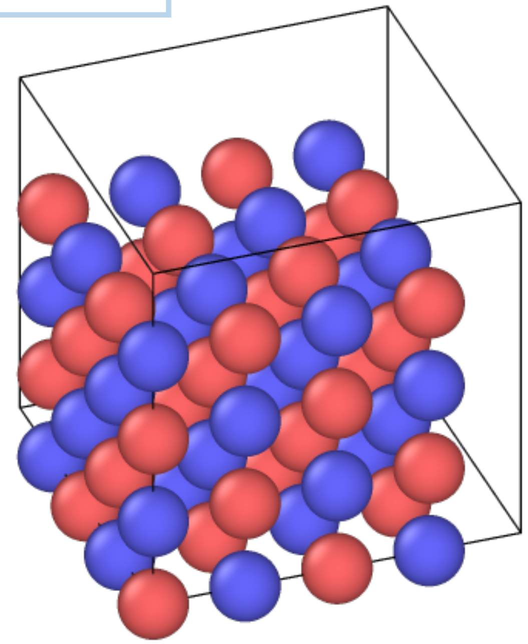

Large-scale Atomic/Molecular Massively Parallel Simulator (LAMMPS)

GSSI

COSINUS: Cryogenic calorimeter based on **NaI crystals**

COSINUS
phenomenology

Molecular Dynamics Simulations

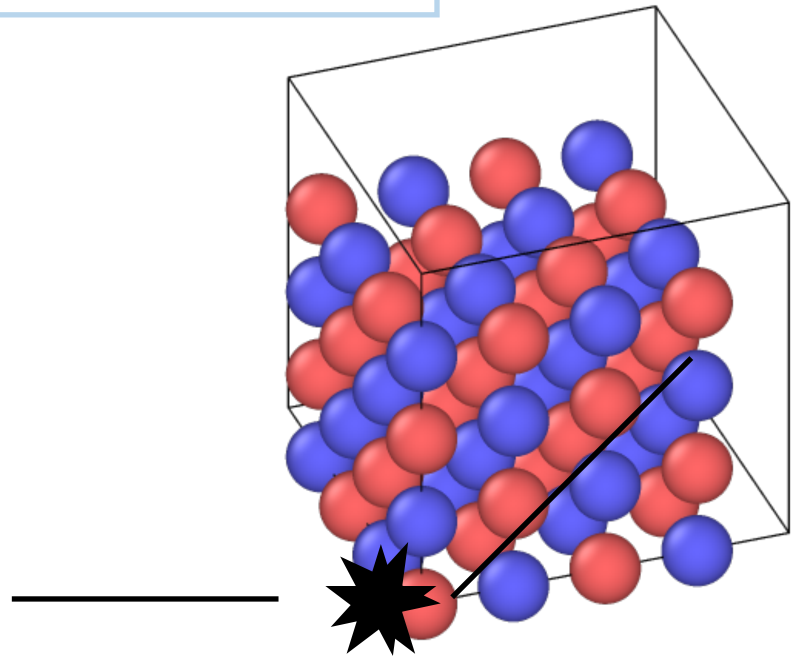

Large-scale Atomic/Molecular Massively Parallel Simulator (LAMMPS)

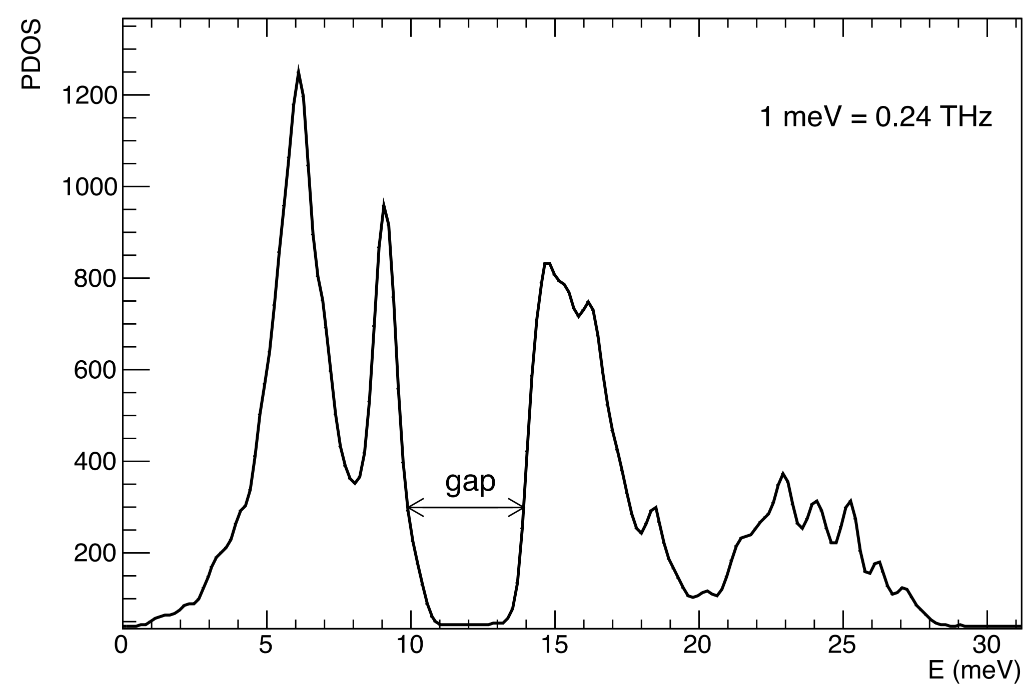

Phonon Density Of States

G S
S I

COSINUS: Cryogenic calorimeter based on **NaI crystals**

Molecular Dynamics Simulations

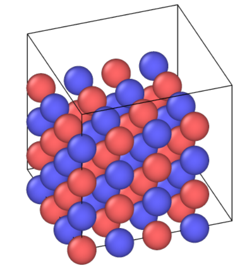

LAMMPS

Anharmonic oscillations can produce phonons in the gap which cannot propagate (intrinsic localised modes)

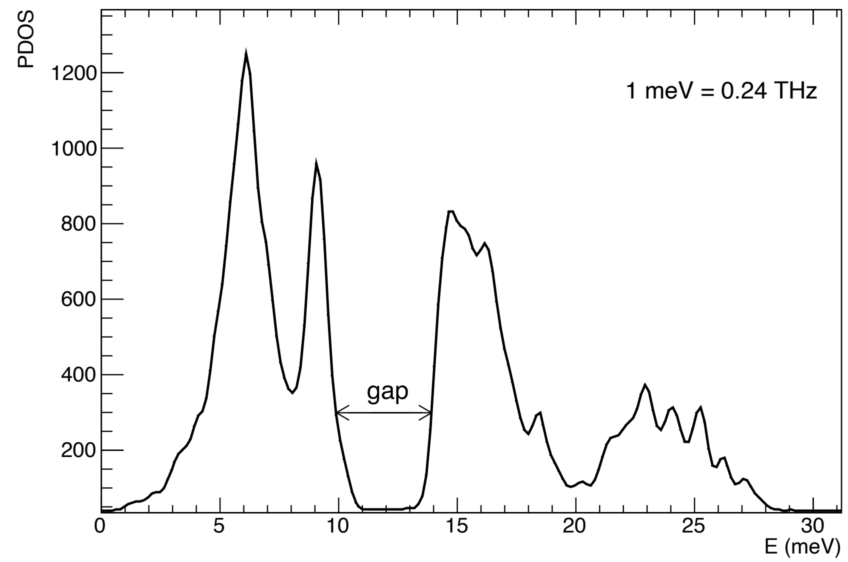

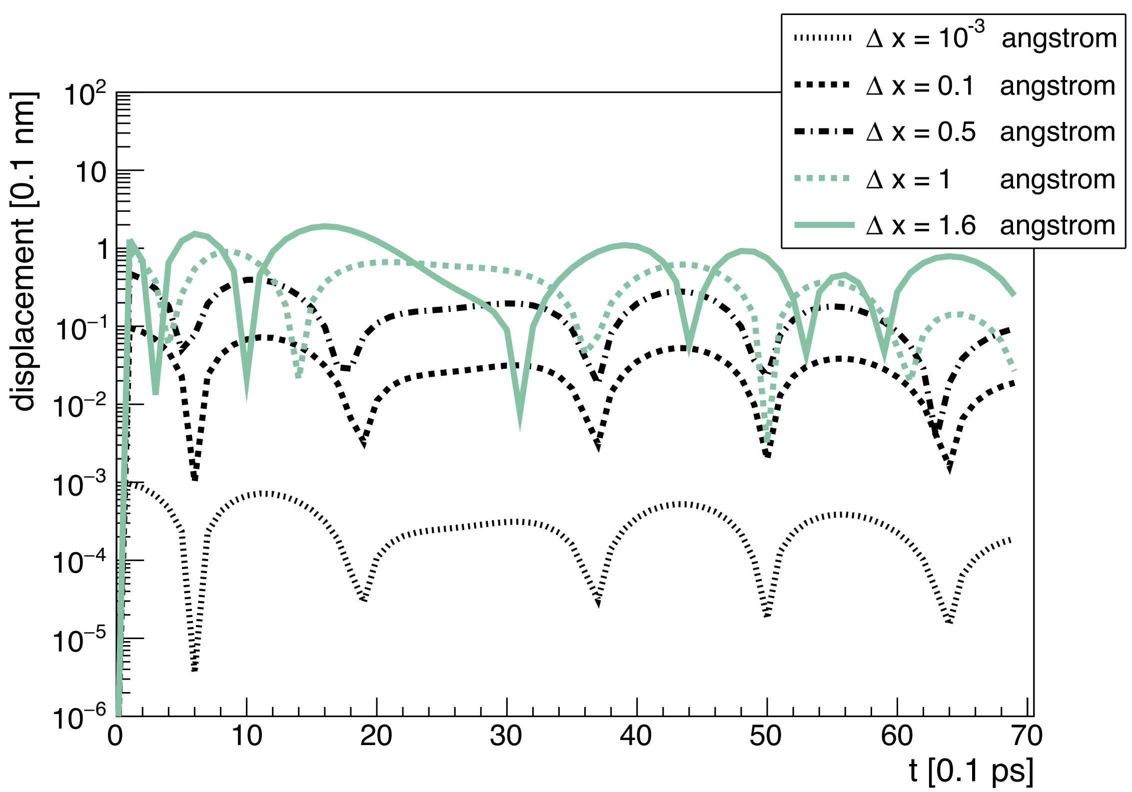

S. A. Kiselev and A. J. Sievers. Generation of intrinsic vibrational gap modes in three-dimensional ionic crystals. Phys. Rev. B, 55:5755{5758, Mar 1997

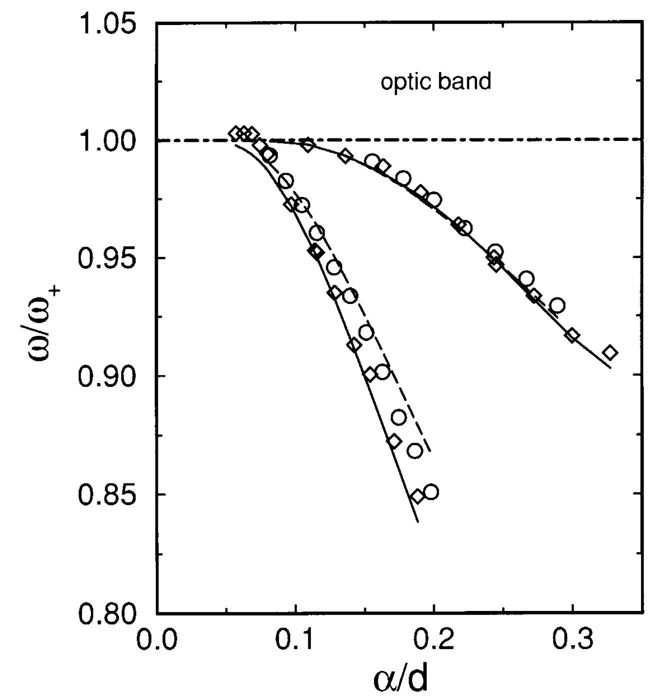

Conclusions

- DM DD effective field theory: two applications
    - Annual modulation properties in NREFT
    - Theoretical formalism for spin-1 dark matter search using polarised nuclei
- DM search with the CRESST experiment
    - Spin-dependent search in ^{7}Li targets
    - First studies on annual modulation search in CRESST-III
- COSINUS phenomenology
    - Elaboration of the extended pulse shape model proposed to explain COSINUS experimental findings
    - New approach based on solid state physics for the study of NaI phonon propagation properties

THANK YOU

G S
S I

Credits

On slide 14: Graphic view of our Milky Way Galaxy. Credit: NASA/Adler/U. Chicago/Wesleyan/JPL-Caltech.

BACK UP

NREFT building blocks

$\hat{\mathcal{O}}_1 = \mathbb{1}_\chi \mathbb{1}_N$	$\hat{\mathcal{O}}_{11} = i\hat{\mathbf{S}}_\chi \cdot \frac{\hat{\mathbf{q}}}{m_N}\mathbb{1}_N$
$\hat{\mathcal{O}}_3 = i\hat{\mathbf{S}}_N \cdot \left(\frac{\hat{\mathbf{q}}}{m_N} \times \hat{\mathbf{v}}^\perp\right)\mathbb{1}_\chi$	$\hat{\mathcal{O}}_{12} = \hat{\mathbf{S}}_\chi \cdot \left(\hat{\mathbf{S}}_N \times \hat{\mathbf{v}}^\perp\right)$
$\hat{\mathcal{O}}_4 = \hat{\mathbf{S}}_\chi \cdot \hat{\mathbf{S}}_N$	$\hat{\mathcal{O}}_{13} = i\left(\hat{\mathbf{S}}_\chi \cdot \hat{\mathbf{v}}^\perp\right)\left(\hat{\mathbf{S}}_N \cdot \frac{\hat{\mathbf{q}}}{m_N}\right)$
$\hat{\mathcal{O}}_5 = i\hat{\mathbf{S}}_\chi \cdot \left(\frac{\hat{\mathbf{q}}}{m_N} \times \hat{\mathbf{v}}^\perp\right)\mathbb{1}_N$	$\hat{\mathcal{O}}_{14} = i\left(\hat{\mathbf{S}}_\chi \cdot \frac{\hat{\mathbf{q}}}{m_N}\right)\left(\hat{\mathbf{S}}_N \cdot \hat{\mathbf{v}}^\perp\right)$
$\hat{\mathcal{O}}_6 = \left(\hat{\mathbf{S}}_\chi \cdot \frac{\hat{\mathbf{q}}}{m_N}\right)\left(\hat{\mathbf{S}}_N \cdot \frac{\hat{\mathbf{q}}}{m_N}\right)$	$\hat{\mathcal{O}}_{15} = -\left(\hat{\mathbf{S}}_\chi \cdot \frac{\hat{\mathbf{q}}}{m_N}\right)\left[\left(\hat{\mathbf{S}}_N \times \hat{\mathbf{v}}^\perp\right) \cdot \frac{\hat{\mathbf{q}}}{m_N}\right]$
$\hat{\mathcal{O}}_7 = \hat{\mathbf{S}}_N \cdot \hat{\mathbf{v}}^\perp \mathbb{1}_\chi$	$\hat{\mathcal{O}}_{17} = i\frac{\hat{\mathbf{q}}}{m_N} \cdot \mathcal{S} \cdot \hat{\mathbf{v}}^\perp \mathbb{1}_N$
$\hat{\mathcal{O}}_8 = \hat{\mathbf{S}}_\chi \cdot \hat{\mathbf{v}}^\perp \mathbb{1}_N$	$\hat{\mathcal{O}}_{18} = i\frac{\hat{\mathbf{q}}}{m_N} \cdot \mathcal{S} \cdot \hat{\mathbf{S}}_N$
$\hat{\mathcal{O}}_9 = i\hat{\mathbf{S}}_\chi \cdot \left(\hat{\mathbf{S}}_N \times \frac{\hat{\mathbf{q}}}{m_N}\right)$	$\hat{\mathcal{O}}_{19} = \frac{\hat{\mathbf{q}}}{m_N} \cdot \mathcal{S} \cdot \frac{\hat{\mathbf{q}}}{m_N}$
$\hat{\mathcal{O}}_{10} = i\hat{\mathbf{S}}_N \cdot \frac{\hat{\mathbf{q}}}{m_N}\mathbb{1}_\chi$	$\hat{\mathcal{O}}_{20} = (\hat{\mathbf{S}}_N \times \frac{\hat{\mathbf{q}}}{m_N}) \cdot \mathcal{S} \cdot \frac{\hat{\mathbf{q}}}{m_N}$

GS SI

Theoretical framework

$$\left.\frac{d\sigma}{dE_R}\right|_{\hat{\mathcal{O}}_1} = \frac{m_T}{2\pi v^2} \sum_{\tau,\tau'} c_1^{(\tau)} c_1^{(\tau')} \tilde{W}_M^{\tau\tau'}(q^2)$$

$$\left.\frac{d\sigma}{dE_R}\right|_{\hat{\mathcal{O}}_7} = \frac{m_T}{2\pi v^2} \sum_{\tau,\tau'} c_7^{(\tau)} c_7^{(\tau')} \frac{(v^2 - v_{min}^2)}{8} \tilde{W}_{\Sigma'}^{\tau\tau'}(q^2)$$

$$\left.\frac{d\sigma}{dE_R}\right|_{\hat{\mathcal{O}}_8} = \frac{m_T}{2\pi v^2} \sum_{\tau,\tau'} c_8^{(\tau)} c_8^{(\tau')} \frac{J_\chi(J_\chi+1)}{3} \left[v^2 \tilde{W}_M^{\tau\tau'}(q^2) - v_{min}^2 \left(\tilde{W}_M^{\tau\tau'}(q^2) - \frac{4\mu^2}{m_N^2} \tilde{W}_\Delta^{\tau\tau'}(q^2) \right) \right]$$

$$\left.\frac{d\sigma}{dE_R}\right|_{\hat{\mathcal{O}}_{11}} = \frac{m_T}{2\pi v^2} \sum_{\tau,\tau'} c_{11}^{(\tau)} c_{11}^{(\tau')} \frac{J_\chi(J_\chi+1)}{3} \times \left[\frac{q^2}{m_N^2} \tilde{W}_M^{\tau\tau'}(q^2) \right]$$

Theoretical framework

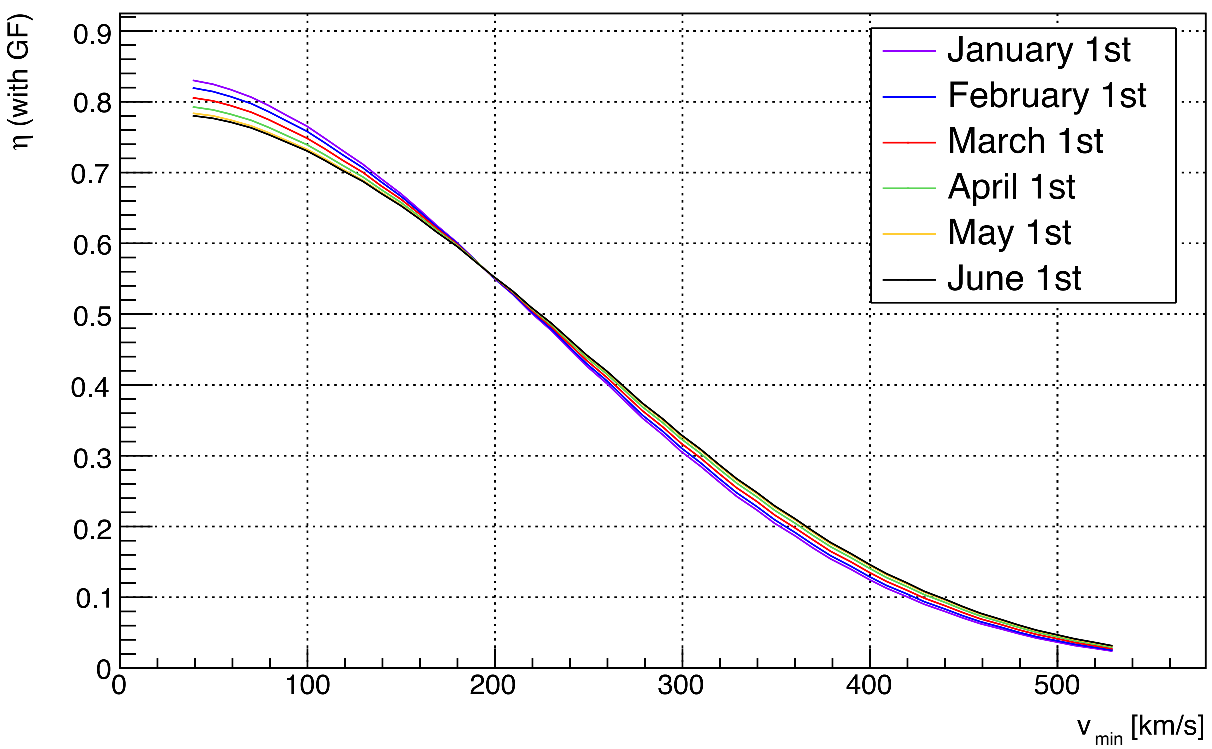

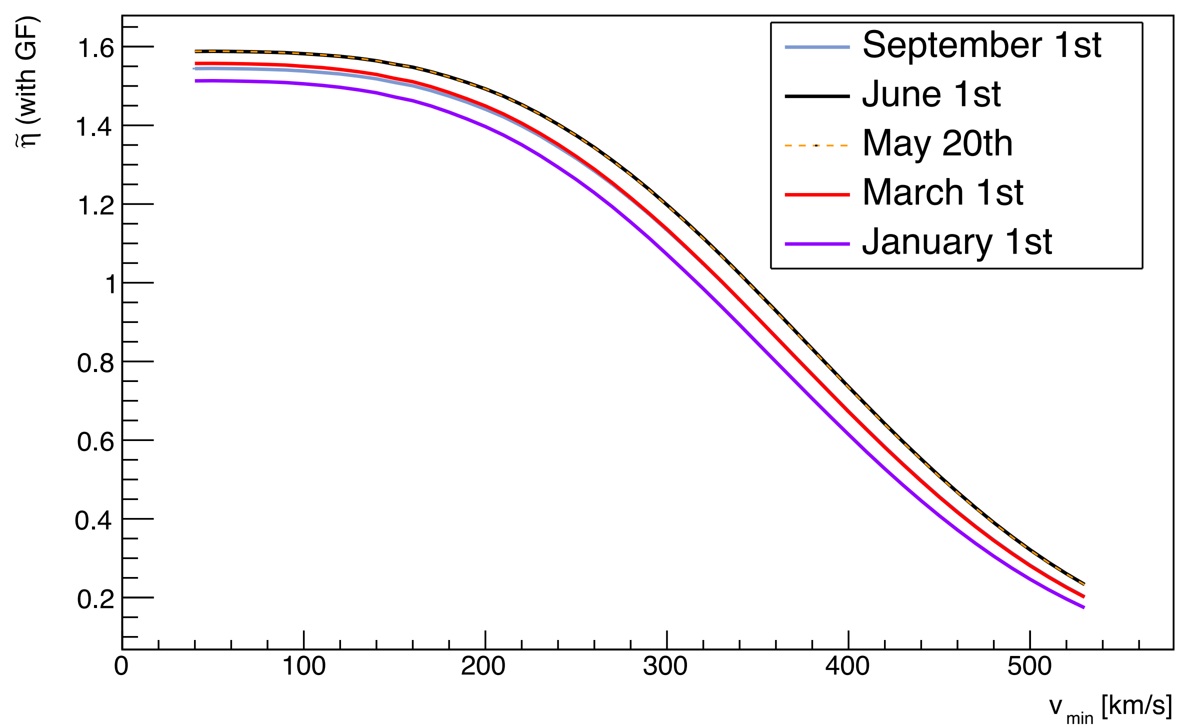

DM direct detection EFT: two applications

1. Annual modulation in NREFT

Results: time of maximal differential rate

Four categories of building-blocks

$$\mathcal{O}_1 \quad \mathcal{O}_5 \quad \mathcal{O}_7 \quad \mathcal{O}_{11}$$

$$\frac{1}{v^2} \cdot \quad 1 \quad (Av^2 + Bv_{min}^2) \quad (v^2 - v_{min}^2) \quad v_{min}^2$$

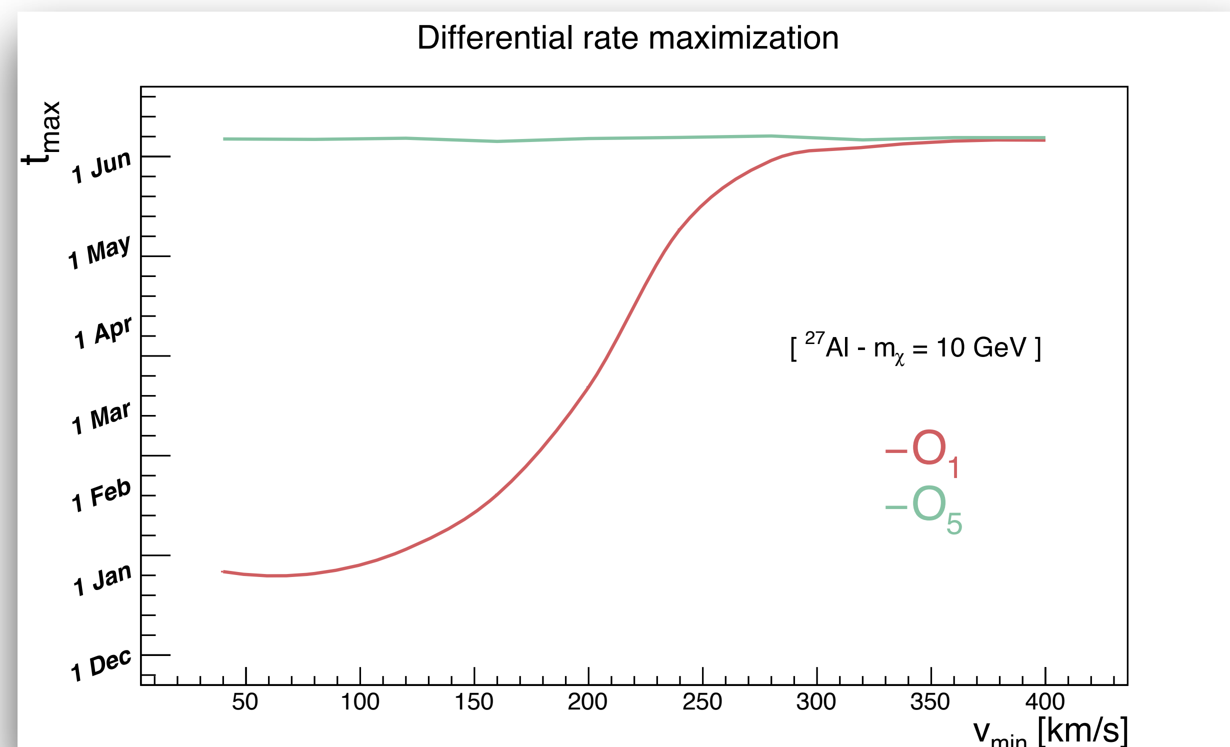

Two classes of building blocks have been identified:

1. the one with "the inversion of phase"
2. the one without inversion of phase.

No target dependence is present if single operators are considered

GSSI

AVANCEZ 1829

DM direct detection EFT: two applications

1. Annual modulation in NREFT

Results: target dependence in CRESST for MDDM (Anapole Dark Matter)

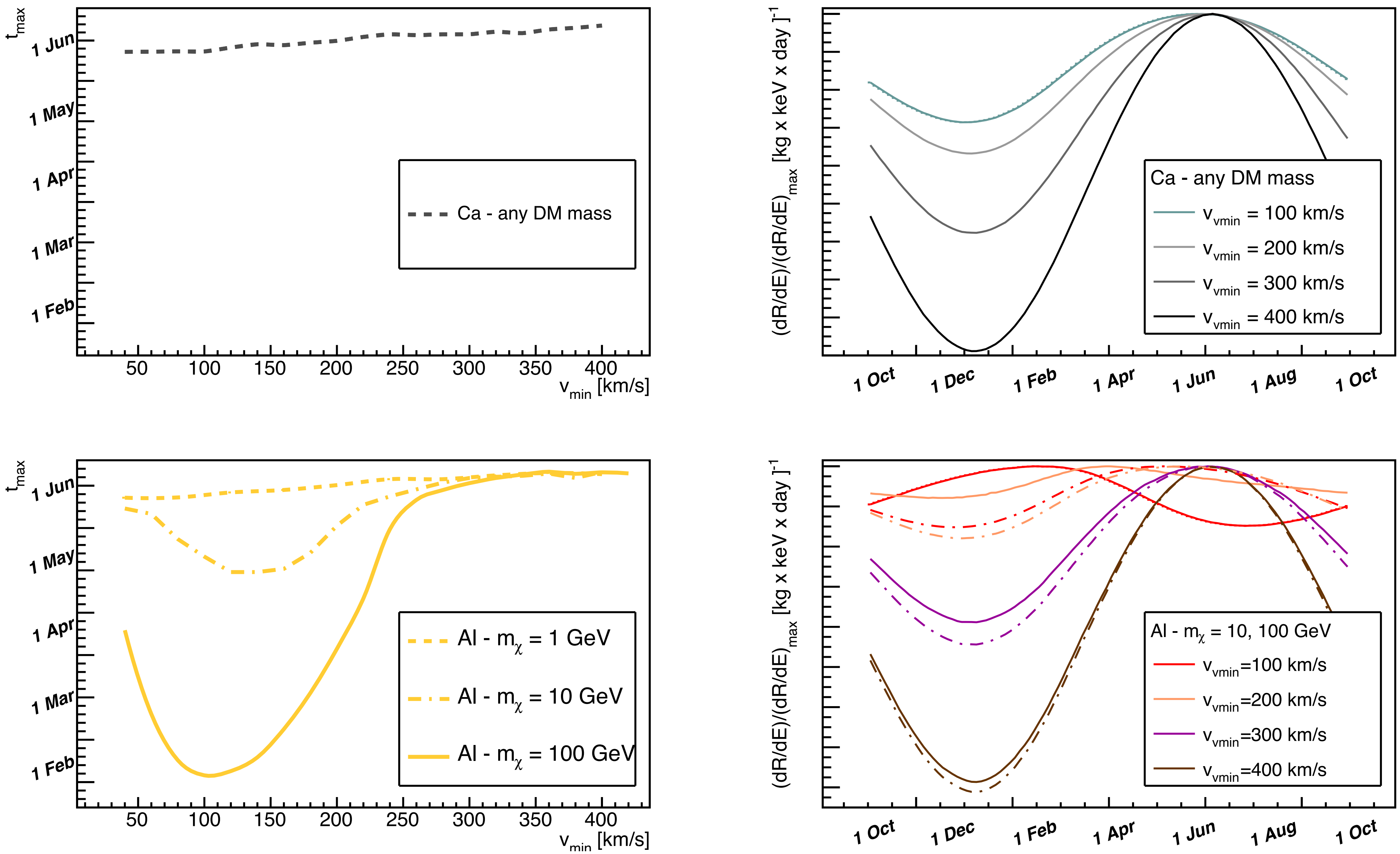

COSINUS: Cryogenic calorimeter based on **NaI crystals**

COSINUS
phenomenology

Validation of the EPSM with experimental data

Implementation by M. Stahlberg

2. **COSINUS neutron calibration problem**: in all the prototypes except for one, the neutrons cannot be identified in the LY plot. However, when a sapphire carrier with an NTD is employed, the neutron band is visible.

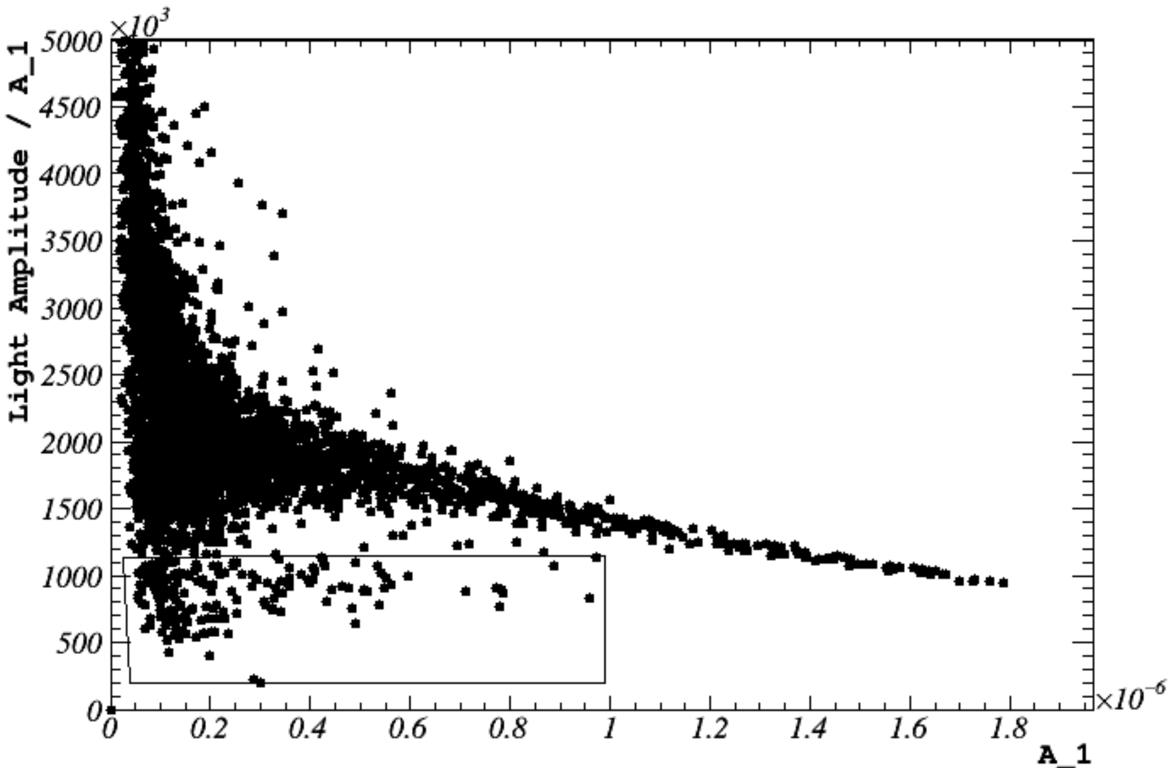

LY with energy reconstructed with the new integrated method based on EPSM

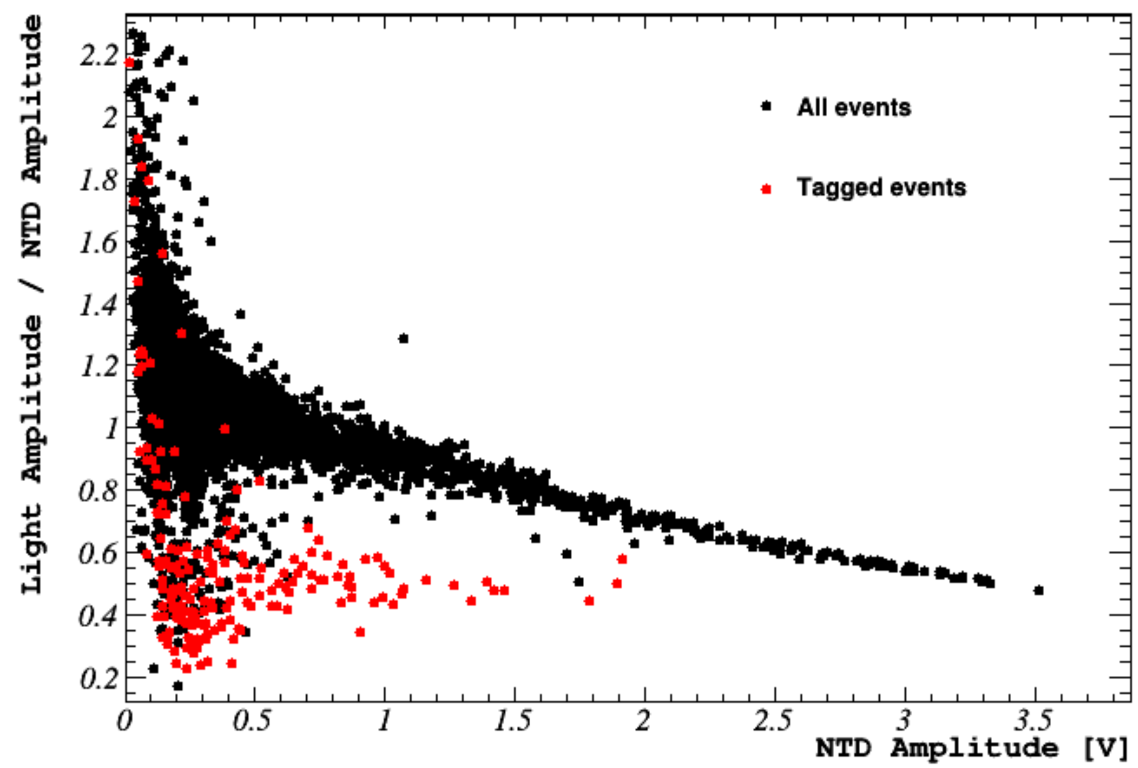

Usual LY obtained using the NTD channel. Neutrons are shown in red

G S
S I

COSINUS: Cryogenic calorimeter based on **NaI crystals**

Molecular Dynamics Simulations